

https://dspace.org/

A Three-dimensional Analysis Of The "hunting" Of An Unflanged Railway Wheelpair In Its Motion Along A Straight Track

Boyd, Charles Olivier

2015-01-12
http://hdl.handle.net/10539/16405

Downloaded from a DSpace repository. https://dspace.org/

UNIVERSITY OF THE WITWATERSRAND

JOHANNESBURG

SCHOOL OF MECHANICAL ENGINEERING

A THREE-DIMENSIONAL ANALYSIS OF THE 'HUNTING' OF AN UNFLANGED RAILWAY WHEELPAIR IN ITS MOTION ALONG A STRAIGHT TRACK

Charles Olivier Boyd

A thesis submitted to the Faculty of Engineering,
University of the Witwatersrand, Johannesburg,
for the degree of Doctor of Philosophy

Johannesburg 1979

A THREE-DIMENSIONAL ANALYSIS OF THE 'HUNTING' OF AN UNFLANGED RAILWAY WHEELPAIR IN ITS MOTION ALONG A STRAIGHT TRACK

Charles Olivier Boyd

A thesis submitted to the Faculty of Engineering,
University of the Witwatersrand, Johannesburg,
for the degree of Doctor of Philosophy

Johannesburg 1979

DECLARATION

This thesis is my own work, and has not been previously submitted to this or any other university.

ABSTRACT

The side-to-side oscillatory motion of a railway wheelpair travelling along a straight track has been investigated as an exercise in three-dimensional dynamics. Whereas existing theories hold that there are three possible regimes in the motion of a wheelpair; that is, pure rolling at very low speeds, creep at intermediate speeds and sliding at high speeds, this work holds that the regimes are:

rolling combined with sliding at very low speeds,
pure rolling at intermediate speeds, and
sliding (combined with a reduced rolling velocity) at speeds above a particular critical value.

Experimental observation of the wheelpair in a test rig evolved to ensure that the path of contact between the wheelpair and the rails in the range of contact between the two bodies takes place along a straight line has shown that the exponential growth in motion amplitude with time predicted by other workers does not occur. It has therefore been concluded that the motion is governed by non-linear differential equations. The derived equations of motion are complex and offer difficulty in providing a satisfactory solution but in their linearised form yield two theoretical frequencies, the higher of which approximates to the experimentally derived frequency. Experiments carried out on the test rig demonstrated that at speeds below the critical speed, the wheelpair would execute a number of cycles (the actual number depending upon the difference between the rail speed and the critical speed) and then revert to pure rolling. It is concluded that

pure rolling at speeds below the critical speed is remarkably stable. This is attributed to the adhesion between the wheelpair and the rails which railway engineers - other than those concerned with railway hunting - have investigated.

For Philip, Julian and Brigid, but especially for Heather, also in memory of Jim and Bee.

"That which has always been accepted by everyone, everywhere, is almost certain to be false".

Paul Valery, Tel Quel (1943)

ACKNOWLEDGEMENTS

I am most grateful to those graduates of the School of Mechanical Engineering in this University who, in executing their Advanced Laboratory Projects during their final year of study, laid a foundation for much of the experimental work on which this thesis is based. They were: Mr R D Venter (1966), Mr J W C Joughin (1967), Messrs P R Abrey and J Harris (1968), Mr B Sacks (1970), Messrs R von Gericke and J H Viviers (1975) and Mr R Smith (1976). The workshop staff and its superintendent, Mr F Bezuidenhout, were always most helpful and cooperative.

Mr J H Loubser, who when this work started was the Chief Mechanical Engineer of the South African Railways and who subsequently became its General Manager, made it possible for me to work with Mr H A Scheffel, presently Mechanical Engineer (Development of Rolling Stock) of the SAR. Not only has Mr Scheffel helped as an external examiner for the various laboratory projects mentioned above and put forward many helpful suggestions, but he has also shown remarkable forbearance in tolerating my heretical views on railway hunting.

Professor A D de Pater of Delft was always generous in sending me copies of papers, while Mr A Wickens kindly sent me photographs of the test rigs operated under his supervision at Derby (and which have been reproduced in this thesis). Professor R E D Bishop of University College, London, also gave me much useful information.

I would also like to acknowledge the assistance given to

me by various colleagues: Mrs Barbara Rotteveel corrected an early mistake in the directions of the systems of co-ordinate axes, Mr T O'D Duggan was most helpful at various stages of the experimental work, Dr R M Walker of the Department of Applied Mathematics found the roots of a number of the frequency equations for various coefficients of friction while Dr H C Duggan calculated the final set of roots. I would like to express my great gratitude to Professor Edgar Bunt, who proofread this thesis in its original form and made many valuable suggestions for its improvement. Professor Beric Skews gave me some of his valuable time to give guidance and help with the timing of the hunting frequency of the wheelpair and I am most appreciative of his generosity. Professor R Jamieson kindly programmed various calculations for me.

TABLE OF CONTENTS

		Page
DECLARATION		i
ABSTRACT		ii
ACKNOWLEDGEMENTS		vi
LIST OF FIGURES		xii
LIST OF TABLES		xiv
NOTATION		xv
CHAPTER 1:	RAILWAY HUNTING: A PROCEDURE FOR ITS INVESTIGATION	1
CHAPTER 2:	REVIEW AND DISCUSSION OF LITERATURE, PART 1: THE KINEMATIC THEORY	13
CHAPTER 3:	SURVEY AND DISCUSSION OF LITERATURE, PART 2: CREEP THEORY VIEWED AS A PARADIGM	23
CHAPTER 4:	REVIEW AND DISCUSSION OF LITERATURE, PART 3: A DISCUSSION OF THE DERIVATION OF THE EQUATIONS OF MOTION AND SOME OTHER TOPICS	37
CHAPTER 5:	DERIVATION OF THE CHARACTERISTIC EQUATIONS OF THE WHEELPAIR - RAILS - RESTRAINING SPRINGS SYSTEM	47
5.1	Introduction	47
5.2	Definition of the systems of coordinate axes	48
5.3	Derivation of the coordinate axes rotation matrices for the case where the origins coincide	50
5.4	Displacement of the centre of mass of the dicone after the yawing and tilting motions have taken place	52
5.4.1	Positions of the points of contact between the axes and the rails	52
5.4.2	Position of the centre of mass of the dicone after rotation about the Ox_2 axis; that is, after yawing	52

		Page
	5.4.3 Position of the centre of mass of the dicone after rotation about the $O'n_1$ axis; that is, after the dicone has tilted through an angle θ_x	54
	5.4.4 The vectorial displacement of the centre of mass of the dicone as movement occurs from the original fixed coordinate axes system to the final coordinate axes system	56
5.5	Coordinates of the points of contact between the dicone and the rails in the $O''\varepsilon_2\varepsilon_3$ plane	58
5.6	Determination of the linear velocities at the points of contact of the wheel-pair with the rails	60
	5.6.1 Introduction	60
	5.6.2 Velocity of the centre of mass of the dicone in the disturbed position	60
	5.6.3 Velocities of the surfaces of the dicone at the points of contact with the rails	61
5.7	Acceleration of the centre of mass of the dicone	65
5.8	The forces acting on the dicone	65
	5.8.1 Introduction	65
	5.8.2 The spring forces	67
	5.8.3 Components of the normal forces	67
	5.8.4 The tangential forces at the points of contact between the dicone and the rails	69
5.9	The linear equations of motion	70
	5.9.1 The matrix form of the linear equations of motion	70
	5.9.2 Expansion of the separate lines of the matrix form	70
	5.9.3 Separation of the (N_A+N_B) and (N_A-N_B) terms	72
	5.9.4 The equation of motion for the linear dicone movement in the direction of the rails	72
5.10	The moments of the forces acting on the dicone about its centre of mass	75
	5.10.1 Introduction	75
	5.10.2 The moments of the spring forces about the centre of mass of the dicone	76

		Page
5.10.3	Moments of the normal forces about the centre of mass of the dicone	77
5.10.4	Moments of the tangential forces at the points of contact about the centre of mass of the dicone	80
5.11	The equations of angular motion	85
5.11.1	Derivations of the equations of angular motion	85
5.11.2	The development of the equations of angular motion	
5.12	The frequency or characteristic equations for the dicone-rails-restraining springs dynamic system	89
5.12.1	The linearising of the equations of motion	89
5.12.2	The characteristic equations of the system	90
CHAPTER 6:	DESIGN OF THE TEST RIG (WITH A DESCRIPTION OF SUBSEQUENT MODIFICATIONS)	93
6.1	Introduction	93
6.2	Design requirements	98
6.2.1	Determination of the initial equipment parameters	98
6.3	Design and development of the first test rig	99
6.3.1	Detailed designs	101
6.3.2	Initial test rig modifications	107
6.3.3	Second test rig modifications	108
6.3.4	Third test rig modifications	112
6.3.5	Final form of the test rig	119
6.3.6	Design of air bearings	121
6.3.7	Optical measuring systems	126
CHAPTER 7:	EXPERIMENTAL WORK PERFORMED ON TEST RIG	130
7.1	Introductory survey	130
7.2	First test series	131
7.3	Second test series	135
7.4	Third test series	141
7.5	Experimental parameter data	145
CHAPTER 8:	A DISCUSSION OF THE THEORETICAL AND EXPERIMENTAL RESULTS	146
8.1	Introductory comments	146
8.2	The problem of Frequency Suppression	148

		Page
8.3	Adhesion between the wheel and the rail	150
8.4	Displacement of the centre of mass of the wheelpair as it yaws and/or tilts	151
	8.4.1 Introduction	151
	8.4.2 Lateral displacement of the centre of mass of the wheelpair as it yaws and/or tilts	152
	8.4.3 Vertical displacement of the centre of mass of the wheelset as it yaws and/or tilts	153
8.5	Cyclic changes in energy in the system	155
8.6	Experimental contact condition	156
8.7	Model tests at Derby	160
8.8	A discussion on the linearised equation of motion	164
8.9	The solution of simultaneous non-linear differential equations	166
CHAPTER 9:	AN OVERALL VIEW OF THE HUNTING PROBLEM	169
REFERENCES		174
APPENDICES		178
A.1	Data for experimental wheelpair	178
A.2	Characteristic equations in terms of test rig data	179
A.3	Calculated roots of characteristic equations for various values of spin speed and coefficients of friction	181¼
A.4	Theoretical first harmonic and experimental frequencies at various spin speeds and rail speeds (wheel diameter = 0.8m)	181
A.5	Translation of article by Heinze and Albrecht	182
A.6	Derivations of equations of motion by Wickens, Brann and Bennington	200
A.7	Are finite angular displacements in three dimensional-space sequence dependent?	213
A.8	Verification of the validity of the roots listed in Appendix 3.	218

LIST OF FIGURES

		Page
1.1 (a)	Angular motion of wheelpair	4
1.1 (b)	Free body diagram of rolling disc	4
1.2	Perspex model to illustrate dicone motion	8
1.3	Diagram to show position relative to roller in perturbed position	11
2.1	Sinusoidal path of wheelpair	17
4.1 (a)	Lomonosoff's figure of dicone motion 7	45
4.1 (b)	Explanatory diagram for figure 3-1(a)	45
5.1	Coordinate axes system	49
5.2	Coordinate axes relationships	49
5.3	Position of dicone after yawing	53
5.4	Position of centre of mass of dicone after yawing	54
5.5	Position of centre of mass of dicone after tilting	55
5.6	Equivalent mechanism	56
5.7	Wheelpair in perspective as a free-body diagram	66
5.8	The normal forces with their components at the points of contact	68
6.1	Possible degrees of freedom in test plant roller unit [26]	94
6.2	Experimental test rig at Derby [8]	96
6.3	Full scale test rig at Derby [8]	96
6.4 (a)	Complete rig without dicone in position showing rails	100
6.4 (b)	Complete rig with dicone in position	100
6.5 (a)	Dicone shaft sleeve	102
6.5 (b)	Assembled dicone	102
6.6	Isometric view of base	103
6.7 (a)	Driving pulley shaft assembly	105
6.7 (b)	Cast iron core	105
6.8	Rail support	106
5.9 (a)	Redesigned wheelpair on test rig	110

		Page
6.9 (b)	Another view of redesigned wheelpair	111
6.10	Dicone yoke and bearing	114
6.11	Plan view of S.A.R. test rig	116
6.12	Elevation of S.A.R. test rig	117
6.13	Rail supporting rollers on S.A.R. test rig	118
6.14 (a)	Cambering rollers in elevation	120
6.14 (b)	Cambering rollers in plan	120
6.15	Isometric view and corss-section of air slide	122
6.16 (a)	Air slide	124
6.16 (b)	Air slide and cambering rollers in plan	124
6.17	Air slide and cambering rollers seen in elevation with the wheelpair	125
6.18	Mirror driving system	127
6.19 (a)	Plan view of mirror driving system	128
6.19 (b)	Elevation of mirror driving system	128
7.1 (a)	Photograph showing squared grids placed under ends of wheelpair shaft	132
7.1 (b)	Mounting of recording cine camera and mirror	132
7.2	Sequence of wheelpair position in various oscillatory positions	133
7.3	Graph of angular positions plotted against time	136
7.4	Graph of longitudinal dislacements plotted against time	138
7.5	Transient response curve	140
7.6	Wheelpair slip in relation to rail speed	142
7.7	Amplitudes of angular displacements plotted against time	143
7.8	Wave form of frequency recording	145
8.1	Variation in lateral displacement of the centre of mass of the wheelpair as tilt angle changes	154
8.2	Variation in vertical displacement of the centre of mass of the wheelpair as tilt angle changes	157

LIST OF TABLES

		Page
6.1	Details of drive particulars	104
7.1	Periods of angular and longitudinal motions	134
7.2	Table of critical speed results	135
7.3	Transient response tests	139
7.4	Slip as a function of wheelpair speed	139
7.5	Relationship between the amplitude of the yawing and tilting movements and belt speeds	141

NOTATION

		Units
M	Mass of dicone	M
R	Radius of base of dicone	L
2α	Cone vertex angle	-
α	Wheel taper angle	-
$2b$	Distance separating rails	L
$2B$	Distance separating restraining springs	L
k	Combined spring constants on each dicone shaft sleeve	MT^{-2}
θ	Angle of tilt	-
ϕ	Angle of yaw	-
n	Wheelpair spin speed	T^{-1}
$\bar{a}$	Position vector of left-hand part of contact	L
$\bar{b}$	Position vector of right-hand point of contact	L
$\bar{F}_i$	ith force in system	MLT^{-2}
$\bar{N}_A, \bar{N}_B$	Normal forces at left- and right-hand points of contact respectively	MLT^{-2}
$\bar{T}_A, \bar{T}_B$	Tangential tractive forces at left- and right-hand points of contact respectively	MLT^{-2}
$\bar{F}_A, \bar{F}_B$	Frictional forces opposing tilting motion at left- and right-hand points of contact respectively	MLT^{-2}
$\bar{\bar{J}}$	Moment of inertia tensor	ML^2
$\bar{\omega}_\varepsilon$	Angular velocity vector in the $O''\xi_1\xi_2\xi_3$ coordinate axes frame	T^{-1}

		Units
$\bar{\bar{\Omega}}_{\varepsilon}$	Matrix form of the angular velocity in the $O''\xi_1\xi_2\xi_3$ coordinate axes frame	T^{-1}
$\omega_{\varepsilon\,\text{dicone}}$	Angular velocity of the dicone in the $O''\xi_1\xi_2\xi_3$ coordinate axes frame	T^{-1}
$\bar{h}(=\bar{\bar{J}}\omega_{\varepsilon\,\text{dicone}})$	Moment of momentum vector of dicone	ML^2T^{-1}
$\bar{g}_i^*$	Moment of ith force about the centre of mass	ML^2T^2

NOTES

1. Square matrices are indicated by capital letters surmounted by a double bar, thus

   $\bar{\bar{J}}$ = Moment of inertia matrix

   $$= \begin{bmatrix} J_1 & 0 & 0 \\ 0 & J_2 & 0 \\ 0 & 0 & J_3 \end{bmatrix}$$

2. Column vectors are written in lower case letters with a bar above the letter, thus,

   $\bar{a}$ = Position vector of the left-hand point of contact

   $= \{a_1 \quad a_2 \quad a_3\}$

3. A subscript added to any vector indicates the coordinate axes frame in which the coordinates of the vector are given. Where appropriate, ordinary vector notation is used, vectors being indicated by a tilde (~) under the letter.

4. The notation used in setting out the equations of motion follows that used by Heading [1], but where appropriate, Chirgwin and Plumpton [2] and Pars [3] have been followed.

5. Angular movement about a horizontal axis is often referred to in the literature as 'rolling'. Since there is always the possibility that confusion could then arise when reference is to be made to the rotation of the wheelpair about the axis of the wheelpair shaft, the term, rolling, has been limited to the

latter form of rotation. The term 'tilt' has been used to indicate rotation of the wheelpair about a horizontal axis normal to the axis of the shaft; that is, about a horizontal axis nominally in the direction of the rails.

6. Unless otherwise stated, any translations included in this work are my own.

CHAPTER 1

RAILWAY HUNTING: A PROCEDURE FOR ITS INVESTIGATION

The investigation of physical phenomena is often difficult in that the actual mechanism causing the particular phenomenon is not readily perceived. If essential features of the mechanism are overlooked then the analysis which follows must be deficient. D'Abro [4] quotes two fundamental canons of natural philosophy, as set out by Max Planck [5] in 1932, to the effect that:

1. *There is a real outer world which exists independently of our knowledge*
2. *The real outer world is not directly knowable.*

It is the second of these canons which is relevant here. Much of our knowledge of how the world functions, says D'Abro, is derived in a roundabout way, by coordinating direct knowledge, elementary inference and rationalisation. Our understanding of physical phenomena is, however, frequently obscured by a combination of preconceived notions, faulty assumptions and a failure to state these assumptions clearly.

Furthermore, if a given phenomenon is studied over a long period of time, particular treatments may assume the character of a vested interest and become, as it were, frozen into a rigid pattern. Various individual theories are postulated and through the passage of time acquire an

apparent validity which is then never questioned. For this reason, it is often useful to re-examine particular theories critically since these enquiries may be fruitful in opening new avenues for further study of how these phenomena occur.

Railways have been in use since the second decade of the last century. Hamilton Ellis [6] gives the date for the first commercial use of steam haulage by a locomotive as August 12, 1812, while the Stephensons succeeded in producing the first locomotive to work public traffic regularly on a company-owned right of way for the Stockton and Darlington Railway which had been incorporated in 1821. The side-to-side movement of railway wheelpairs as the vehicle travelled along the track, and which has always been known as 'railway hunting', had (according to an unidentified source) already been commented on by Stephenson in 1821.

A great number of papers have been written on the subject of railway hunting. Lomonosoff [7] refers to observations of the phenomenon made by M von Weber in 1848. Because hunting has been studied so intensively over such an extended period of time, there is always the possibility referred to in a previous paragraph that some of the theories may justify critical re-evaluation since the theories may not in fact accord with reality.

Although the wheelpair is described in the literature as having a linear lateral displacement, that is, it hunts in the plane normal to the direction of the rails, it would appear to be more correct to believe that the actual movement of the wheelpair is made up of two angular movements, as shown in Figure 1.1(a). It can be shown that what appears to be a lateral displacement is caused by the wheelpair tilting.

Since railway hunting is often thought to be the cause of derailments, research into the way wheelpairs behave as they travel along the rails is of great practical importance. A H Wickens of the Engineering Research Division of British Railways at Derby, explains the problem as follows [8]:

> Recent work... has established by experiment that existing railway vehicles possess critical speeds. Below the critical speed the motion of the vehicle is determined by track features, but above the critical speed a continuous hunting oscillation occurs which is limited only by the action of the flanges, slipping of the wheels, and by suspension non-linearities. The critical speeds of existing four-wheeled vehicles are in some cases as low as 20 mile/h, and bogie vehicles exist with critical speeds as low as 55 mile/h. The hunting oscillation has several practical consequences which tend to limit train speeds. In addition to the unsatisfactory vibration levels experienced by the payload, the large lateral forces which occur contribute to derailment proneness, overheated axle bearings, damage to track, and fatigue failures of the vehicle structure.
>
> Railway vehicles are fitted with coned wheels to provide a measure of static stability. The hunting oscillation arises from the dynamic instability of the vehicle caused by the interaction between the conicity of the wheels, the forces acting between the wheels and the rails, and the action of the suspension.

In general, railway vehicles consist of a body resting on soleplates on the tops of the supporting bogies. These soleplates make it possible for the bogies to rotate with respect to the body they support. The wheelpairs are usually fastened to the bogie frames through springs fixed to the wheelpair bearings. The behaviour of the wheelpairs is transmitted through the bogie suspension to the vehicle and is therefore of great practical interest.

This work has been confined to an examination of the

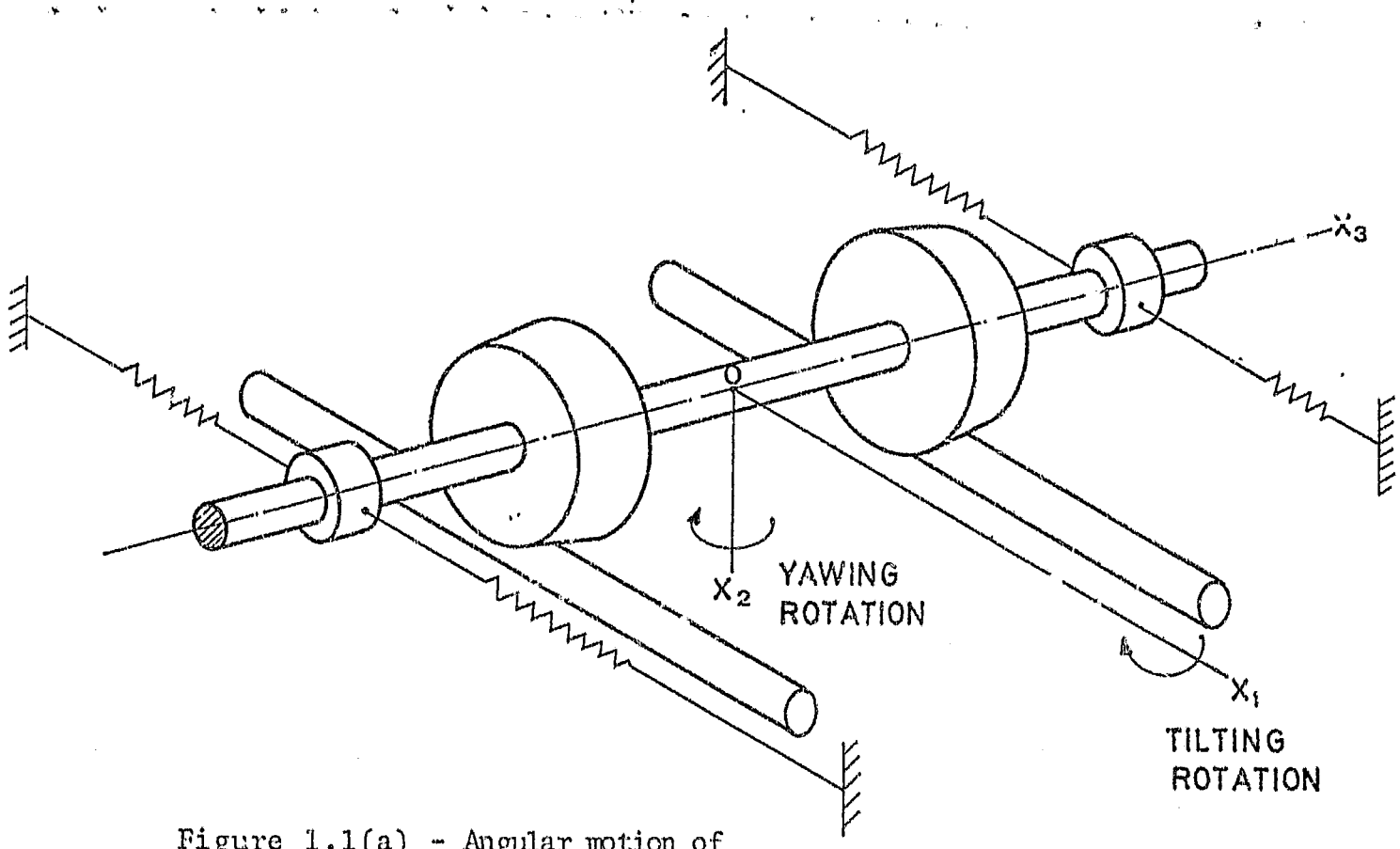

Figure 1.1(a) - Angular motion of wheelpair

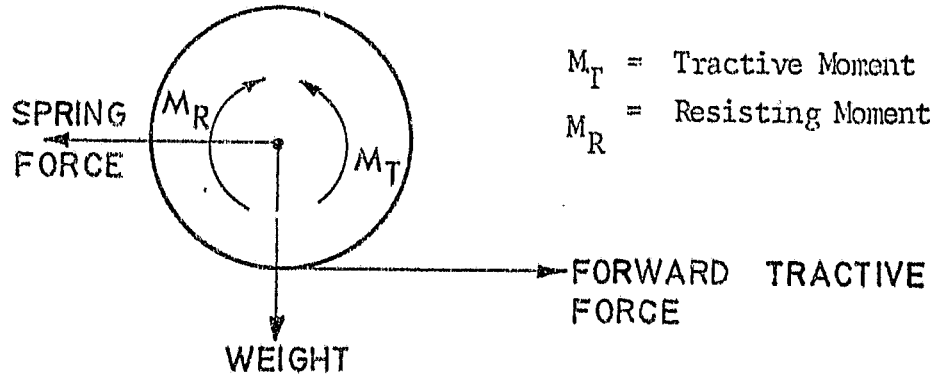

M_T = Tractive Moment

M_R = Resisting Moment

FREE BODY DIAGRAM OF FORCE ON WHEEL

Figure 1.1(b)

behaviour of the wheelpair as it travels along a straight track. Every effort has been made to simplify the problem in the belief that the removal of extraneous complications will facilitate the understanding of how hunting occurs. The wheelpair has uniformly tapered conical running surfaces so that point contact between the wheelpair surface and the rounded supporting rail head can be assumed. An important assumption made in the analysis is that the respective wheels which together comprise the wheelpair are constrained to remain in contact with the rails at all times. As will subsequently be seen, this assumption then makes it possible to determine the position of the centre of mass of the wheelpair as a function of the angular displacements incurred by it as it yaws and/or tilts. The acceleration of the centre of mass of the wheelpair can then be found by differentiating the position vector of the centre of mass. The only gravity force on the wheelpair is its own weight. The forces between the wheelpair surfaces and the rails are opposed by horizontal springs acting on sleeves free to slide along the wheelpair shaft: between them these forces make up the couple causing the wheelpair to rotate, as shown in Figure 1.1(b)

The analysis presented in this work is based on rigid body dynamics which precludes any allowance being made for elastic deformations. Rigid body dynamics, in effect, recognises only those kinematic displacements, which are of first order magnitude and rejects those kinematic displacements, which are due to elastic deformation on the grounds that such displacements are of the second order in magnitude and may therefore be overlooked. As a consequence, it is argued that either the wheelpair has pure rolling motion or that it slides, with reduced spin velocity, across the rails, and that in the latter case the forces between the wheels and the rails are Coulomb frictional

forces which are proportional to the normal forces and which act in the direction of the rails.

All the information will then have been made available so that the linear equations of motion as well as the angular equations of motion can be found. This total of six equations corresponds to the number of variables which are: The angles of yaw and tilt, the spin velocity, the linear displacement in the track direction and the normal forces.

It is appropriate at this point to suggest that other workers in this field have not always been sufficiently appreciative of the fact that considerable discrepancies exist between two- and three-dimensional analysis. The distinction between the two approaches is lucidly explained by Marris and Stoneking [9]:

> There is a yawning chasm between plane motion and three-dimensional dynamics, and principles and methods learned in the context of plane motion appear as almost unrecognizable specializations of three-dimensional results. Finite angular displacement may be considered to be a vector in plane motion; three-dimensional motion shows that it is not a vector. Again, moment of inertia may appear as a scalar, perhaps even analogous to mass, in plane motion; three-dimensional considerations show its true nature as a tensor. Plane-motion dynamics dealing with rods, hoops, and disks generally avoids mention of principal axes and the use of rotating coordinate axes embedded along the principal axes of the body, even though it uses the method implicitly.
>
> The new kinematical concepts required for three-dimensional motion make the direct *extension* of plane-motion ideas to include the three-dimensional case nearly impossible. On the other hand, once the fundamentals of three-dimensional kinematics are grasped, a new and wider understanding of the special plane-motion case follows immediately.

Since the three-dimensional dynamic model is far more complex than the apparently equivalent two-dimensional counterpart, it is not surprising that other workers in this field should have confined their analysis to two-dimensional models on the grounds that the deviations from three-dimensional behaviour as the wheelpair travels along the straight track are so small that they can be ignored. These deviations may be slight, but it is ironical that these workers should then proceed to analyse elastic deformations, which are much smaller than the kinematic displacements they have decided to overlook. As will be shown later, the assumption that a two-dimensional model is adequate is not justified.

In the introductory paragraph of this chapter, the canon stated by Max Planck to the effect that the real world can only be seen indirectly was quoted. If this canon is to be taken seriously, it is necessary to invoke any possible aid to determine what could be involved in any particular physical phenomenon - such as the construction of adequate models - so as to improve the likelihood that the basic elements of the problem may be properly understood. The perspex model shown in Figure 1.2 shows in three dimensions what occurs when a dicone whose surfaces taper at an angle of 30° is caused to yaw and to tilt. The 'rolling circles' of the dicone would be those circles of the dicone which touch the rails at the points of contact. As shown in the model, these circles may differ widely in diameter. If there were no constraints on the motion of the dicone, the motion of the following points on the circumferences of the rolling circles would have the direction shown in the model. Since constraints do exist, such movement is not possible and alternative forms of motion then have to be considered.

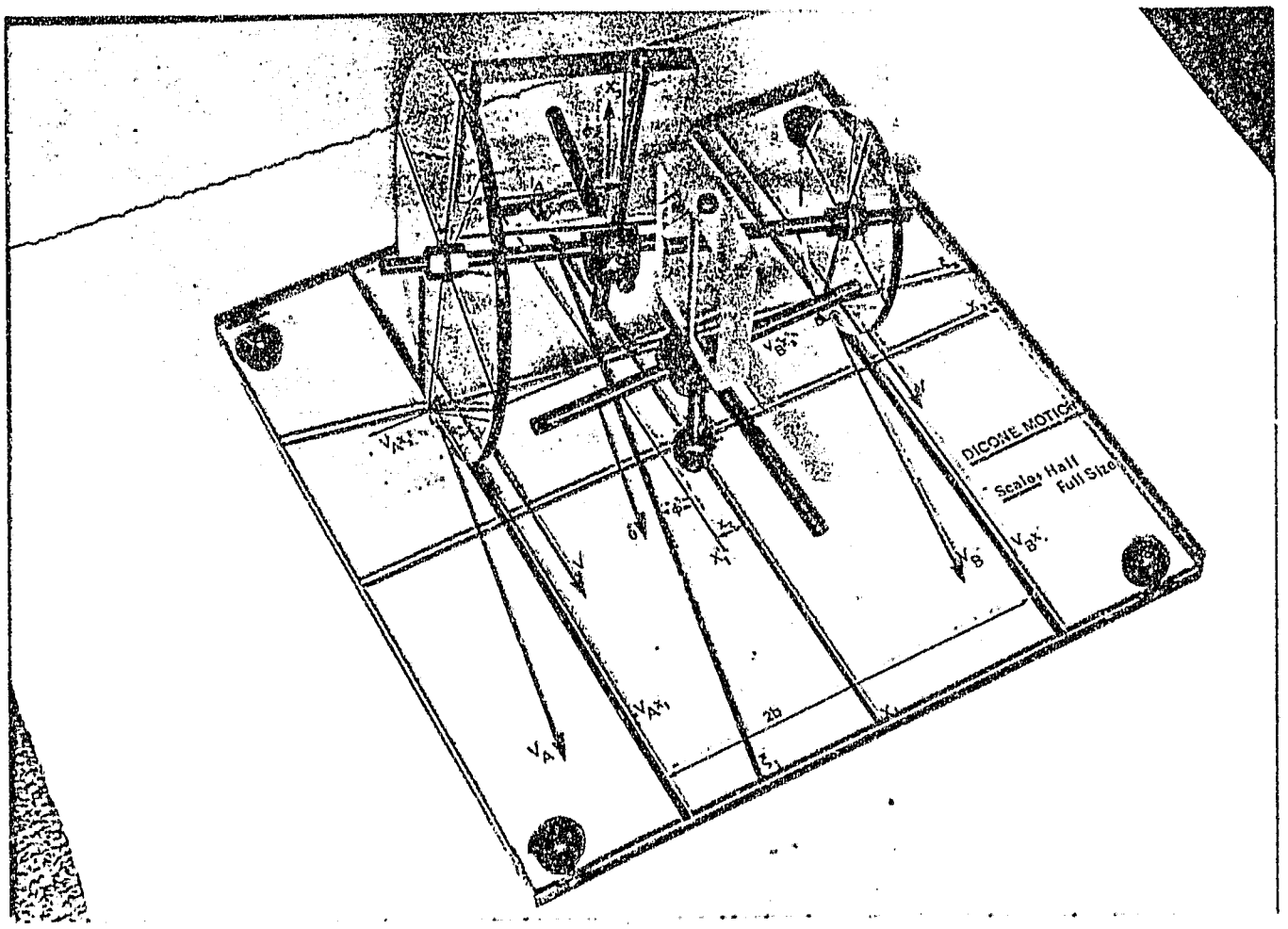

FIG. 1 - 2:

PERSPEX MODEL TO ILLUSTRATE DICONE MOTION

The application of Newton's Laws of Motion to the movement of the wheelpair requires that the centre of mass of the equivalent dicone should be known; that is, the position vector, which establishes the position of the centre of mass with reference to a given set of coordinate axes, has to be determined. But this in turn requires that the positions of the points of contact of the wheelpair with the supporting rails should be known. These points would serve to locate the centre of mass in the space. The first approach made to determine the contact point was mathematical, that is, the points of intersection with the surface of the dicone of two parallel lines at the correct distance from each other should be found and the actual contact points would be those points where the two intersecting points for each rail coalesce into a single point. Fortunately a simpler method (as described in section 5.4.1 of Chapter 5) was found and this eliminated the clumsy mathematical approach referred to in the previous sentence.

Information as to the nature of the forces at the points of contact between the dicone and the rails had also to be obtained. The position of the centre of mass of the dicone having been obtained, it was possible to determine the velocities of the surface of the dicone at the points of contact with the rails. Since these velocities are not identical with the rail velocities, it has to be concluded that the dicone must slide over the rails, if it has yawed and/or tilted. If the dicone slides, then the forces at these contact points must be the normal and the tangential forces, which act in the direction opposite to the direction of the dicone surface velocity at that instant, and which are proportional to the normal forces. On the other hand, other workers in this field have, basing their assumptions on creep theory, assumed that the tangential forces are proportional to the relative

velocities of the surfaces in the 'areas' of contact.

Judging by the resulting publications, all other experimental work on railway hunting has been conducted exclusively on 'roller rigs' where the wheelpairs rest on the upper surfaces of supporting rollers which take the place of the rails on which they would normally rest. The wheelpair is prevented from moving by elastic constraints and so the required relative motion between the wheelpair and the 'rails' is obtained by driving the supporting rollers. Apart from the fact that each wheel would follow a curved path related to the surface on which it rests as the wheelpair yaws, there could be objections to the constraints controlling the movement of the isolated wheelsets tested on these rigs. Photographs of these rigs suggest that the supporting rollers are 'discs' rather than 'rollers' since their thickness is minimal. Figure 1.3 shows how contact would occur between the supporting disc and the dicone as the latter yaws. Whereas in reality, the dicone would sink further between the discs as yawing proceeded, the position of the disc has been raised in the figure so that this contact continues to be possible. It is true, as is inevitable in any diagram designed to show the importance of certain aspects of the process under investigation, that the angle of yaw has been exaggerated, yet the figure emphasizes how the motion of a dicone on a roller rig is not equivalent to the movement which would occur if it were supported on a pair of straight tracks. Attempts have been made to overcome this objection, but these very attempts defeat the objectives of the research procedure. Figure 6.2 in Chapter 6 is a photograph of a test rig used at Derby [8] to investigate how a single wheelset would behave on a roller rig. Since the form of the constraint on the wheelpair in this case is such that the movement of yaw of which it is capable has been so arranged that the argument against the use

velocities of the surfaces in the 'areas' of contact.

Judging by the resulting publications, all other experimental work on railway hunting has been conducted exclusively on 'roller rigs' where the wheelpairs rest on the upper surfaces of supporting rollers which take the place of the rails on which they would normally rest. The wheelpair is prevented from moving by elastic constraints and so the required relative motion between the wheelpair and the 'rails' is obtained by driving the supporting rollers. Apart from the fact that each wheel would follow a curved path related to the surface on which it rests as the wheelpair yaws, there could be objections to the constraints controlling the movement of the isolated wheelsets tested on these rigs. Photographs of these rigs suggest that the supporting rollers are 'discs' rather than 'rollers' since their thickness is minimal. Figure 1.3 shows how contact would occur between the supporting disc and the dicone as the latter yaws. Whereas in reality, the dicone would sink further between the discs as yawing proceeded, the position of the disc has been raised in the figure so that this contact continues to be possible. It is true, as is inevitable in any diagram designed to show the importance of certain aspects of the process under investigation, that the angle of yaw has been exaggerated, yet the figure emphasizes how the motion of a dicone on a roller rig is not equivalent to the movement which would occur if it were supported on a pair of straight tracks. Attempts have been made to overcome this objection, but these very attempts defeat the objectives of the research procedure. Figure 6.2 in Chapter 6 is a photograph of a test rig used at Derby [8] to investigate how a single wheelset would behave on a roller rig. Since the form of the constraint on the wheelpair in this case is such that the movement of yaw of which it is capable has been so arranged that the argument against the use

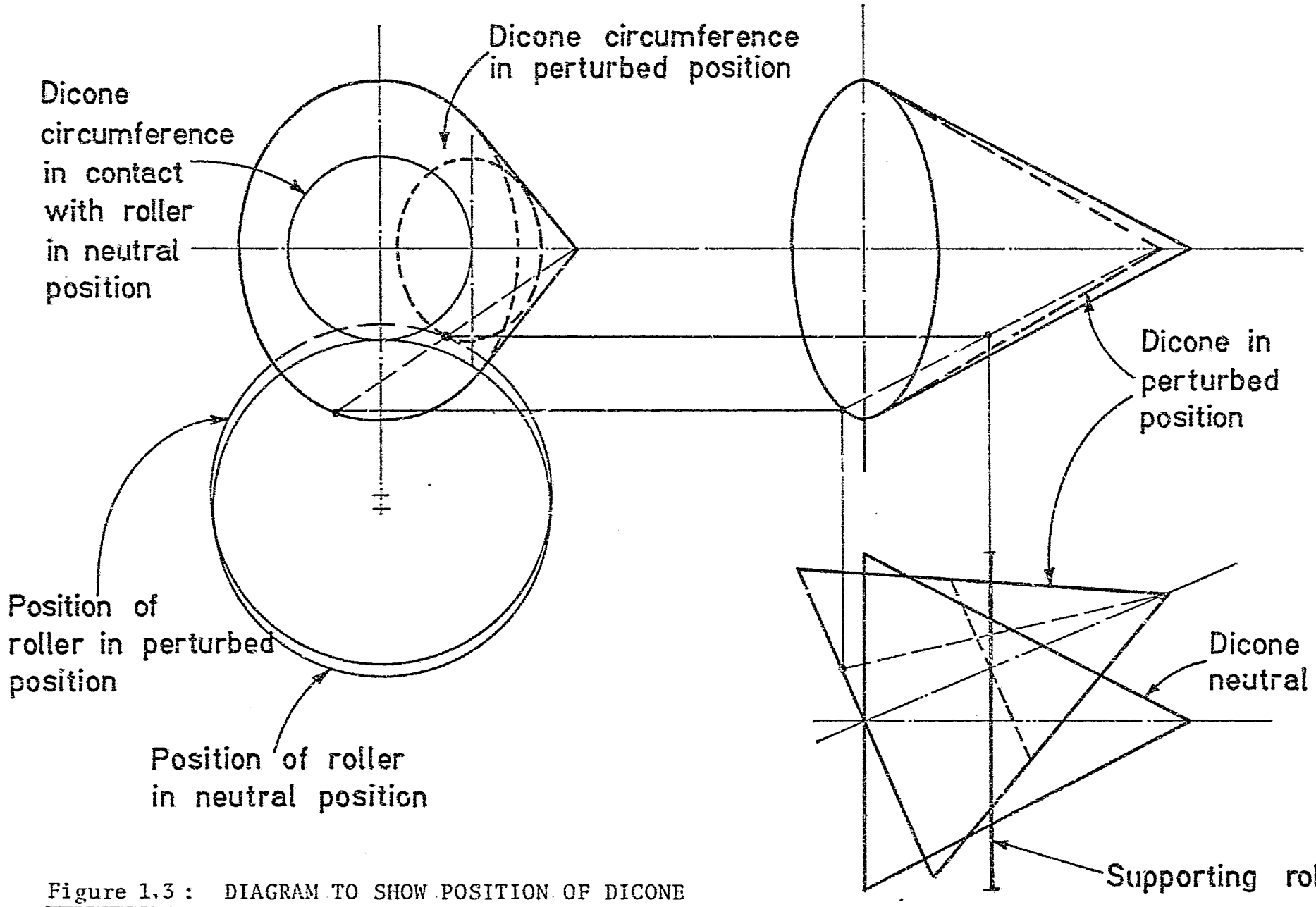

Figure 1.3 : DIAGRAM TO SHOW POSITION OF DICONE RELATIVE TO ROLLER IN PERTURBED POSITION

of a roller rig raised in the previous sentences, has been minimized, it would seem that the entire purpose of the research objective has thereby been negated. If the wheelpair movement is to be tested under the correct dynamic conditions, it would appear important that it should be allowed to move as freely as possible as it yaws and/or tilts; moreover the path of contact between the wheels and the rails should be a straight line as is the case in the situation which it is supposed to model.

Roller rigs are undoubtedly easier to design and maintain, but nevertheless, it seemed possible that the movement between the wheelpair and the rails could be simulated in a different manner. Consequently, one of the aims of this work has been to devise what was thought to be a more s tisfactory form of test rig. The results which were obta ned here show that the required relative motion can be more adequately reproduced in an experimental test rig in a better (and original) way, namely, by making use of a rail simulating surface comprised of a driven steel strip supported on an air slide.

Succeeding chapters review various current and out-moded theories which have been proposed to explain the causes of railway hunting. These chapters are followed by a different form of analysis of the problem, an outline of the design and construction of the experimental test rig, a review of the tests run on this rig to investigate the degree of correspondence between the theoretically predicted results and the experimental behaviour of the wheelpair in the new form of rig, a discussion of the theory and the theoretical results and finally, by a summing up of what has been attempted and to what extent this has been achieved in this work.

CHAPTER 2

REVIEW AND DISCUSSION OF LITERATURE, PART 1: THE KINEMATIC THEORY

Some concepts, thought to be so simple that they are usually described as 'elementary', may on closer observation show that the processes involved are more complex than are initially believed to be the case. It is suggested that such a concept is that of pure rolling and that this requires to be precisely defined, if misunderstandings are to be avoided. MacMillan [10] interpreted the mechanism involved in pure rolling as follows:

> Since any displacement of a rigid body parallel to a fixed plane can be effected by a rotation about a suitable axis perpendicular to the plane any continuous motion of a body parallel to a fixed plane can be resolved into a series of infinititesimal rotations about an axis which, in general, is itself in continuous motion both with respect to the body and with respect to the plane. If the motion of the axis were discontinuous, the motion of the body also would be regarded as discontinuous.

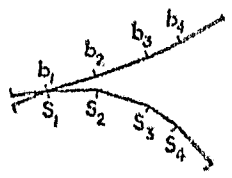

The axis about which the body is rotating at any instant in this resolution of the motion is called the instantaneous axis of rotation. The locus of the instantaneous axis in the body is called the body centrode, and the locus of the axis with respect to the fixed plane is called the space centrode. It is fairly evident that the motion of the body is just the same as though the body centrode, rigidly attached to the body, were rolling without slipping upon the space centrode. In order to make this clear, however, imagine a series of small but finite rotations. In the figure let s_1, s_2, s_3, s_4, be four consecutive positions of the instantaneous axis on the fixed plane at the instants t_1, t_2, t_3, t_4, and b_1, b_2, b_3, b_4, be the positions in the body at the same instant. In the interval $t_2 - t_1$ the body pivots on b_1 which coincides

with s_1. This rotation brings b_2 into coincidence with s_2. In the interval $(t_3 - t_2)$ the body pivots on s_2 and b_2 until b_3 is brought into coincidence with s_3, etc. The motion is the same as the rolling of one polygon on another. The motion is discontinuous at each corner, and the axis jumps by finite amounts. The rate of rolling may vary in any manner whatever, but the displacement at each pivot is definite. If the sides of the polygons are diminished indefinitely, the centrodes become smooth curves, and if the motion of the body is continuous, the body centrode rolls without slipping upon the space centrode. The instantaneous axis is at the point of contact of the two centrodes and the motion is always one of pivoting on the instantaneous axis.

In the case of the wheel travelling on the rail, the body centrode is the circumference of the wheel ('the rolling circle') and the space centrode is the rail, where it facilitates one's thinking if this is viewed as a straight line. MacMillan has defined his discussion to movement parallel to a fixed plane and although it is possible to conceive that the body and space centrodes could be situated in a three-dimensional space, this would introduce considerable complexity into the analysis. Since the space centrode in this case is a straight line, it can be concluded that pure rolling occurs only if the rolling circle is planar; that is, the wheelpair has pure rolling motion only when it is rolling in the neutral position, mid-way between the rails, with zero angles of tilt and yaw.

It is useful to examine the free body diagram of the wheel as shown in the following discussion taken from Huddleston [11].

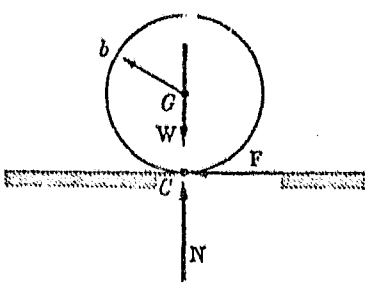

The free body diagram in the figure shows the external forces. In reality, the wheel is observed to slow down, an occurrence which is

due to the rolling resistance accompanying small deformations of the wheel surface and that of the plane at the point of contact.

This account is a fair representation of conventional thinking on pure rolling and yet, it is incorrect. For force equilibrium in the horizontal direction, the free body diagram should show an additional force placed at the centre of the wheel, equal in magnitude and opposite in direction to the force at the contact point. When Huddleston states that in reality the wheel is observed to slow down, this is also theoretically correct. Since if there is no opposing force at the wheel centre, this force in effect becomes an inertial force. To round off these observations, it is necessary to note that in addition to the pure rolling situation, two other possibilities exist, namely:

a. If there were no force at the contact point, which would be the case if both surfaces were ideally smooth, the wheel would not roll and it would simply slide bodily over the supporting surface.

b. If the force applied at the wheel centre exceeded the maximum possible friction force, the wheel would both slide and roll.

The preliminary remarks serve as an introduction to a theory originally proposed by Klingel [12] in 1883 and generally referred to in the literature as the 'Klingel theory' or the 'kinematic theory'. It has been used by Rocard [13] and Inglis [14] to illustrate instances of simple harmonic motion; however, it would appear that the mechanism of the oscillatory motion may be more subtle and complex than can be adequately handled by this theory. The Klingel theory is prompted by the experimental observation that if a wheelpair with uniformly tapered running surfaces is so placed that it is not in the neutral position on two parallel straight rails, the plane of which is inclined at a slight angle to the horizontal so that the rolling friction in the direction of the rails is overcome by the appropriate component of the weight of the wheelpair,

the wheelpair moves slowly down the rails, oscillating from side to side as it does so. Figure 2.1 shows this motion. Not only does the wheelpair yaw about an axis perpendicular to the plane of the rails, but it also tilts about an axis in the direction of the rails. The distances between the centre of mass of the wheelpair and the points of contact on either rail alters steadily during the movement. What was in many ways a perceptive analysis of the situation was given by Robert Levi [15] , the Technical Director of the French Railways, who wrote in his official capacity one of the reports issued after a serious accident had occurred in 1933. Because of its value, a translation of the first half of the paper will be given:

> An essential question which suggests itself in investigating the reciprocal action between the rolling stock and the permanent way is the manner in which the wheels progress along the rails. Is there any sliding associated with the wheelpairs?
>
> Researches made so far pose a dilemma in answering the question: the motion consists either of pure rolling, in which case the advance of the respective wheels proceeds at equal and parallel velocities along the track, or by pure sliding, characterized by a force of definite magnitude in the directions of the movement of the wheel at the point of contact with the rail. We proceed first of all to indicate briefly in what way these two solutions differ from what really occurs and we then insist that a more accurate account of what is occurring should be proposed.
>
> In a separate section, we will indicate - and attempt to demonstrate - that the wheels progress both by rolling and by sliding and that the combined movement extends from the case of pure rolling, where there is no force, to the case of pure sliding, where the force reaches a maximum value.
>
> Case of a wheelpair in isolation. In discussing the effects of conicity of the tyres, it is necessary to discuss how a wheelpair behaves and to suppose that the wheels roll without sliding along the rails.

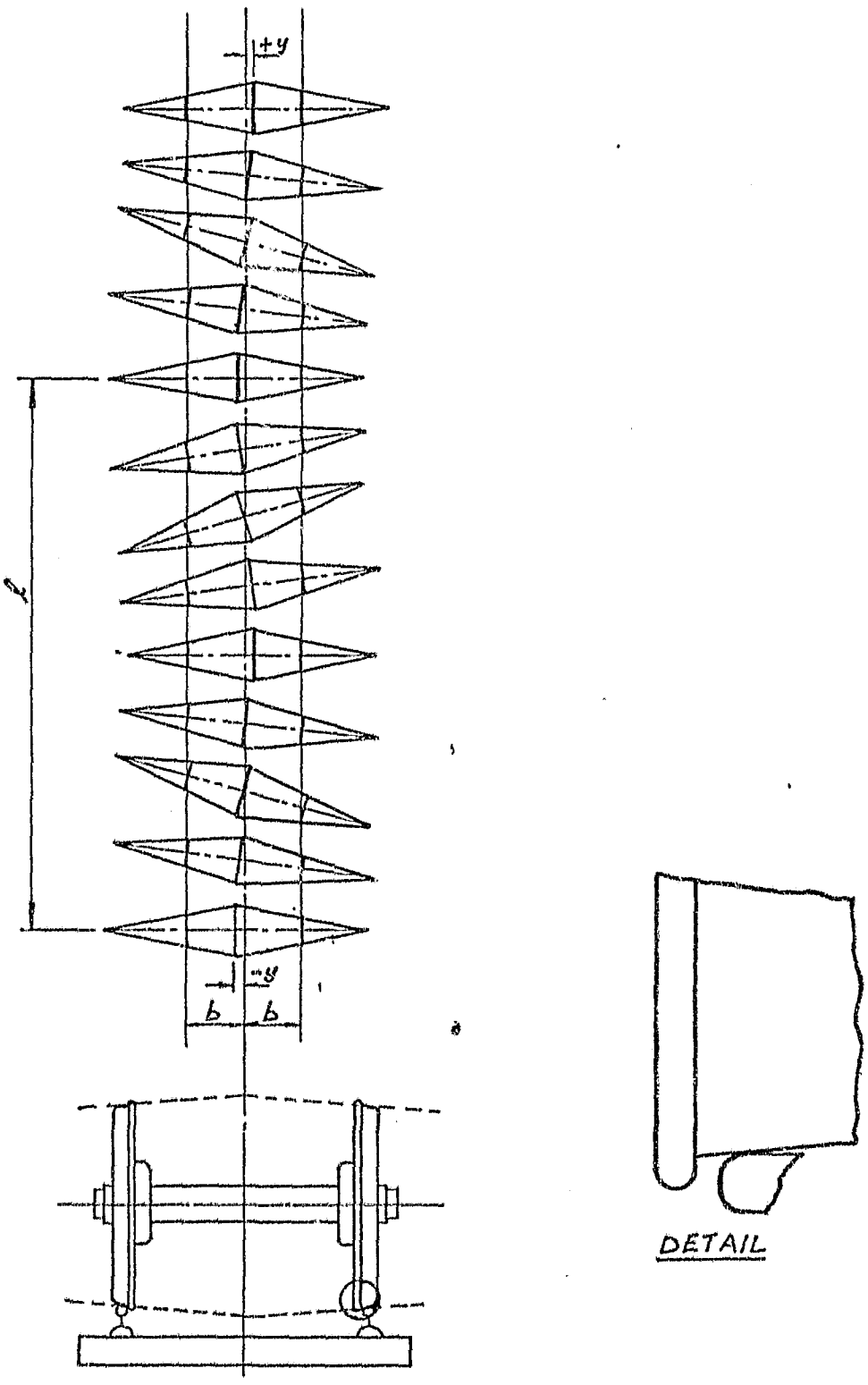

Figure 2 - 1. Sinusoidal Path of Wheelpair (with acknowledgements to Schutzbach [15])

Since the rolling radii are in general different, the trace O where the extension of the axis of symmetry of the wheelpair meets the plane in which the rolling occurs is at a finite distance ρ. On the basis that this hypothesis is adopted, the point O - being on the same straight line as the contact points P and Q, fixed at that instant of time - is equally fixed. It should be observed that the conicity of the tyres has been exaggerated in the figure for purposes of clarity. This

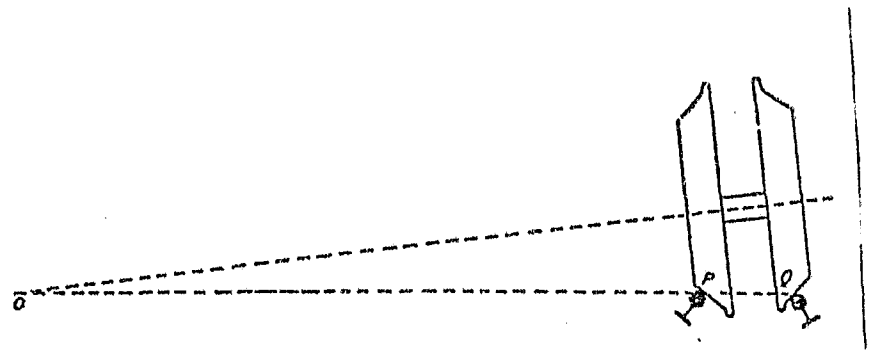

reasoning supposes in essence that the wheelpair behaves like a rigid body which is rolling without sliding along the two rails which are equally rigid.

Does this happen in reality? Yes, without question, if the movement of the wheelpair is extremely slow; but, if the velocity is no longer negligible then it is obvious that if the movement of the wheelpair is defined by the kinematic mode described, inertial forces would be experienced in the mass of the wheelpair since the motion is neither uniform nor in a straight line. These inertial forces would show themselves as forces applied to the rails in the plane of the rolling contact.

If the movement of the wheelpair remains the same at the velocities customary in practice as that required by the hypothesis stated previously, then this can only occur if the inertial forces do not in their turn cause any displacements, no matter how small these may be. Since nature yields no case where a force does not disturb the state of the system to which it is applied, it can be seen that the hypothesis of pure rolling does not account for the inertial forces which would arise.

As for the hypothesis of pure sliding, this is only possible if the forces of inertia, transferred to the plane of the rails, exceed the limits imposed by the coefficient of friction. Below this limit the problem is indeterminate as it is not sufficiently defined to make a solution possible.

The basis for the Klingel theory as generally given is that the displacements of the centres of the respective rolling circles are proportional to their radii if the wheelpair has moved away from the neutral position. It is convenient to quote the explanation given by Rocard:

> Let us take a single axle fitted with its two conical wheels, place it on rails, and cause it to roll. This is the problem of a double cone rolling on two wires (if we approximate the rails to wires), the double cone being formed by the rolling path of the two wheels. Let c be the conicity (1/20 is normal practice), $r + cy$ the radius at A and $r - cy$ the radius at B with r as a certain mean radius, finally $2h$ the distance between the rails (gauge). If the axle rolls through an angle $d\phi$ about its own axis, A advances by $(r+cy)d\phi$ and B by $(r-cy)d\phi$. As a result the point Q advances by $dx = rd\phi$ and the angle ψ increases by $d\psi$ (in this case negative) such that $2hd\psi$ = difference in displacements of A and B
>
> $$= -2cyd\phi = -\frac{2cy}{r}dx.$$
>
> Hence
>
> $$\frac{d\psi}{dx} = -\frac{cy}{rh}.$$
>
> However, $dy = \psi\, dx$ so that, differentiating the preceding equation, we find
>
> (20) $$\frac{d^2\psi}{dx^2} = -\frac{c}{rh}\frac{dy}{dx} = -\frac{c}{rh}\psi$$
>
> or
>
> (21) $$\frac{d^2\psi}{dx^2} + \frac{c}{rh}\psi = 0$$
>
> The same differential equation would be obtained for y. Consequently both, ψ and y, have a *purely sinusoidal oscillation* with a spatial period X to be found from
>
> (22) $$\frac{4\pi^2}{X^2} = \frac{c}{rh}, \text{ i.e. } X = 2\pi\sqrt{\frac{rh}{c}}.$$

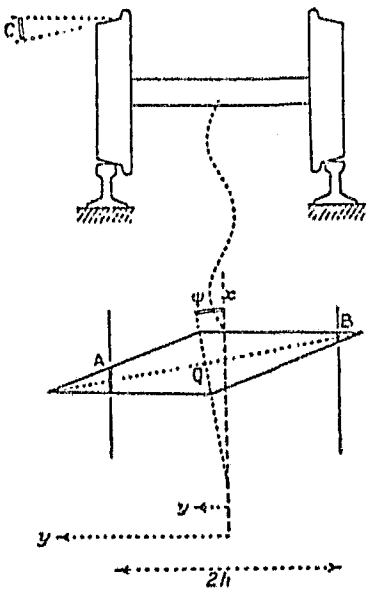

The theoretically predicted wavelength agrees remarkably well with that experienced in practice. This is illustrated by using the data given in Appendix 1 on page 178 where r = 0.085m, h = 0.124m and the conicity c = (Tan 5°) is 0.087. From these figures, the wavelength is $2\pi r$ x 4.08 or 12.82 wheel diameters. Anticipating the results to be discussed later in this work, the data listed in Table 7.5 on page 141 provides an interesting confirmation of this figure. If the revolutions per second are divided by the oscillatory frequencies, the number of revolutions per oscillation is obtained, and if this figure is multiplied by the wheel circumference, the length of rail traversed by the wheel pair during each oscillation would be obtained, thus if the figures in the third column are divided by the figures in the fifth column, the ratios are found to vary from $2\pi r$ x 3.80 for the lowest spin speed to $2\pi r$ x 4.73 for the highest spin speed. These figures provide the required wavelengths and it will be seen that there is remarkable agreement with the Klingel figure.

The Klingel theory therefore agrees surprisingly well with experimentally determined values: nevertheless, there are some difficulties in the analysis as given which should not be ignored. Thus, it is essential that the angle of yaw must decrease if the eventual differental equation is to have the desired form, yet this decision as it is given in the analysis

as it is given by Rocard is somewhat arbitrary, since no reason is advanced why this should be the case. At higher speeds, inertial forces would cause the wheelpair to move in the direction transverse to the rails but the Klingel theory does not offer any suggestions as to what forces would cause the transverse movement to occur at low speeds. What it does is to relate the distance through which the centre of the wheelpair shaft moves along the path of its motion at any instant to the radius of curvature of the path at that instant, but it offers no explanation how the length of this radius changes. If the theory were to be satisfactory, some explanation should be forthcoming.

Such an explanation is possible if it is recognised that as indicated earlier, the wheelpair moves in three-dimensional space; that is, not only can it yaw but it can tilt as well. Since the angle of tilt which is experienced by the wheelpair is small, its effect on the analysis which has been given is insignificant, but as the analysis to be given in Chapter 5 shows, any change in the angle of tilt,even if it is small, has a marked effect on the lateral displacement of the centre of mass of the wheelpair and therefore on the normal reactions at the points where the wheelpair contacts the rails.

Before continuing this explanation, it is useful to refer to an experiment quoted by Klein and Sommerfeld [16] to demonstrate how dry frictional forces would determine the movement of a uniform wooden stick placed on the outstretched index fingers of the demonstrator in such a way that the stick is horizontal. As the fingers are moved slowly towards each other, it is observed that the stick first moves in one direction and then in the other . This movement is caused by the fact that as the fingers move, the position of the centre of mass of the stick with respect to the supporting fingers alters, the normal forces change and therefore the respective dry frictional forces at these points change. The horizontal force at the finger towards which the stick is moving increases and reversal of the direction of the motion occurs as soon as the difference in the magnitudes of the frictional forces reaches the required level.

During the movement of the wheelpair, there is then at any instant a tangential displacement of the centre of the wheelpair along the path of its motion which corresponds to that which is the case if pure rolling occurred but at the same time there is a normal displacement caused by the difference in the frictional forces at the points of contact and it is this movement in the normal direction which produces the required change in the magnitude of the radius of curvature of the path. When the angle of tilt is at a maximum, the difference in the magnitude of the frictional forces is greatest, the direction of the transverse displacement reverses, reaches a maximum and then decreases again. A more adequate explanation of the observed motion is then possible, if it is acknowledged that the wheelpair both tilts and yaws.

CHAPTER 3

SURVEY AND DISCUSSION OF LITERATURE, PART 2 :

CREEP THEORY VIEWED AS A PARADIGM

How scientific theories develop and change has been discussed by a number of academic workers, such as Kuhn [17, 18] Popper [19] and Medawar [20]; thus, Kuhn argues that normal science is a tradition-bound activity, using text books to expound the body of accepted theory. This process constitutes what he designates a paradigm, but he then notes that there are 'scientific revolutions' when time-honoured scientific theories are rejected in favour of others which are incompatible with them. Kuhn's suppositions make it obvious why anyone who questions time-honoured theories would be labelled as someone who 'impugns all the other workers in the given field'. This is hardly accurate since what is being questioned is the theory and not the man who formulates it. Failure to tolerate free debate is an admission of weakness, not of strength.

Although the part played by creep forces in railway hunting has for the past sixty years been universally regarded as an acceptable (and thus time-honoured) part of theory., it is nevertheless possible to question whether the concept is so firmly based that its premises are not open to doubt. Thus, there are two significant omissions in the literature on creep in its relationship to railway hunting, the most important of which is the failure to recognise that what is being examined is a wheelpair. In its place, there is much speculation about what happens in the contact area between one of the wheels and the rail on which it rests. What is, however, of more significance is not what happens at the single contact area, but the interaction between the events

at the two separate areas of contact. This is not to suggest that the effect of creep at the individual wheel-rail contact area should not be investigated, but having done so, it would appear essential that the restriction placed on one's concepts by the existence of the other contact area should not be overlooked. The second omission is perhaps the consequence of changed views in recent years in pedagogy. It is now widely held that if one is to investigate the effect of the forces applied to any individual element in a given system, the first step to be adopted in the investigation is to show on a sketch of the element (the 'free body diagram') all the forces which could be supposed to act on it. In discussing the forces acting on the wheel, the literature on creep often refers vaguely to forces which may be imposed on it by spring connected masses instead of using a suitable diagramatic representation.

It is now appropriate to quote the initial proponent of the theory of creep, namely, Carter [21] :

> Interaction between Wheel and Rail. - There are three general modes of progress of a wheel on a rail, which may be designated respectively, rolling, slipping and creeping. The first is the natural function of the wheel and requires no explanation. The second also is readily apprehended as a form in which there is relative motion between wheel and rail at their point of contact. The third, however, is somewhat more recondite and requires explanation. The interaction between wheel and rail is really a very complicated one - the material in the region of the area of contact being strongly stressed. When the wheel simply rolls on the rail, the state of stress is symmetrical about the axial plane bisecting the area of contact and the resultant interaction is a simple pressure. If, however, as the wheel rolls, a force is applied to it in any direction tangential to the area of contact, the material in the region of this area is deformed, extended elements of one member being successively brought into contact with compressed elements of the other, with the visible result

that the wheel, besides rolling, creeps slowly in the general direction of the force. Thus a driving wheel makes a somewhat greater number of revolutions in a given distance than an idly running wheel of the same size, and the difference, considered in relation to the tractive effort, measures the creepage. As the tangential force is increased, a value is ultimately reached at which the surfaces in contact can no longer grip with sufficient intensity to transmit the force, and slipping then commences, continuing as long as the force is maintained. Conversely when the motion and the geometrical connections are such as to compel creeping as an accompaniment to the rolling of the wheels, a tangential force is set up at the contact face. The value of this force depends upon the rate of creeping as compared with that of rolling, until a certain limiting rate is attained, at which slipping commences, and the force becomes sensibly independent of the rate. Under ideally uniform conditions it is possible to conceive an abrupt transition from creeping to slipping, but with the unevenness of actual surfaces and the vibration of running the boundary between the two states is naturally indistinct.

Creepage. - It is convenient to define creepage as the ratio of the rate of displacement by creeping to the rate of displacement by rolling, and to adopt the word 'gliding' to include either slipping or creeping. With the above definition, the creepage, within limits set by the yielding of the material, is clearly proportional to the elastic deformation in the region of the interface and therefore to the tangential force between wheel and rail, at any rate for displacements in principal directions. If accordingly α and α' are components of creepage in the longitudinal and transverse directions respectively, the corresponding components of tangential force on the wheel may be written $-f\alpha$ and $-f'\alpha'$. No data are available from which to determine values of f and f', and although conjecture may set limits, there is difficulty even in obtaining a plausible estimate. It may, however, be assumed as the result of experience that the stresses

> involved in creeping are not in general sufficiently great to cause continuous yielding in the materials of the rail or wheel-rims. This limitation appears at first sight to reduce the possibility of creeping to a very small range, for from tests made on standard test pieces of the material, a permanent set is usually obtained at stresses of the order of 35,000 lbs. per sq. inch (2,500 kg. per sq. cm.), corresponding to a maximum recoverable strain of the order of 0.15 per cent. for each member, or a maximum creepage of 0.3 per cent. As is well known, however, the stresses in a well-ironed surface layer may greatly exceed those possible in a machined test piece, without fracture of the material; and a steel which would commence to yield at 35,000 lbs. per sq. inch in the mass, may be found to stand 150,000 lbs. per sq. inch without yielding if drawn into a wire of 1/10 inch diameter, whilst the amount of flexure that such a wire will stand without permanent set indicates an even greater limit of allowable stress in the surface layers. It would appear accordingly that there is nothing in the nature of steel to prevent creepage, even up to 1 per cent., when the surfaces have been well-ironed by use, and this is the order of most of the gliding motions incidental to progress along curves. Whilst therefore it may be necessary, in the interests of definiteness and in order to obtain limiting forces, to assume that the gliding motions on curves are of the nature of slipping, it appears not unlikely that creeping is the more normal condition and actual slipping somewhat exceptional.

Carter's views were eagerly seized upon and have dominated thinking in railway hunting since 1920. An explanation as to why the validity of his views were not questioned may be found in the fact that around that time, engineers had become increasingly aware of the necessity for becoming more familiar with the consequences of mechanical vibratory phenomena. An important element in the accompanying analysis of many of these investigations was the introduction of damping forces and these, fortunately, were generally found to be adequately represented by linear velocity dependent terms. For these

workers attempting to investigate the intricacies of railway hunting, Carter's hypothesis supplied the required velocity dependent element and this consideration may have assisted in making its general acceptance so wide-spread. Furthermore, the resulting linear equations were helpful in investigating the behaviour of the more complex assemblies involved in general vehicle suspension. However, these considerations apart, there are grounds for a more critical examination of Carter's hypothesis.

A detailed examination of his hypothesis yields the following observations:

. The first three sentences explain how Carter thought the wheels progressed over the rails. The explanation given in the previous chapter as to what was required for pure rolling to occur might be thought to be tedious pedantry but in light of the comments made by Carter would appear to be a elementary precaution to ensure that one's understanding of what constituted pure rolling was well founded. According to him, pure rolling was merely 'a natural function of the wheel', a phrase showing little real insight. His views on the state of stress in the contact area between the wheel and rail 'when the wheel simply rolls over the rail' were incorrect in that although the state of stress is obviously symmetrical about the axial plane when the wheel is stationary, this is not the case when the wheel is rolling, as will be seen if the following argument is considered. If the surfaces of the wheel and the supporting rail were ideally smooth, any force exerted on the wheel would as stated in a previous chapter cause it to slide bodily over the rail without rolling taking place. If the wheel is to roll, a tangential force must be applied to the wheel at the area of contact in the direction of the intersection of the plane of rolling and the plane in which the area of contact

lies so that the symmetry envisaged by Carter vanishes and the interaction is not a simple pressure, as claimed by him.

b. Two principal objections can be raised against the 'more recondite' type of motion envisaged by Carter, e.g.:

i. the hypothesis as established by him is generally vague and lacks clarity, thus:

'If, as the wheel rolls, a force is applied to it in any direction tangential to the area of contact.'

Apart from the necessity that a force must exist in the contact area for the wheel to roll, it would be helpful if if it were revealed how the proposed force was transmitted to the wheel.

ii. The basis for the hypothesis proposed by Carter is that as a consequence of the applied force, the material in the area of contact is deformed and that the wheel then creeps 'slowly' in the direction of the force. The key word here is 'slowly' and if the hypothesis is to be thought to be adequate, some form of numerical evaluation must be made possible to test its validity. A situation, which although not directly related to that envisaged by Carter, but which nevertheless is sufficiently similar for a comparison to be made is the belt-pulley situation which will now be described.

Several years after Carter had put forward his hypothesis, a paper was read by Swift [22] , in which the latter discussed the manner in which forces were transmitted by a belt wrapped around a pair of pulleys. Some sixty years previously,

Reuleaux [23] had attempted a classification of various machine elements. Both the wheel-rail and the belt-pulley systems (which are referred to on pages 171 - 173 of his book) are examples of what he called a higher pair of elements in which force closure is necessary, if the motion of the one element relative to the other is to be completely restrained and if there is to be no sliding. However, since friction is often a necessary counterpart of the closing force, the frictional force may prove to be insufficient to prevent sliding between the bodies and the force closure is then said to be incomplete. A pulley and that portion of the belt in contact with it (as in the case of the wheel and the length of rail in contact with it) constitute an incompletely constrained higher pair, and in this way is kinematically equivalent to a lower pair of elements, since there is movement between them. Here then is a situation which affords some measure of comparison whereby Carter's concept of 'slowly' may be evaluated.

Swift suggested that although the belt did not slip bodily over the pulley, if the ratio of the belt tensions on either side of the pulley, designated as T_1 and T_2, was less than $e^{\mu\alpha}$ (where μ is the limiting coefficient of friction and α is the angle of lap), nevertheless, reached its limiting value over an 'active' arc, less than α, as shown in figure a and that it was over this arc that T_1 was reduced to T_2. Because the belt is elastic, it stretches and, as a consequence,

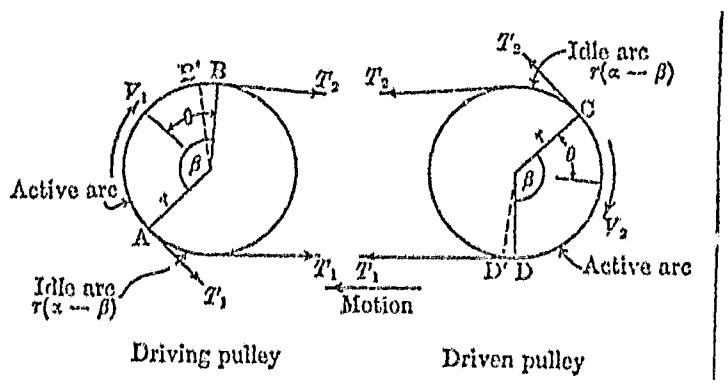

Figure a

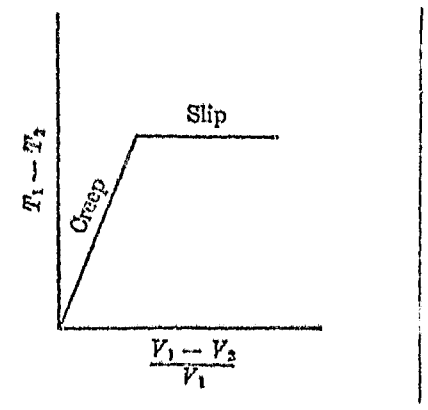

Figure b

'creeps'. Green [24] gives a summary of the theory developed by Swift, demonstrating that a relationship exists between the peripheral velocity of the driving pulley (V_1) and that of

the driven pulley (V_2) - where it is supposed that the pulleys are of equal diameter - and the belt tensions. As the power which is to be transmitted by the pulleys increases, the idle arc diminishes until $\beta = \alpha$, that is, the whole arc of contact becomes active. Having reached this condition, the belt starts to slip bodily over the pulleys, as suggested in figure b. In a numerical example, Green shows that for the particular conditions quoted by him, the loss of peripheral speed of the driven pulley is 1.2 per cent. This is an interesting figure in that it is now possible to conjecture what might be the order of magnitude of Carter's concept of 'slowly'. Not only is the rail much stiffer than the materials from which belts are generally made (the ratio of the moduli of elasticity would exceed 1000) so that the extension possible in the area of contact would be considerably less but, in addition, the length of the belt in the active arc would exceed greatly the length of the rail in contact with the wheel. If the loss of peripheral speed in the case of the driven pulley is of the order of 1%, then in the case of the wheel moving over the rail, it would be incomparably smaller. It would appear that in using the word 'slowly', Carter was sketching a type of motion, the effect of which was so small as to be negligible.

Many workers have subsequently been active in investigating creep theory, thus, basic work has been done by Johnson [25], Johnson & Vermeulen [26], and Kalker [27], while the results of this work have been applied to railway hunting by Wickens [28, 29], Brann [30], Bennington [31] and Royer [32]. A recent review of the research into the phenomenon of creep is given by Heinze and Albrecht [33], where much of the emphasis is on the work done in Europe. To make it possible to inspect this latter work, a translation of the paper is given in Appendix 5. (Since the primary aim of the translation is to provide an understanding of the essential philosophy on which creep theory is based, the mathematical development and some sections thought to be irrelevant for the pur-

poses of this discussion have been omitted.)

Several aspects of the paper by Heinze and Albrecht invite comment; thus, for example, it is believed, as proposed in the previous chapter, that in referring to the Klingel theory, it is incorrect to suggest that the mechanism involved is one of pure rolling and that, instead, it is thought to be a combination of rolling and sliding. The insistence that allowance must be made for 'spin' (that is, for rotation to occur about an axis normal to the surface of contact) is strange, if it is remembered that the primary purpose of this research is to determine, not the behaviour of a single wheel, but the behaviour of a pair of wheels. If the maximum amount of creep which is possible before the locked region vanishes is 1%, then since the length of the area of contact between the wheel and the rail is small, 1% of this short length is an appreciably smaller amount. The angular displacement of the wheelpair about an axis normal to the plane of the rails when the creep has reached its limit at both contact points would be the sum of these small amounts divided by the distance separating the areas of contact. One can only conclude that spin is of negligible practical importance. Another point is that if there is to be a locked region, then that part of the wheel in the locked region must at that instant of time be stationary with respect to the rail with which it is in contact. On the basis of kinematic considerations, it can be shown that this condition occurs only if the wheel has pure rolling motion over the rails and that this in turn is possible only if the wheelpair is in the neutral position, that is, if it is running mid-way between the rails. Lastly, it is worthy of note that the belief that in addition to the locked region, there is a region of creep strengthens the case put forward earlier in this chapter that it is possible to compare the wheel-rail and the belt-pulley systems.

The views of those later workers who, in their attempts to explain railway hunting, have based their equations of motion on creep forces may have been more sanguine of the extent of

its validity than its basic assumptions allow for, that is, in their eagerness to use creep theory, they may have overlooked certain of the limitations on which the theory was based. Moreover, it would appear possible that the theory itself has not been fully comprehended. In verbal and written discussions with those who defend the use of creep theory, one reaches the conclusion that if asked to support their views, their defence might take the following form:

1. Creepage does not pretend to explain the actual mechanism of what happens at the wheel-rail interface. It is simply a convenient and relatively simple way of describing certain macroscopic occurrences which have been observed experimentally. Coulomb's law of friction is a similar attempt to explain the behaviour at the interface under different conditions.

2. The creepage concept is an attempt to represent a particular phenomenon in terms of rigid body concepts, despite the admission that it is known that some deformation occurs. It is a recognition of the fact that if a wheel rolls and at the same time, it is subjected to forces normal to the plane of rolling, it will creep in the lateral direction. It is insisted that such a phenomenon does occur and the fact that such is the case, makes it possible to establish the magnitudes of the creep coefficients.

These comments are given, because it is suspected that they are surprisingly widely held. The first claim apparently suggests that, somehow, in investigating the dynamics of railway hunting, dry frictional forces are not possible and that in their place, creep forces occur. This is strange if it is noted that the words 'in the presence of dry friction' occur in the title of the thesis (presently held to be the

authoritative guide to creep theory) which was submitted by Kalker to Delft Technological University* [27]. Furthermore, Kalker took painstaking care to attempt to understand what happened at the wheel-rail interface. However, he did emphasize that the theory of the 'locked region' which he put forward was valid only for limited amounts of creep. What is contended in this work is that the conditions under which hunting occurs are outside these limits within which the Kalker theory is valid. This contention will be discussed further in the next chapter.

If it can be shown with regard to the second claim that the lateral displacement or creep of a wheel under the application of a sideways force is unlikely to occur, one is led to suspect that the claim to universal validity is, after all, not so well founded and that instead, it fails to consider other possibilities. Although this has been said earlier in this chapter, it is necessary to reaffirm that it is not a single wheel which is under consideration. Instead, it is a pair of wheels solidly locked through a common axle. Suppose that the wheelpair is moving at constant velocity along a horizontally laid, straight track and that it is in the central position mid-way between the rails. The forces on the wheelpair would be as shown in figure 3.1. Because the velocity of the centre of mass of the wheelpair is constant and in a direction parallel to that of the rails, the forces acting on the wheelpair must be in static equilibrium. The tangential forces in the directions of the rails at the points of contact must be equal and opposite to the forces acting on the wheelpair shaft bearings and together they form a couple which opposes the bearing and rolling frictional moments. The normal forces at the two points of contact can be separated into vertical and horizontal components where the sum of the vertical components equals the weight of the wheelpair (and attachments such as the bearings),

---

*. The full title of the thesis is 'On the Rolling of Two Elastic Bodies in the Presence of Dry Friction'.

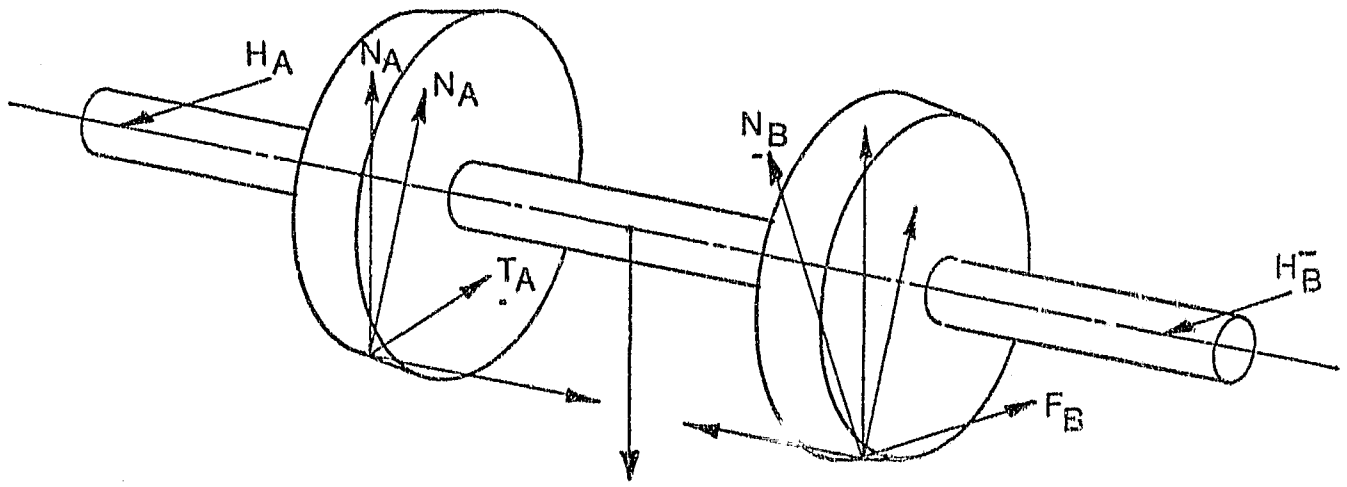

FIGURE 3.1 - FREE BODY DIAGRAM SHOWING FORCES ON WHEELPAIR MIDWAY BETWEEN RAILS

while the horizontal components are equal to each other in magnitude and opposite in direction. If it were a physically observable fact that the wheels undergo creepage, the lateral displacements would be in opposite directions, but since it is an assumption that the wheelpair is rigid, this is not possible. This flaw in the logical development goes back to the belief that each wheel can be viewed as a separate entity.

In concluding this argument, there is obviously a possibility that there could be some conflict of opinion as to what is physically observable. This work has an advantage in this respect in that as far as a survey of the literature shows, it would appear that the test rig constructed here is the only rig on which a wheelpair is able to move without any restraint being placed on it as to the extent to which it can yaw and/or tilt. For that reason it has been possible to actually observe the wheelpair movement and not to rely on speculation as to how the wheelpair might move. Observations made of how a wheelpair moves on a roller rig, for example, will not give much guidance; thus, as the discussion in chapter 1 shows, the path of contact between the wheels and the supporting rollers, as the wheelpair yaws, is not along a straight line, as would be the case if it were moving along a straight pair of rails. An even stronger objection to the use of roller rigs is based on the changes in the directions of the normal forces. As the wheelpair travels along a straight pair of rails, the normal forces remain in what was described by Carter as the axial plane, that is, the plane at right angles to the plane of the rails in which the points of contact between the wheels and the rail, the wheelpair centre of mass and the centreline of the shaft are situated. As can be seen from figure 1.3, the directions of the normal forces between each wheel and the roller on which it rests, after yawing, will no longer lie in the axial plane. If the force situation on a roller rig is unlike that which occurs in the wheels-rails system it is intended to simulate, how is it

possible for valid comparisons to be made? To obviate this disadvantage, one might have recourse to restrict the possible angles of yaw of the wheelpair but this would then defeat the object of the exercise. Nor is it really adequate to base one's observations on the behaviour of a wheelpair in a bogie since how is one to know the effect of the interaction between the separate wheelpairs?

Having made these points, it is possible to assert that several aspects of the experimental work reject the possibility that creep could be of significance in determining the oscillatory behaviour of the wheelpair. The wear pattern on the bands simulating the rails with a dicone with a taper angle of 30° (which will be discussed in chapter 6) showed clearly demarcated zones where there was pure rolling and where a difference in surface velocities caused scuffing to occur between the dicone and the bands. Creep theory would shed no light on such behaviour. Moreover, according to creep theory, a change in the character of the driving surfaces would cause the oscillatory behaviour of the wheelpair to alter. No such change was observed which is contrary to what creep theory would predict. Summing up then, it can be conjectured that the phenomenon of creep is important during that extremely brief transitional period when the wheelpair breaks away from pure rolling in the neutral position and then proceeds to slide with diminished spin speed from side to side across the rails. Why and how this break occurs is, at this stage, not at all clear. Should an adequate explanation be forthcoming as to the cause of the transition, it would constitute an important advance in understanding wheelpair behaviour. The present work restricts itself to a recognition that the transition occurs and to the investigation of the character of the oscillatory behaviour.

CHAPTER 4

REVIEW AND DISCUSSION OF LITERATURE, PART 3:

A DISCUSSION OF THE DERIVATION OF THE EQUATIONS OF MOTION AND SOME OTHER TOPICS

In examining the literature on railway hunting, it is noteworthy that, apart from the common feature that creep forces are invariably referred to, there is a wide variation in the manner in which the equations of motion for the wheelpair as it travels along a straight pair of rails have been developed, whereas one might have expected that a more or less standard form would have evolved. The aim of this chapter is to comment on several of these procedures and then to refer briefly to other relevant topics mentioned in the literature.

Before discussing the derivations referred to, it is useful to examine two figures taken from Wickens [28]:

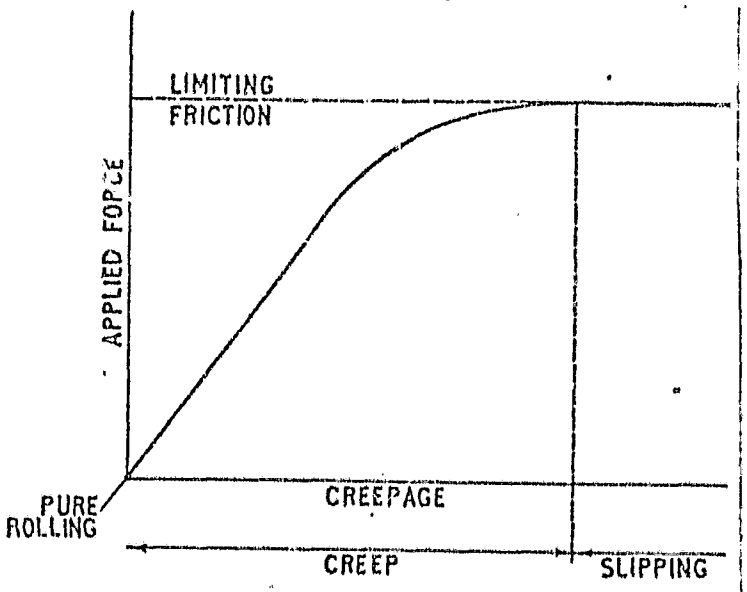

The relationship between longitudinal creepage and longitudinal creep force, for constant values of lateral creepage and spin

Figure a

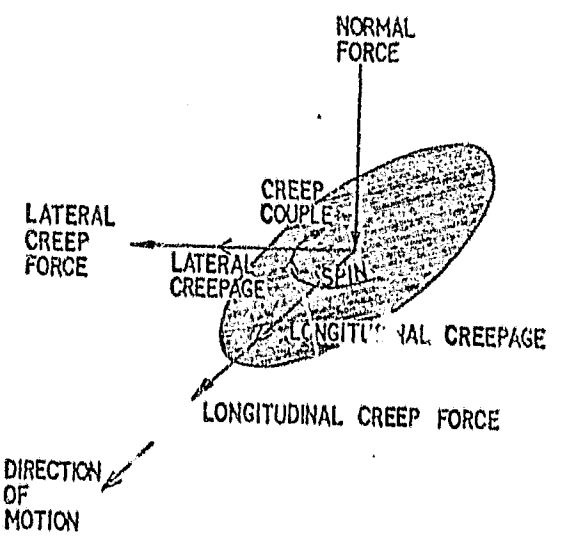

Deviations from a pure rolling motion can be described in terms of longitudinal creepage, lateral creepage, and spin. These quantities give rise to corresponding creep forces and a couple.

Figure b

Figure a shows the relationship between creepage and applied force, while figure b illustrates how Wickens conceives the various forces, as well as a creep couple, to exist in the contact area between the wheel and the rail. A belief that a creep couple will exist is a logical development if it is

believed that spin exists in the contact area; nevertheless, in view of the small size of the contact area, it is difficult to envisage how such a creep couple could have a magnitude of any significance. The linear relationship, where the slope is a function of the elastic constants of the wheel and the rail, their curvatures and the normal reaction, is of crucial importance since it is this linear relationship upon which reliance has been placed in developing the equations of motion. As the figure shows, the region of creep is not extensive and the straight line regime is appreciably less in extent. The question then to be faced is how far the existence of the straight line portion justifies its extensive use in formulating the equations of motion.

In order to answer the question just raised, it is necessary to see how creep forces have been formulated so that they may be inserted in the equations of motion. Here, a further innovation is found, namely, that whereas creep theory itself was concerned with elastic body theory (and as a consequence, with elastic body deformations), in the application of the theory it has been thought appropriate to make use of kinematic displacements in order to determine the creep forces. Thus the argument used by Wickens [8] runs as follows: First, longitudinal and lateral creeps are defined; taking the lateral creep γ^1 as an example:

$$\gamma^1 = \frac{\text{Actual lateral displacement - pure rolling lateral displacement}}{\text{Forward displacement attributable to rolling}}$$

$$= \frac{dq_1 - q_2\, Vdt}{Vdt}$$

$$= \frac{q_1}{V} - q_2$$

The lateral creep force is then given as f^1 where f^1 is the lateral creep coefficient (that is, the constant of proportionality relating the creep force to the amount of creep), hence:

$$\text{Lateral creep force} = -f'\left(\frac{q_1}{V} - q_2\right)$$

According to this equation, the lateral creep force is a constant multiplied by the difference between the ratio of the lateral velocity and the forward speed of the centre of the wheel-set and the angle of yaw. Since these are kinematic quantities, it has to be considered whether this relationship is compatible with the premises on which creep theory was based.

The justification, for example, for the concept of rigid bodies (as customarily followed in dynamics) lies in the fact that the kinematic displacements of most bodies, if allowance is made for elastic distortion, differ from those which would occur if the bodies were thought to be rigid by an amount whose order of magnitude, if compared with the kinematic displacements, would be sufficiently small so as to justify their neglect. Although creep theory has been based on elastic body theory, in the application of creep theory, kinematic displacements are used, which are of a completely different order of magnitude to the elastic deformation on which the theory itself has been founded. This, in turn, aggravates considerably the restriction that the theory is valid only within a limited range, a range which from the point of view of kinematic displacements, (as was the case used in the argument justifying rigid body theory) would appear to be negligible.

The manner in which creep theory has been used in deriving the equations of motion is best seen by examining the procedures followed by some of the various workers; the derivations by Wickens [299, Brann [30 and Benington 31] have been used for this purpose and in order to facilitate a comparison, the appropriate pages from these papers are reproduced in Appendix 6. Each derivation will be considered briefly and individually, and an attempt will then be made to find common ground between the various derivations. For the purposes of this discussion, the validity of the concept of

creep forces has been accepted.

Looking at the first of the derivations, that by Wickens, it is seen that several equations are quoted as having been originally formulated by other workers and for that reason, it would appear that this derivation is more broadly based than the others; further, it will be noted that equations 2a - 4b are aimed at obtaining a relationship between the running radius of the wheel and the natural displacement q_1. Although the wheel tread and the rail head are assumed to be curved, the relationship is eventually approximated to that of a uniformly tapered rolling surface so that the additional equations are to some extent misleading. It could also be argued that in practice since R is very much greater than R', the effective conicity is for all practical purposes equal to λ. A possible objection to the derivation of the normal reaction N and N' is that in deriving the generalised force Q_1, a term involving the vertical displacement of the centre of mass of the wheelpair has been included. If it is thought necessary to include this term in the relationship for Q_1, why is its second derivative ignored in the equation for N and N'?

Turning to the analysis made by Brann, the following comments may be made on his free body diagram (which has been reproduced here with certain additions):

a. Since the point of contact between the right hand wheel and the rail on which it rests is incorrectly shown in the original drawing, the intersection of the plane of the rails - which presumably passes through the points of contact - is wrongly placed. This in turn means that the angle of tilt is much less in the correct version.

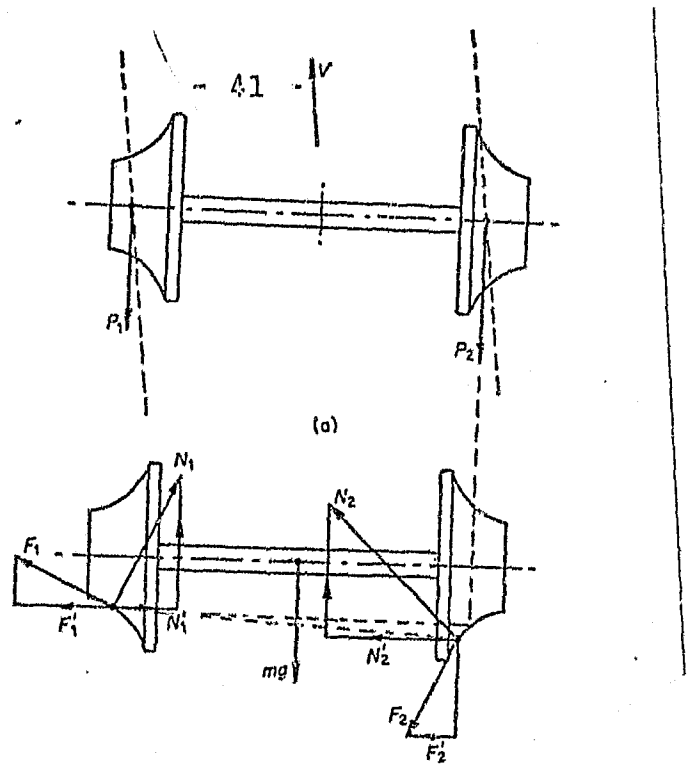

b. In this work, it is believed that the only forces in the plane of the rails act in the direction of the rails. According to Brann, however, these forces act in the direction in which the wheelpair is moving. It would have been helpful if reasons had been given for this choice of direction.

c. Although N_1 and F_1 are at right angles to each other - which would appear to be correct - this procedure has not been followed with N_2 and F_2.

d. No forces are shown to act on the wheelpair shaft and since the wheelpair would then be unable to turn, it is not clear why these forces have been omitted.

Because Brann has interpreted the forces acting on the wheelpair differently from Wickens, the resulting equations of motion are different. The same is true in the last of the analyses namely, that by Bennington, where there is a strange choice of generalised coordinates. No recognition appears to have been given by him to the constraints on the wheelpair, that is, that its running surfaces must remain in contact with the rails at all times. For this reason it would seem that q_1 and q_3 are related to each other, and since they are not independent, they should be combined.

This would reduce the equations numbered 1 - 4 to 3. As the last of these equations determines the wheelpair motion about its centreline, the remaining equations would then correspond to the number used by Wickens and Brann. The equations derived by Bennington are then not comparable in their present form with the other sets of equations.

The equations derived by Wickens and Brann are most easily compared when arranged in matrix form, where the symbols for the variables are those used by Wickens. A further discussion of the matrix coefficients is made in chapter 8. The first set of equations is that derived by Wickens while the second set is that derived by Brann:

$$\begin{bmatrix} M & 0 \\ 0 & C \end{bmatrix}\begin{bmatrix} \ddot{q}_1 \\ \ddot{q}_2 \end{bmatrix} + 2\begin{bmatrix} d_2+\frac{f'}{V} & 0 \\ 0 & d^2d_1+\frac{f}{V} \end{bmatrix}\begin{bmatrix} \dot{q}_1 \\ \dot{q}_2 \end{bmatrix} + 2\begin{bmatrix} k_2+\frac{We}{2\ell} & -f_1 \\ \frac{f\lambda\ell}{r_o} & d^2k_1 \end{bmatrix}\begin{bmatrix} q_1 \\ q_2 \end{bmatrix} = \begin{bmatrix} 0 \\ 0 \end{bmatrix}$$

$$\begin{bmatrix} M & 0 \\ 0 & C \end{bmatrix}\begin{bmatrix} \ddot{q}_1 \\ \ddot{q}_2 \end{bmatrix} + f\begin{bmatrix} k & 0 \\ 0 & \frac{\ell}{V^2r} \end{bmatrix}\begin{bmatrix} \dot{q}_1 \\ \dot{q}_2 \end{bmatrix} + \begin{bmatrix} \frac{mg}{2}\Sigma e_s Y^{2s+1} & -fk \\ 0 & 0 \end{bmatrix}\begin{bmatrix} q_1 \\ q_2 \end{bmatrix} = \begin{bmatrix} 0 \\ 0 \end{bmatrix}$$

It is not unreasonable to suppose that if the same comparisons were made with equations by other workers, a similar difference in the matrix equations would be found. This is a serious matter, since in effect, the matrix coefficients are the raw data which these workers use as a basis to test various theoretical procedures. If there is no agreement about the raw data, the effectiveness of these developments is open to some doubt and it would seem appropriate that attention should be given to securing a widely accepted set of equations of motion. If agreement were then possible, subsequent comparisons would be facilitated.

Turning from the equations of motion, other topics raised in the literature warrant brief examination, thus:

Royer [32] who based his theories on creep, proposed that the torques at the respective wheels of the wheelset would change as the rolling radii and the creep forces altered. Because of the differences in the torques at the wheels, the axle joining the wheels would twist, and potential energy would then be stored in the axle. This energy would be partly released as heat but the balance would be transformed into kinetic energy. As the wheelpair kinetic energy increased, a stage of instability would be reached. This theory appeared initially to be quite plausible and as a consequence an attempt was made early in the experimental program described here to test its validity by using a flexible shaft. Faith in the theory was, as a result of the experience then gained, lost and since the incorporation of a flexible shaft was thought to be an unnecessary and unjustified complication, work in this direction was consequently abandoned.

An interesting confirmation of the comments made earlier in the discussion of the theory of creep is contained in the paper by Savage and Loewenthal [34] which dealt with an investigation into the requirements necessary for the kinematic stability of wheelpairs in free rolling contact. It was found that unless the rollers ran true (that is, in their plane of contact without axial displacement), axial thrusts occurred. Certain kinematic corrections could then be used to cause the rollers to return to the pure rolling position.

Some of the features of the methods used in this work to determine the position of the centre of mass of the wheelpair are foreshadowed in an analysis put forward by Lomonosoff [7]. Unfortunately this author failed to develop his ideas very far and there are considered to be strange basic errors in his work. The figure used by him to demonstrate the gravitational restoring force is reproduced at twice its original size in Figure 4.1(a). What according to the data given in the figure should be the

centre line between the points of contact, has been placed to the left of the correct position; furthermore, Figure 4.1(b) is an explanatory diagram which shows that Lomonosoff has chosen a dicone, the proportions of which are such that the centre of the circle passing through the points of contact B and B_0 coincides with the centre of mass of the dicone. As shown in Figure 5.5 of Chapter 5, this is not generally the case.*

His conclusions based on the assumption that only gravity forces needed consideration, is that the restoring forces is negligible and he then says:

> The axis of the wheels is always parallel to a ruler placed across the rail heads, ie, it is normally horizontal.

It will be shown that although the angle of tilt may be small, it is nevertheless of great importance in deciding the character of the motion of the wheelpair. Lomonosoff's error lies in not recognising that dynamic forces could be far more influential in their effect on the motion of the wheelpair as compared with the relatively small gravitational force envisaged in his analysis. The experimental work to be discussed in a subsequent chapter confirmed that the transverse forces experienced during the cyclic motion of the wheelpair are far from negligible.

---

* Lomonosoff used the diagram to show that

$BH = (e+y)\,\mathrm{Tan}(\mu-\psi) = (e-y)\mathrm{Tan}(\mu+\psi)$

He then states that

$\mathrm{Tan}\psi = \frac{y}{e}\mathrm{Tan}\mu$

Instead, the correct relationship is

$\mathrm{Sin}2\psi = \frac{y}{e}\mathrm{Sin}2\mu$

On approximating, the end result is the same.

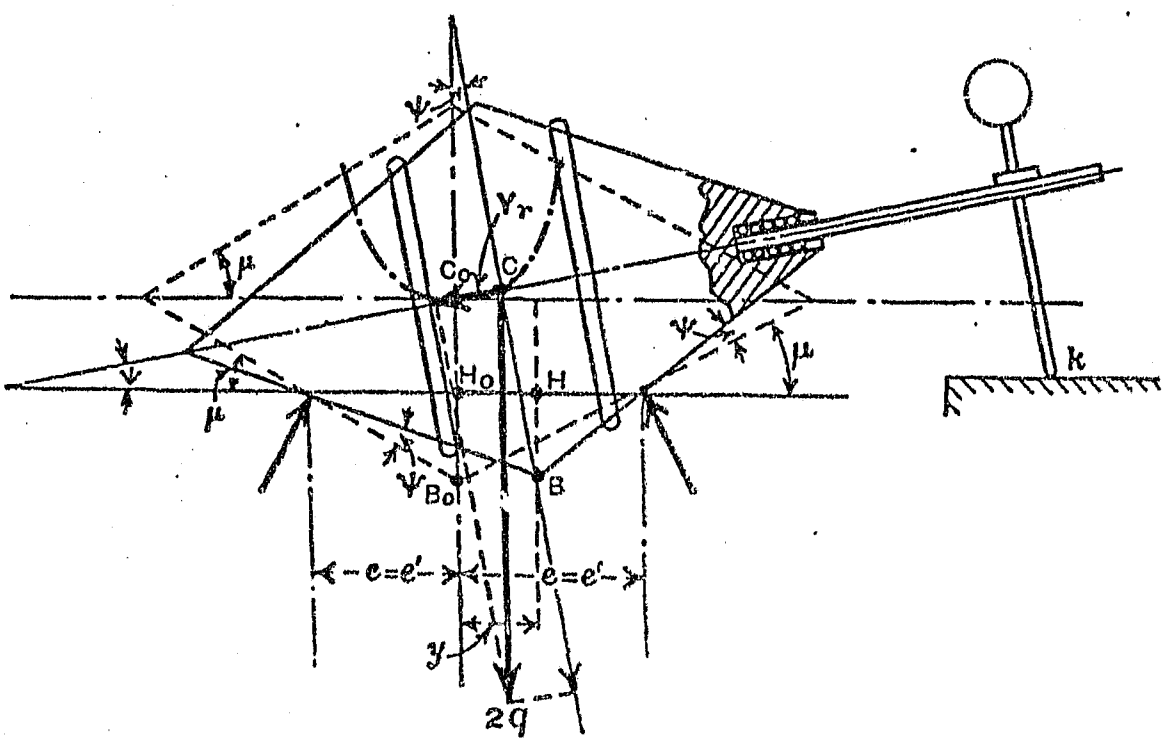

Figure 4.1(a): LOMONOSOFF'S FIGURE OF DICONE MOTION [7]

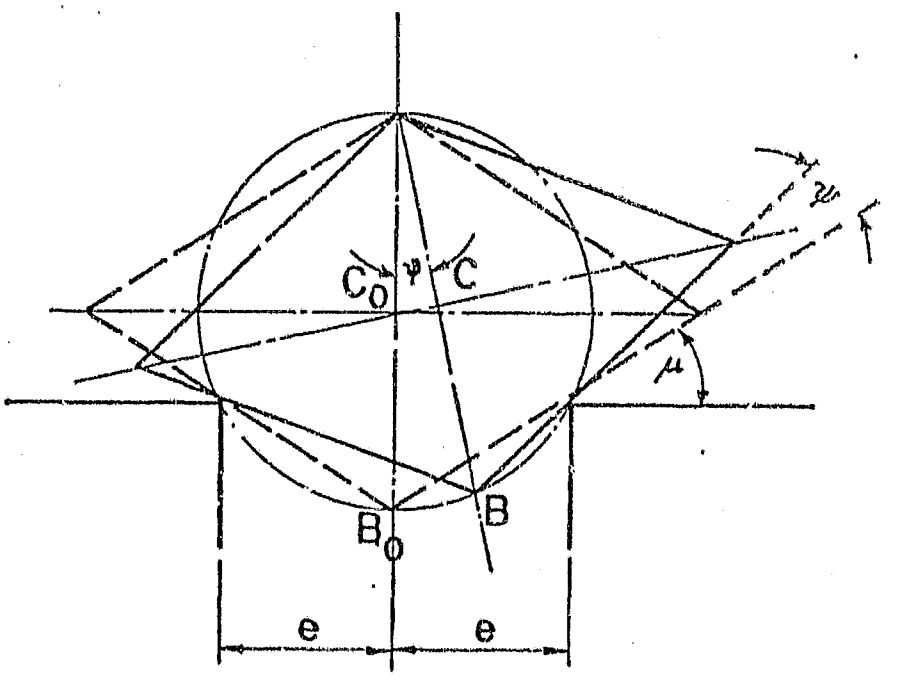

Figure 4.1(b): EXPLANATORY DIAGRAM FOR FIGURE 4.1(a)

In concluding this last section of the review and discussion of the literature, this chapter has examined how creep theory has been applied to the formulation of the equations of motion by various workers. Examples of such formulations have been quoted and commented on. After this, the equations have been arranged in matrix form so as to compare them in chapter 8 with the matrix equations derived from the linearised forms of the equations developed in the next chapter. Finally, there are comments from the literature which were thought to be relevant to this thesis.

CHAPTER 5

THE DERIVATION OF THE CHARACTERISTIC EQUATIONS OF THE WHEELPAIR - RAILS - RESTRAINING SPRINGS SYSTEM

5.1 INTRODUCTION

The model of the dynamic systems envisaged in this work was discussed in the first chapter; that is, it is a wheelpair with uniformly tapered running surfaces, which is caused to rotate through contact with two parallel moving rail simulating surfaces; translation of the wheelpair in the direction of travel of the rail surfaces is to be restricted by horizontal springs attached to sleeves able to slide freely along the wheelpair shaft; and there is no gravity force other than that of the wheelpair itself. As a conceptual device, the wheelpair will be considered as if it were a dicone.

Apart from the fact that the dicone can rotate (or spin) about its axis of symmetry, it has three degrees of freedom; that is, it has translatory freedom of movement in the direction of the tracks, it can tilt or rotate about an axis nominally in the direction of the tracks, and it can yaw about an axis which is nominally vertical.

5.2 DEFINITION OF THE SYSTEMS OF COORDINATE AXES

Before describing the various coordinate axes systems shown in Figure 5.1, it is necessary to mention that since the rails are used as the reference points in a fixed space, the position of the centre of mass of the uniform homogenous dicone will alter in accordance with the way its position has changed in the fixed space. In the position of rest, the position of the centre of mass is designated as O_S. If the rail simulating surfaces move, the dicone moves to a position where the forces in the restraining springs are equal and opposite to the frictional forces between the dicone and the rail simulating surfaces. The centre of mass is then at O; after yawing and tilting, the centre of mass will be at O' and O'' respectively (The actual displacement of the centre of mass will be discussed in Section 5.4.) Parallel systems of coordinate axes systems will exist at the three origins, O, O' and O''.

The three coordinate axes systems conform to the positions of the body fixed axes systems in each of the three possible cases. In the $Ox_1x_2x_3$ system, the Ox_2 axis would coincide with the direction of the spin axis of the dicone while the Ox_1 axis is in a horizontal plane. After the wheelpair has yawed, the body fixed axes system would be $O'\eta_1\eta_2\eta_3$ (with $O'\eta_1$ remaining in a horizontal plane) and if the wheelpair then tilts, the coordinate axes system would be $O''\xi_1\xi_2\xi_3$, with $O''\xi_1$ again remaining in a horizontal plane. Figure 5.1 shows how the rotations take place from one system to the next where, for convenience, the parallel axes systems with the origins at O are shown. The various coordinate axes systems make it possible to establish the position of any point in the dicone at any stage in its motion.

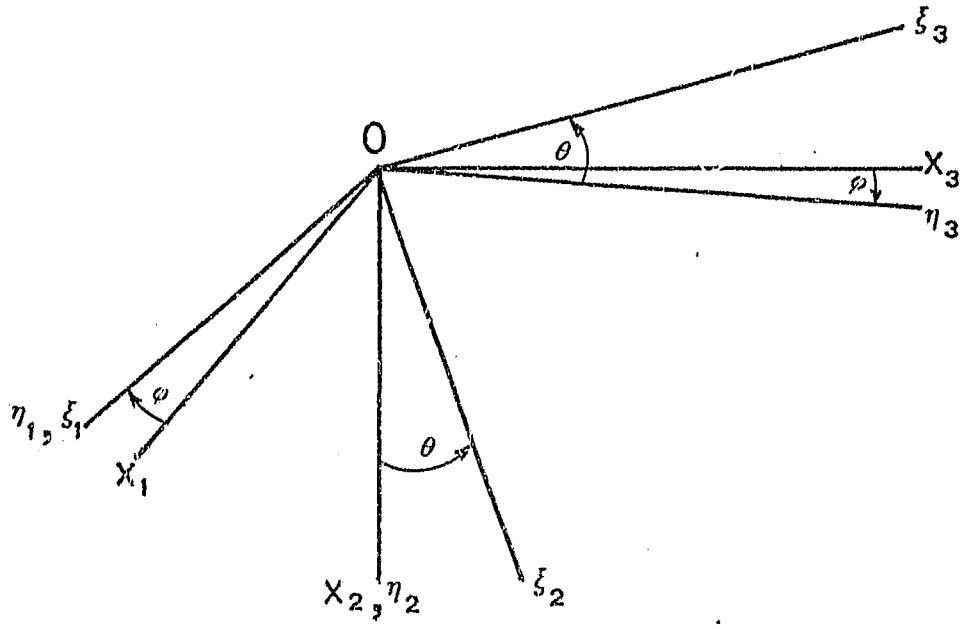

Figure 5.1: COORDINATE AXES SYSTEMS

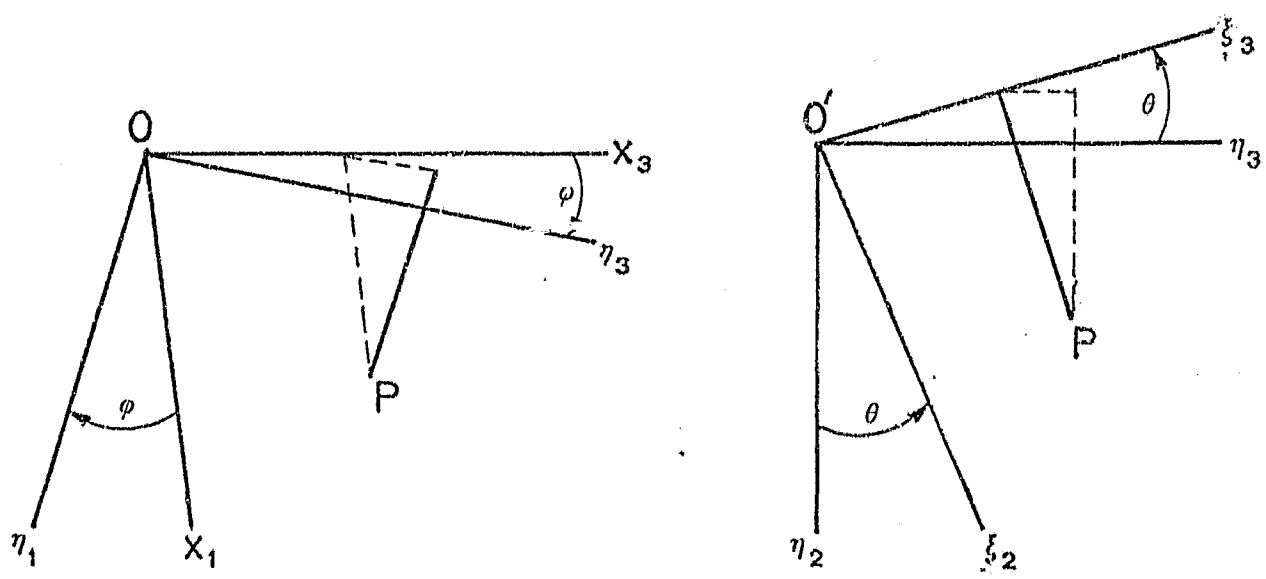

Figure 5.2: COORDINATE AXES RELATIONSHIPS

As has been explained, the dicone rests on two horizontal rail simulating surfaces. For the purposes of this analysis, these are not surfaces but lines, since it is assumed that there is point contact between the dicone and the supporting surfaces, or rails, as they will be referred to in the subsequent discussion.

5.3 DERIVATION OF THE COORDINATE AXES MATRICES FOR THE CASE WHERE THE ORIGINS COINCIDE

The origins of the three coordinate axes frames are made to coincide in Figure 5.1, while Figures 5.2(a) and 5.2(b) show the relationships between the coordinates in the various frames when this has been done. As explained in the previous section, the centre of mass of the dicone would move from O to O'. In terms of the systems of coordinate axes, this movement takes place by rotating the $Ox_1x_2x_3$ axes system about the Ox_1 axis through an angle ϕ into the $O'\eta_1\eta_2\eta_3$ coordinate axes system, and in so doing the dicone settles deeper between the rails. If the origins were to coincide, as shown in Figure 5.2(a), the relationships between the two systems of coordinates would be:

$$\eta_1 = x_1\text{Cos}\phi - x_3\text{Sin}\phi \qquad x_1 = \eta_1\text{Cos}\phi + \eta_3\text{Sin}\phi$$

$$\eta_3 = x_1\text{Sin}\phi + x_3\text{Cos}\phi \qquad x_3 = -\eta_1\text{Sin}\phi + \eta_3\text{Cos}\phi$$

After the yawing movement, the dicone tilts and the centre of mass moves from O' to O''. (The way in which this takes place will be discussed in Section 5.4.3.) In terms of the coordinate axes systems, the $O'\eta_1\eta_2\eta_3$ coordinate axes system rotates about the $O'\eta_1$ axis through an angle θ into the $O''\xi_1\xi_2\xi_3$ coordinate axes system. Again, if the origins were to coincide, the coordinates in the two systems

would be given by:

$$\xi_2 = \eta_2\text{Cos}\theta + \eta_3\text{Sin}\theta \qquad \eta_2 = \xi_2\text{Cos}\theta - \xi_3\text{Sin}\theta$$

$$\xi_3 = -\eta_2\text{Sin}\theta + \eta_3\text{Cos}\theta \qquad \eta_3 = \xi_2\text{Sin}\theta + \xi_3\text{Cos}\theta$$

Hence

$$\begin{bmatrix}\xi_1\\ \xi_2\\ \xi_3\end{bmatrix} = \begin{bmatrix}1 & 0 & 0\\ 0 & \text{Cos}\theta & \text{Sin}\theta\\ 0 & -\text{Sin}\theta & \text{Cos}\theta\end{bmatrix}\begin{bmatrix}\eta_1\\ \eta_2\\ \eta_3\end{bmatrix} = \begin{bmatrix}1 & 0 & 0\\ 0 & \text{Cos}\theta & \text{Sin}\theta\\ 0 & -\text{Sin}\theta & \text{Cos}\theta\end{bmatrix}\begin{bmatrix}\text{Cos}\phi & 0 & -\text{Sin}\phi\\ 0 & 1 & 0\\ \text{Sin}\phi & 0 & \text{Cos}\phi\end{bmatrix}\begin{bmatrix}x_2\\ x_2\\ x_3\end{bmatrix}$$

$$= \begin{bmatrix}\text{Cos}\phi & 0 & \text{Sin}\phi\\ \text{Sin}\phi\text{Sin}\theta & \text{Cos}\theta & \text{Cos}\phi\text{Sin}\theta\\ \text{Sin}\phi\text{Cos}\theta & -\text{Sin}\theta & \text{Cos}\phi\text{Cos}\theta\end{bmatrix}\begin{bmatrix}x_1\\ x_2\\ x_3\end{bmatrix}$$

or $\bar{\xi} = \bar{\bar{L}}\bar{x}$

where $\bar{\bar{L}}$ is the rotation matrix.

Alternatively,

$$\begin{bmatrix}x_1\\ x_2\\ x_3\end{bmatrix} = \begin{bmatrix}\text{Cos}\phi & 0 & \text{Sin}\phi\\ 0 & 1 & 0\\ -\text{Sin}\phi & 0 & \text{Cos}\phi\end{bmatrix}\begin{bmatrix}1 & 0 & 0\\ 0 & \text{Cos}\theta & -\text{Sin}\theta\\ 0 & \text{Sin}\theta & \text{Cos}\theta\end{bmatrix}\begin{bmatrix}\xi_1\\ \xi_2\\ \xi_3\end{bmatrix}$$

$$= \begin{bmatrix}\text{Cos}\phi & \text{Sin}\phi\text{Sin}\theta & \text{Sin}\phi\text{Cos}\theta\\ 0 & \text{Cos}\theta & -\text{Sin}\theta\\ -\text{Sin}\phi & \text{Cos}\phi\text{Sin}\theta & \text{Cos}\phi\text{Cos}\theta\end{bmatrix}\begin{bmatrix}\xi_1\\ \xi_2\\ \xi_3\end{bmatrix}$$

or $\bar{x} = \bar{\bar{L}}^{-1}\bar{\xi}$

5.4 DISPLACEMENTS OF THE CENTRE OF MASS OF THE DICONE AFTER THE VARIOUS ROTATIONS

5.4.1 Positions of the points of contact between the dicone and the rails

The positions of the points of contact between the dicone and the rails now have to be established since once this is known the position of the centre of mass of the dicone can be determined. This information is obtained from Figure 5.3, where projections are shown of the right-hand half of the dicone before and after yawing.

These projections show that contact occurs along the generator of the cone joining the cone vertex to the lowest point on the dicone base; that is, in planes normal to the plane in which the rails lie. Since it has been required that the Ox_1 axis, the $O\eta_1$ axis and the $O\xi_1$ axis should always lie in a horizontal plane, the planes normal to the listed axes will always be vertical. The centre of mass of the dicone and the points of contact will lie either in the Ox_2x_3 plane, the $O\eta_2\eta_3$ or the $O\xi_2\xi_3$ planes.

5.4.2 Position of the centre of mass of the dicone after rotation about the Ox_2 axis; that is, after yawing has occurred

In the auxiliary projection of Figure 5.4, it is seen that the yawing of the dicone causes the dicone to settle deeper between the rails. The centre of mass changes its height above the rails as follows:

Height of centre of mass above rails before yawing

$$= -(R-b\text{Tan}\alpha)$$

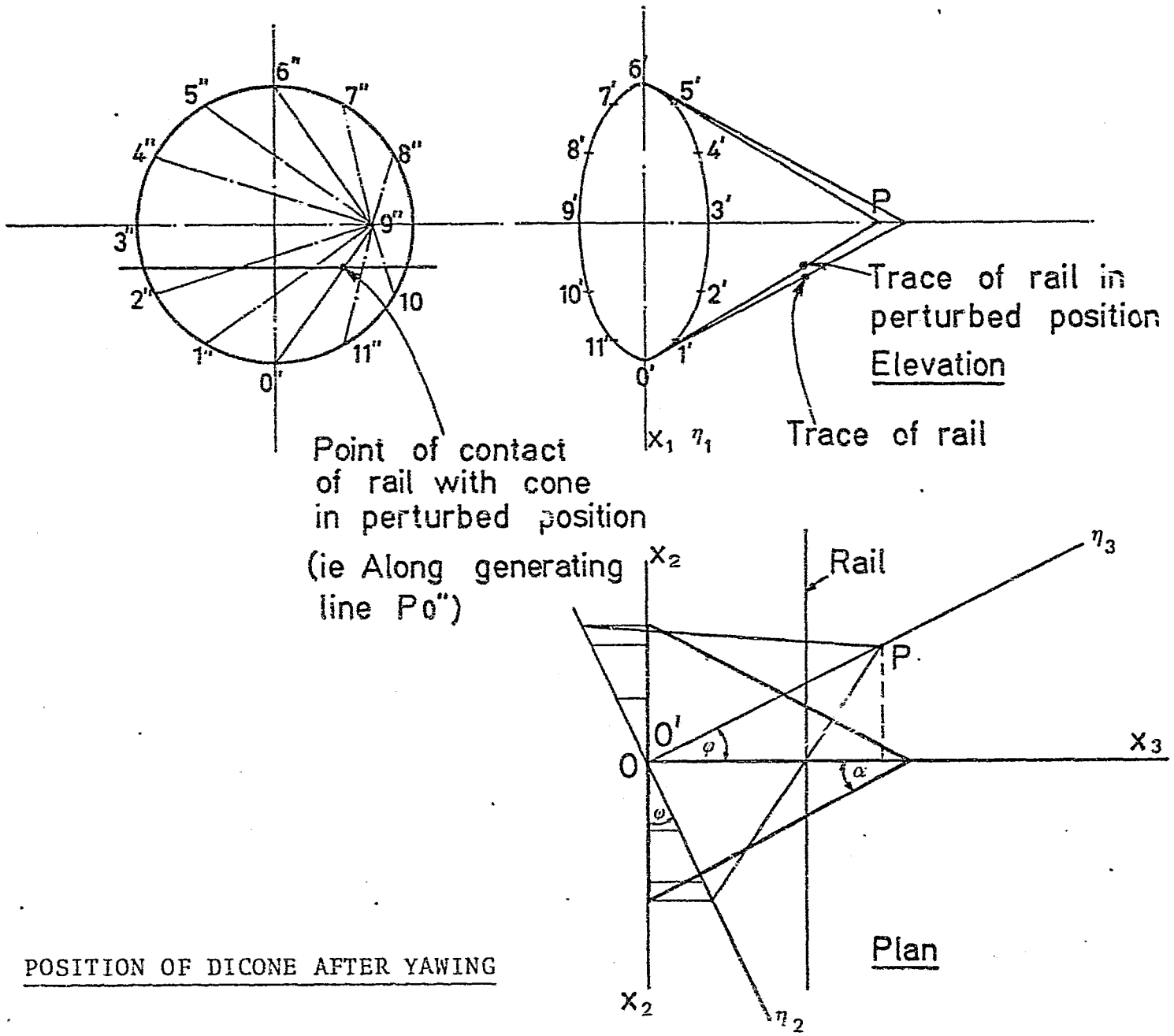

Figure 5.3: POSITION OF DICONE AFTER YAWING

H of centre of mass above rails after yawing

$$= -(R-b\,Tan\alpha\,Sec\phi)$$

The distance moved by the centre of mass from O to O' is the difference of these two heights:

$$OO'' = b\,Tan\alpha(Sec\phi - 1)$$

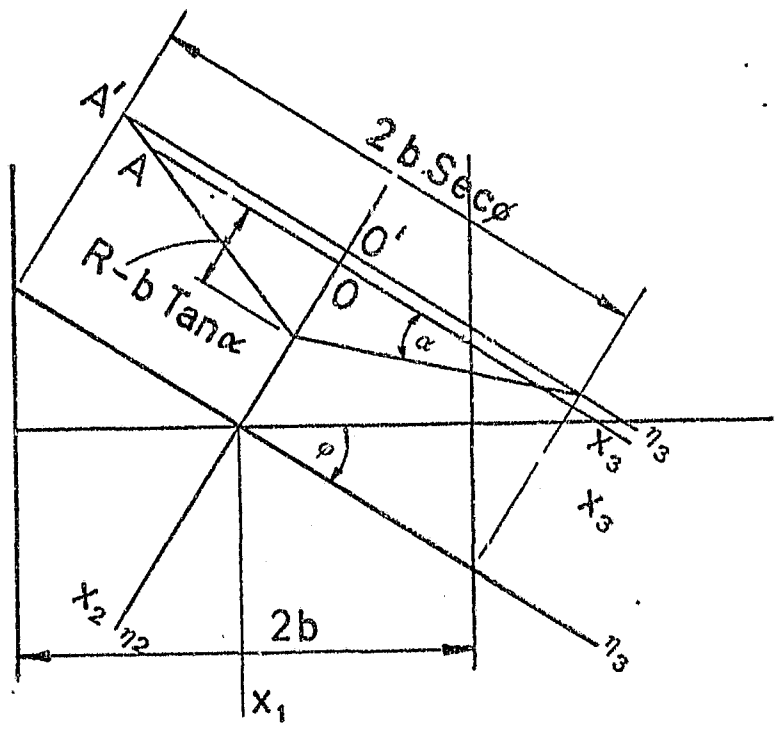

Figure 5.4: POSITIONS OF THE CENTRE OF MASS OF DICONE AFTER YAWING

5.4.3 Position of the centre of mass of the dicone after the rotation about the $O'\eta_1$ axis; that is after the dicone has tilted through an angle θ

The more complex movement of the centre of mass of the dicone is shown in Figure 5.5, where the lower half of the vertical cross-section of the dicone is represented by the triangle MNC. $M\hat{C}N$ in this triangle has a constant magnitude since the other angles in the triangle are each equal

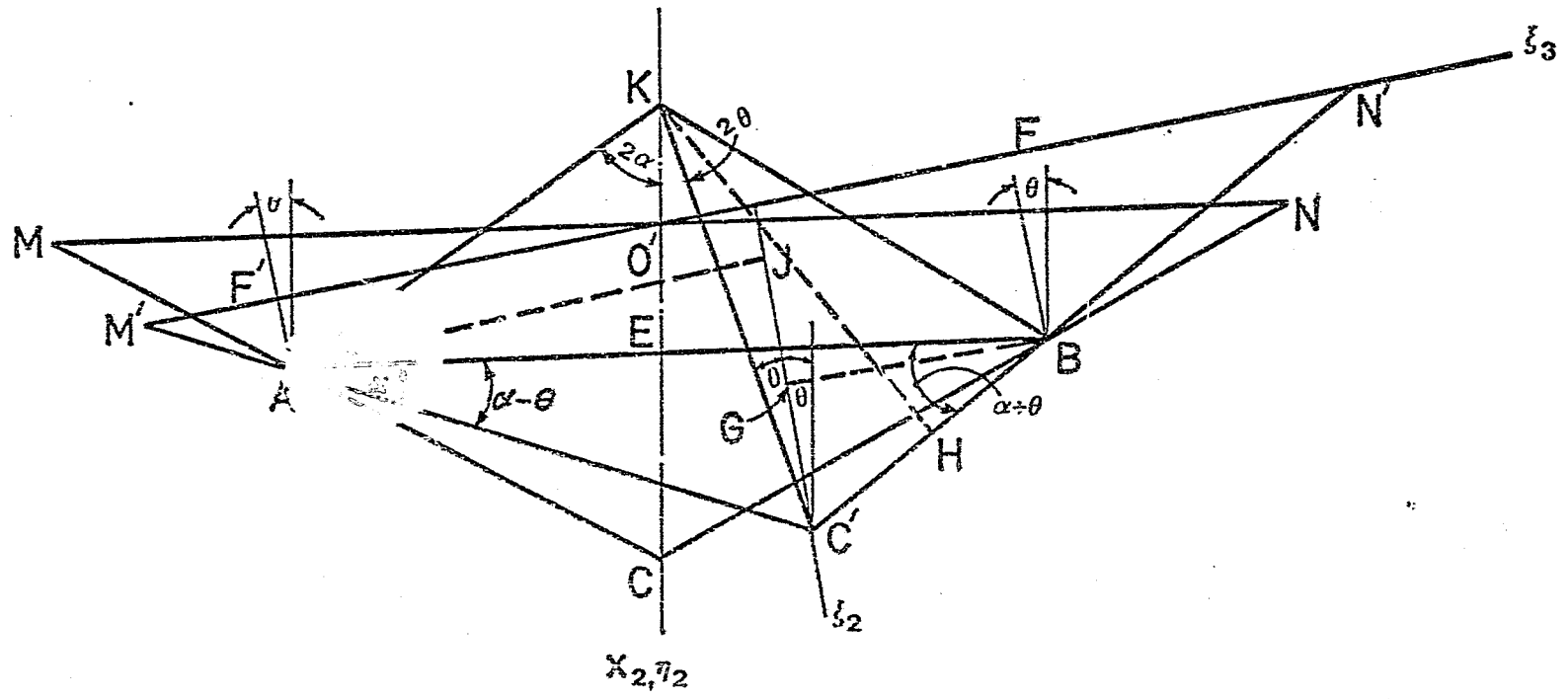

Figure 5.5: POSITION OF CENTRE OF MASS OF DICONE AFTER TILTING

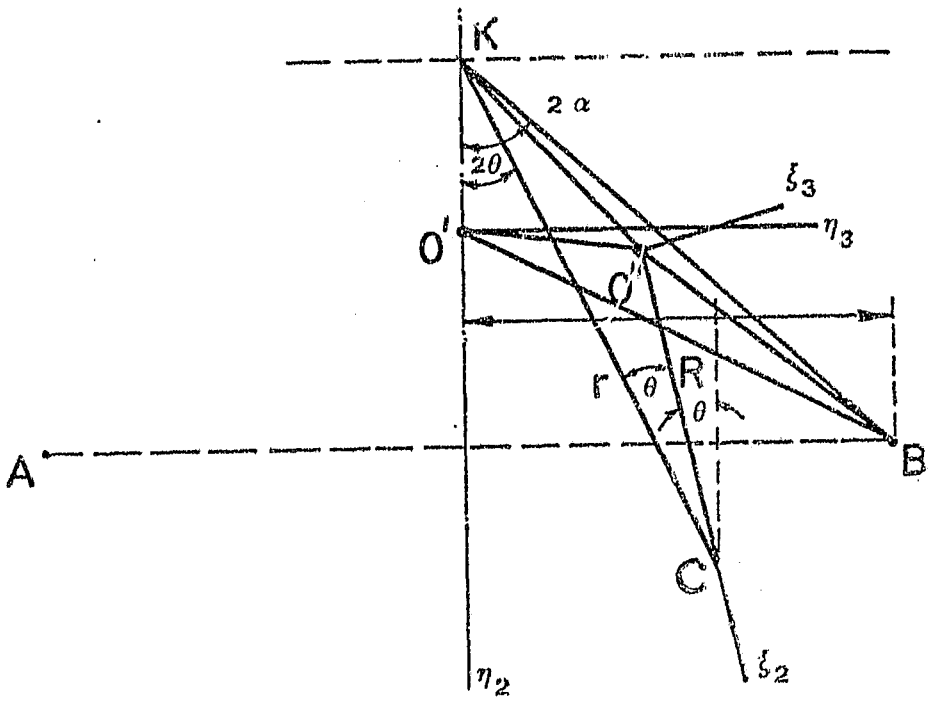

Figure 5.6: EQUIVALENT MECHANISM

5.4.4 The vectorial displacement of the centre of mass of the dicone as movement occurs from the original fixed coordinate axes system to the final coordinate axes system

The vectorial sum of the movements of the centre of mass after the dicone has been moved in the direction of the track and has then undergone two successive rotations is

$$\overline{O_s O''} = \overline{O_s O} + \overline{OO'} + \overline{O'O''}$$

where all the components of the vectors must relate to the fixed coordinate axes system. The position vector of the centre of mass which has just been derived has as coordinates those determined by the $O'\eta_1\eta_2\eta_3$ coordinate axes system, and these must then be transformed into

by considering the motion of an equivalent mechanism consisting of two pivotted links, as shown in Figure 5.6. The link of length r is pivotted at one end to the kinematic pivot K and at the other end to a link of length R. A mechanism (not shown in the figure) arranges that the angular movement between the links is half the absolute angular movement of the link of length r.

From the figure, since

$\underset{\sim}{KO'} + \underset{\sim}{O'O''} = \underset{\sim}{KO''}$,

then

$\underset{\sim}{O'O''} = \underset{\sim}{KO''} - \underset{\sim}{KO'}$

But

$$\overline{KO''}_\eta = \overline{KC'}_\eta + \overline{C'O''}_\eta = \begin{bmatrix} 0 \\ r\text{Cos}2\theta - R\text{Cos}\theta \\ r\text{Sin}2\theta - R\text{Sin}\theta \end{bmatrix} = \begin{bmatrix} 0 \\ 2r\text{Cos}^2\theta - r - R\text{cos}\theta \\ 2r\text{Sin}\theta\text{Cos}\theta - R\text{Sin}\theta \end{bmatrix}$$

Hence

$$\overline{O'O''} = \begin{bmatrix} 0 \\ 2r\text{Cos}^2\theta - r - R\text{Cos}\theta \\ 2r\text{Sin}\theta\text{Cos}\theta - R\text{Sin}\theta \end{bmatrix} - \begin{bmatrix} 0 \\ r - R \\ 0 \end{bmatrix} = \begin{bmatrix} \\ R(1-\text{Cos}\theta) - 2r\text{Sin}^2\theta \\ 2r\text{Sin}\theta\text{Cos}\theta - R\text{Sin}\theta \end{bmatrix}$$

$$= \begin{bmatrix} 0 \\ R(1-\text{Cos}\theta) - 2b\text{Cosec}2\alpha\text{Sec}\phi\text{Sin}^2\theta \\ 2b\text{Cosec}2\alpha\text{Sec}\phi\text{Sin}\theta\text{Cos}\theta - R\text{Sin}\theta \end{bmatrix}$$

coordinates in the O'x x x coordinate axes system as follows:

$$\overline{O'O''}_{\eta} = \begin{bmatrix} 0 \\ R(1-\cos\theta) - 2b\,\mathrm{Cosec}2\alpha\,\mathrm{Sec}\phi\,\sin^2\theta \\ b\,\mathrm{Cosec}2\alpha\,\mathrm{Sec}\phi\,\sin 2\theta - R\sin\theta \end{bmatrix}$$

$$\overline{O'O''}_{x} = \begin{bmatrix} \cos\phi & 0 & \sin\phi \\ 0 & 1 & 0 \\ -\sin\phi & 0 & \cos\phi \end{bmatrix} \begin{bmatrix} 0 \\ R(1-\cos\theta) - 2b\,\mathrm{Cosec}2\alpha\,\mathrm{Sec}\phi\,\sin^2\theta \\ b\,\mathrm{Cosec}2\alpha\,\mathrm{Sec}\phi\,\sin 2\theta - R\sin\theta \end{bmatrix}$$

$$= \begin{bmatrix} b\,\mathrm{Cosec}2\alpha\,\mathrm{Tan}\phi\,\sin 2\theta - R\sin\phi\sin\theta \\ R(1-\cos\theta) - 2b\,\mathrm{Cosec}2\alpha\,\mathrm{Sec}\phi\,\sin^2\theta \\ b\,\mathrm{Cosec}2\alpha\,\sin 2\theta - R\cos\phi\sin\theta \end{bmatrix}$$

Hence

$$\overline{O_S O''} = \begin{bmatrix} x_1 + b\,\mathrm{Cosec}2\alpha\,\mathrm{Tan}\phi\,\sin 2\theta - R\sin\phi\sin\theta \\ b\,\mathrm{Tan}\alpha(\mathrm{Sec}\phi - 1) + R(1-\cos\theta) - 2b\,\mathrm{Cosec}2\alpha\,\mathrm{Sec}\phi\,\sin^2\theta \\ b\,\mathrm{Cosec}2\alpha\,\sin 2\theta - R\cos\phi\sin\theta \end{bmatrix}$$

5.5 COORDINATES OF THE POINTS OF CONTACT BETWEEN THE RAILS AND THE DICONE IN THE $O''\xi_2\xi_3$ PLANE

From Figure 5.5, the coordinate of B in the $O''\xi_2$ direction is given by

$b_2 = FB = O''G$

$= O''C' - GC'$

But

$$GC' = BC'\mathrm{Sin}\alpha = 2HB\mathrm{Sin}\alpha$$

where KH is the perpendicular bisector dropped from the vertex of the isosceles triangle KBC' on to its base BC'. Further, since $B\hat{A}C'$ and $B\hat{K}C'$ both subtend the same arc of the circle

$$B\hat{A}C' = \tfrac{1}{2}B\hat{K}C' = B\hat{K}H$$

$$= \alpha - \theta$$

Hence

$$GC' = 2KB\mathrm{Sin}\alpha\mathrm{Sin}(\alpha-\theta)$$

$$= 2b\mathrm{Cosec}2\alpha\mathrm{Sin}\alpha\mathrm{Sec}\phi\mathrm{Sin}(\alpha-\theta)$$

$$= b\mathrm{Sec}\phi(\mathrm{Tan}\alpha\mathrm{Cos}\theta-\mathrm{Sin}\theta)$$

from which

$$b_2 = R - b\mathrm{Sec}\phi(\mathrm{Tan}\alpha\mathrm{Cos}\theta - \mathrm{Sin}\theta)$$

The coordinate of B in the $O''\xi_3$ direction is given by

$$b_3 = O''F = BG$$

$$= BC'\mathrm{Cos}\alpha$$

$$= 2b\mathrm{Cosec}2\alpha\mathrm{Cos}\alpha\mathrm{Sec}\phi\mathrm{Sin}(\alpha-\theta)$$

$$= b\mathrm{Sec}\phi(\mathrm{Cos}\theta - \mathrm{Cot}\alpha\mathrm{Sin}\theta)$$

Hence

$$\bar{b} = \begin{bmatrix} 0 \\ R-b\mathrm{Sec}\phi(\mathrm{Tan}\alpha\mathrm{Cos}\theta-\mathrm{Sin}\theta) \\ b\mathrm{Sec}\phi(\mathrm{Cos}\theta-\mathrm{Cot}\alpha\mathrm{Sin}\theta) \end{bmatrix}$$

Similarly

$$\bar{a} = \begin{bmatrix} 0 \\ R-b\,Sec\phi\,(Tan\alpha\,Cos\theta+Sin\theta) \\ -b\,Sec\phi\,(Cos\theta+Cot\alpha\,Sin\theta) \end{bmatrix}$$

5.6 THE DETERMINATION OF THE LINEAR VELOCITIES AT THE POINTS OF CONTACT OF THE WHEELPAIR WITH THE RAILS

5.6.1 Introduction

Since the running radii of the individual wheels of the wheelpair are equal in magnitude when the wheelpair is in the neutral, or equilibium position, there can be no doubt that pure rolling can then occur, but it is not valid to assume that similar conditions exist if the wheelpair is displaced from the neutral position. Pure rolling is possible only if the wheels at the points of contact with the stationary rails are instantaneously at rest.

5.6.2 The velocity of the centre of mass of the dicone in the disturbed position

The position vector of the centre of mass of the dicone in the $O'\eta_1\eta_2\eta_3$ coordinate axes frame was found in Section .4.3 to be

$$\overline{O'O''}_{\eta} = \begin{bmatrix} 0 \\ R(1-Cos\theta)-2b\,Cosec2\alpha\,Sec\phi\,Sin^2\theta \\ Sin\theta\,(2b\,Cosec2\alpha - R) \end{bmatrix}$$

Hence

$$\overline{OO''_x} = \begin{bmatrix} 0 \\ b\text{Tan}\alpha(\text{Sec}\phi-1) \\ 0 \end{bmatrix} + \begin{bmatrix} b\text{Cosec}2\alpha\text{Tan}\phi\text{Sin}2\theta - R\text{Sin}\phi\text{Sin}\theta \\ R(1-\text{Cos}\theta) - 2b\text{Cosec}2\alpha\text{Sec}\phi\text{Sin}^2\theta \\ b\text{Cosec}2\alpha\text{Sin}2\theta - R\text{Cos}\phi\text{Sin}\theta \end{bmatrix}$$

$$= \begin{bmatrix} b\text{Cosec}2\alpha\text{Tan}\phi\text{Sin}2\theta - R\text{Sin}\phi\text{Sin}\theta \\ b\text{Tan}\alpha(\text{Sec}\phi-1) + R(1-\text{Cos}\theta) - 2b\text{Cosec}2\alpha\text{Sec}\phi\text{Sin}^2\theta \\ b\text{Cosec}2\alpha\text{Sin}2\theta - R\text{Cos}\phi\text{Sin}\theta \end{bmatrix}$$

Hence

$$\bar{V}_{O''} = \frac{d}{dt}\begin{bmatrix} b\text{Cosec}2\alpha\text{Tan}\phi\text{Sin}2\theta - R\text{Sin}\phi\text{Sin}\theta + x_1 \\ b\text{Tan}\alpha(\text{Sec}\phi-1) + R(1-\text{Cos}\theta) - 2b\text{Cosec}2\alpha\text{Sec}\phi\text{Sin}^2\theta \\ b\text{Cosec}2\alpha\text{Sin}2\theta - R\text{Cos}\phi\text{Sin}\theta \end{bmatrix}$$

$$= \begin{bmatrix} (b\text{Cosec}2\alpha\text{Sec}^2\phi\text{Sin}2\theta - R\text{Cos}\phi\text{Sin}\theta)\dot{\phi} + (2b\text{Cosec}2\alpha\text{Tan}\phi\text{Cos}2\theta - R\text{Sin}\phi\text{Cos}\theta)\dot{\theta} + \dot{x}_1 \\ b(\text{Tan}\alpha - 2\text{Cosec}2\alpha\text{Sin}^2\theta)\text{Sec}\phi\text{Tan}\phi\dot{\phi} + (R\text{Sin}\theta - 2b\text{Cosec}2\alpha\text{Sec}\phi\text{Sin}2\theta)\dot{\theta} \\ R\text{Sin}\phi\text{Sin}\theta\dot{\phi} + (2b\text{Cosec}2\alpha\text{Cos}2\theta - R\text{Cos}\phi\text{Cos}\theta)\dot{\theta} \end{bmatrix}$$

5.6.3 Velocities of the surfaces of the dicone at the points of contact with the rails

The angular velocity of the $O''\xi_1\xi_2\xi_3$ coordinate axes frame is

$$\bar{\omega}_{\xi\text{frame}} = \{\dot{\theta} \quad \dot{\phi}\text{Cos}\theta \quad -\dot{\phi}\text{Sin}\theta\}$$

Since the dicone has a spin velocity n in the $O''\xi_1\xi_2\xi_3$

coordinate axes frame, the dicone has an angular velocity given by

$$\bar{\omega}_{\xi' dicone} = \{\dot{\theta} \quad \dot{\phi}Cos\theta \quad n-\dot{\phi}Sin\theta\}$$

The velocity of A as a point on the dicone surface relative to O'', namely, $\underset{\sim}{V}_{O''A_\xi}$, is obtained as follows:

$$\bar{V}_{O''A_\xi} = \frac{d}{dt}(\overline{O''A_\xi}) + \bar{\bar{\Omega}}_{frame} \times \overline{O''A_\xi}$$

$$\bar{V}_{O''A_\xi} = \frac{d}{dt}\begin{bmatrix} 0 \\ R-bSec\phi(Tan\alpha Cos\theta+Sin\theta) \\ -bSec\phi(Cos\theta+Cot\alpha Sin\theta) \end{bmatrix}$$

$$+ \begin{bmatrix} 0 & \dot{\phi}Sin\theta-n & \dot{\phi}Cos\theta \\ n-\dot{\phi}Sin\theta & 0 & -\dot{\theta} \\ -\dot{\phi}Cos\theta & \dot{\theta} & 0 \end{bmatrix} \begin{bmatrix} 0 \\ R-bSec\phi(Tan\alpha Cos\theta+Sin\theta) \\ -bSec\phi(Cos\theta+Cot\alpha Sin\theta) \end{bmatrix}$$

$$= \begin{bmatrix} (\dot{\phi}Sin\theta-n)\{R-bSec\phi(Tan\alpha Cos\theta+Sin\theta)\}-b\dot{\phi}Sec\phi Cos\theta(Cos\theta+Cot\alpha Sin\theta) \\ -b\dot{\phi}Sec\phi Tan\phi(Tan\alpha Cos\theta+Sin\theta)+b\dot{\theta}Sec\phi(Tan\alpha Sin\theta-Cos\theta)+b\dot{\theta}Sec\phi(Cos\theta+Cot\alpha Sin\theta) \\ -b\dot{\phi}Sec\phi Tan\phi(Cos\theta+Cot\alpha Sin\theta)+b\dot{\theta}Sec\phi(Sin\theta-Cot\alpha Cos\theta)+\dot{\theta}\{R-bSec\phi(Tan\alpha Cos\theta+Sin\theta)\} \end{bmatrix}$$

$$= \begin{bmatrix} n\{bSec\phi(Tan\alpha Cos\theta+Sin\theta)-R\}+R\dot{\phi}Sin\theta-b\dot{\phi}Sec\phi\{(Tan\alpha+Cot\alpha)Sin\theta Cos\theta+Sin^2\theta+Cos^2\theta\} \\ -b\dot{\phi}Sec\phi Tan\phi(Tan\alpha Cos\theta+Sin\theta)+2b\dot{\theta}Cosec2\alpha Sec\phi Sin\theta \\ -b\dot{\phi}Sec\phi Tan\phi(Cos\theta+Cot\alpha Sin\theta)+R\dot{\theta}-2b\dot{\theta}Cosec2\alpha Sec\phi Cos\theta \end{bmatrix}$$

$$\bar{V}_{O''A_x} = \begin{bmatrix} \text{Cos}\phi & \text{Sin}\phi\text{Sin}\theta & \text{Sin}\phi\text{Cos}\theta \\ 0 & \text{Cos}\theta & -\text{Sin}\theta \\ -\text{Sin}\phi & \text{Cos}\phi\text{Sin}\theta & \text{Cos}\phi\text{Cos}\theta \end{bmatrix} \begin{bmatrix} n\{b\text{Sec}\phi(\text{Tan}\alpha\text{Cos}\theta+\text{Sin}\theta)-R\}+\dot{\phi}\{R\text{Sin}\theta \\ -b\dot{\phi}\text{Sec}\phi\text{Tan}\phi(\text{Tan}\alpha\text{Cos}\theta+\text{Sin}\theta)+ \\ -b\dot{\phi}\text{Sec}\phi\text{Tan}\phi(\text{Cos}\theta+\text{Cot}\alpha\text{Sin}\theta)+R\dot{\theta} \end{bmatrix}$$

$$\begin{bmatrix} -b\text{Sec}\phi(\text{Cosec}2\alpha\text{Sin}2\theta+1)\} \\ 2b\dot{\theta}\text{Cosec}2\alpha\text{Sec}\phi\text{Sin}\theta \\ -2b\dot{\theta}\text{Cosec}2\alpha\text{Sec}\phi\text{Cos}\theta \end{bmatrix}$$

$$= \begin{bmatrix} n\{b(\text{Tan}\alpha\text{Cos}\theta+\text{Sin}\theta)-R\text{Cos}\phi\}+\{R\text{Cos}\phi\text{Sin}\theta-b\text{Sec}^2\phi(\text{Cosec}2\alpha\text{Sin}2\theta+1)\}\dot{\phi} \\ b\dot{\phi}(2\text{Cosec}2\alpha\text{Sin}^2\theta-\text{Tan}\alpha)\text{Sec}\phi\text{Tan}\phi+(2b\text{Cosec}2\alpha\text{Sec}\phi\text{Sin}2\theta-R\text{Sin}\theta)\dot{\theta} \\ n\{R\text{Sin}\phi-b\text{Tan}\phi(\text{Tan}\alpha\text{Cos}\theta+\text{Sin}\theta)\}-R\dot{\phi}\text{Sin}\phi\text{Sin}\theta+(R\text{Cos}\phi\text{Cos}\theta \end{bmatrix}$$

$$\begin{bmatrix} -(2b\text{Cosec}2\alpha\text{Tan}\phi\text{Cos}2\theta-R\text{Sin}\phi\text{Cos}\theta)\dot{\theta} \\ -2b\text{Cosec}2\alpha\text{Cos}2\theta)\dot{\theta} \end{bmatrix}$$

$$\bar{V}_{A_x} = \bar{V}_{O''_x} + \bar{V}_{O''A_x}$$

$$= \begin{bmatrix} n\{b(\text{Tan}\alpha\text{Cos}\theta+\text{Sin}\theta)-R\text{Cos}\phi\}-b\dot{\phi}\text{Sec}^2\phi+\dot{x}_1 \\ 0 \\ n\{R\text{Sin}\phi-b\text{Tan}\phi(\text{Tan}\alpha\text{Cos}\theta+\text{Sin}\theta)\} \end{bmatrix}$$

Similarly,

$$\bar{V}_{B_x} = \begin{bmatrix} n\{b(\text{tan}\alpha\text{Cos}\theta-\text{Sin}\theta)-R\text{Cos}\phi\}-b\dot{\phi}\text{Sec}^2\phi+\dot{x}_1 \\ 0 \\ n\{R\text{Sin}\phi-b\text{Tan}\phi(\text{Tan}\alpha\text{Cos}\theta-\text{Sin}\theta)\} \end{bmatrix}$$

In order that pure rolling should occur at the points of contact between the dicone surfaces and the rails, the velocities of the surfaces of the dicone at the points of contact would have to be equal to each other and to the rail velocities. First of all, since the dicone is required to remain in contact with the rails, it is apparent that these equations meet this condition since the velocities in the Ox_2 direction vanish in both equations.

The velocities in the transverse direction, that is in the Ox_3 direction, must vanish, since the rails cannot move in this direction. This is the case only if ϕ is zero, which implies also that $\dot{\phi}$ vanishes. Using these requirements, the velocities in the Ox_1 direction at A and B respectively must be equal to each other, that is,

$$n\{b(\mathrm{Tan}\alpha\mathrm{Cos}\theta+\mathrm{Sin}\theta)-R\} + \dot{x}_1 = n\{b(\mathrm{Tan}\alpha\mathrm{Cos}\theta-\mathrm{Sin}\theta) - R\} + \dot{x}_1.$$

This relationship is possible only if θ vanishes.

It has then to be concluded that the dicone, except in the neutral position, slides over the rails and that pure rolling motion does not occur. This conclusion is confirmed experimentally by the fact that the dicone has a lower spin velocity when it hunts than that required by the rail speed; furthermore, if the rails are dusty, sparks are seen to fly from the contact region if the room in which the experiments are conducted is darkened. (The sparks are caused by the specks of dust being heated into incandescence by the energy lost as the dicone slides over the rails.)

5.7 ACCELERATION OF THE CENTRE OF MASS OF THE DICONE

The acceleration of the centre of mass of the dicone, $\bar{a}_{g_X}$, is obtained by differentiating the velocity of the centre of mass, as found in section 6.2:

$$\bar{a}_{g_X} = \frac{d}{dt}\begin{bmatrix} (b(\text{Cosec}2\alpha\text{Sec}^2\phi\text{Sin}2\theta - R\text{Cos}\phi\text{Sin}\theta)\dot{\phi} + (2b\text{Cosec}2\alpha\text{Tan}\phi\text{Cos}2\theta - R\text{Sin}\phi\text{Cos}\theta)\dot{\theta} + \dot{x}_1 \\ b(\text{Tan}\alpha - 2\text{Cosec}2\alpha\text{Sin}^2\theta)\text{Sec}\phi\text{Tan}\phi\dot{\phi} + (R\text{Sin}\theta - 2b\text{Cosec}2\alpha\text{Sec}\phi\text{Sin}2\theta)\dot{\theta} \\ R\text{Sin}\phi\text{Sin}\theta\dot{\phi} + (2b\text{Cosec}2\alpha\text{Cos}2\theta - R\text{Cos}\phi\text{Cos}\theta)\dot{\theta} \end{bmatrix}$$

$$= \begin{bmatrix} (b\text{Cosec}2\alpha\text{Sec}^2\phi\text{Sin}2\theta - R\text{Cos}\phi\text{Sin}\theta)\ddot{\phi} + (2b\text{Cosec}2\alpha\text{Sec}^2\phi\text{Tan}\phi\text{Sin}2\theta + R\text{Sin}\phi\text{Sin}\theta)\dot{\phi}^2 \\ b\ddot{\phi}\text{Sec}\phi\text{Tan}\phi(\text{Tan}\alpha - 2\text{Cosec}2\alpha\text{Sin}^2\theta) + b\text{Sec}\phi(\text{Sec}^2\phi + \text{Tan}^2\phi)(\text{Tan}\alpha - 2\text{Cosec}2\alpha\text{Sin}^2\theta)\dot{\phi}^2 \\ R\ddot{\phi}\text{Sin}\phi\text{Sin}\theta + R\dot{\phi}^2\text{Cos}\phi\text{Sin}\theta + 2R\dot{\phi}\dot{\theta}\text{Sin}\phi\text{Cos}\theta + (R\text{Cos}\phi\text{Sin}\theta - 4b\text{Cosec}2\alpha\text{Sin}2\theta)\dot{\theta}^2 \end{bmatrix}$$

$$\begin{bmatrix} +2(2b\text{Cosec}2\alpha\text{Sec}^2\phi\text{Cos}2\theta - R\text{Cos}\phi\text{Cos}\theta)\dot{\phi}\dot{\theta} + (R\text{Sin}\phi\text{Sin}\theta - 4b\text{Cosec}2\alpha\text{Tan}\phi\text{Sin}2\theta)\dot{\theta}^2 \\ -4b\text{Cosec}2\alpha\text{Sec}\phi\text{Tan}\phi\text{Sin}2\theta\dot{\phi}\dot{\theta} + (R\text{Cos}\theta - 4b\text{Cosec}2\alpha\text{Sec}\phi\text{Cos}2\theta)\dot{\theta}^2 + R\text{Sin}\theta \\ +2b\text{Cosec}2\alpha\text{Cos}2\theta - R\text{Cos}\phi\text{Cos}\theta)\ddot{\theta} \end{bmatrix}$$

$$\begin{bmatrix} +(2b\text{Cosec}2\alpha\text{Tan}\phi\text{Cos}2\theta - R\text{Sin}\phi\text{Cos}\theta)\ddot{\theta} + \ddot{x}_1 \\ -2b\text{Cosec}2\alpha\text{Sec}\phi\text{Sin}2\theta)\ddot{\theta} \end{bmatrix}$$

5.8 THE FORCES ACTING ON THE DICONE

5.8.1 Introduction

The forces acting on the dicone are its weight, the spring restraining forces and the forces at the points of contact. The latter forces are the forces normal to the surface of

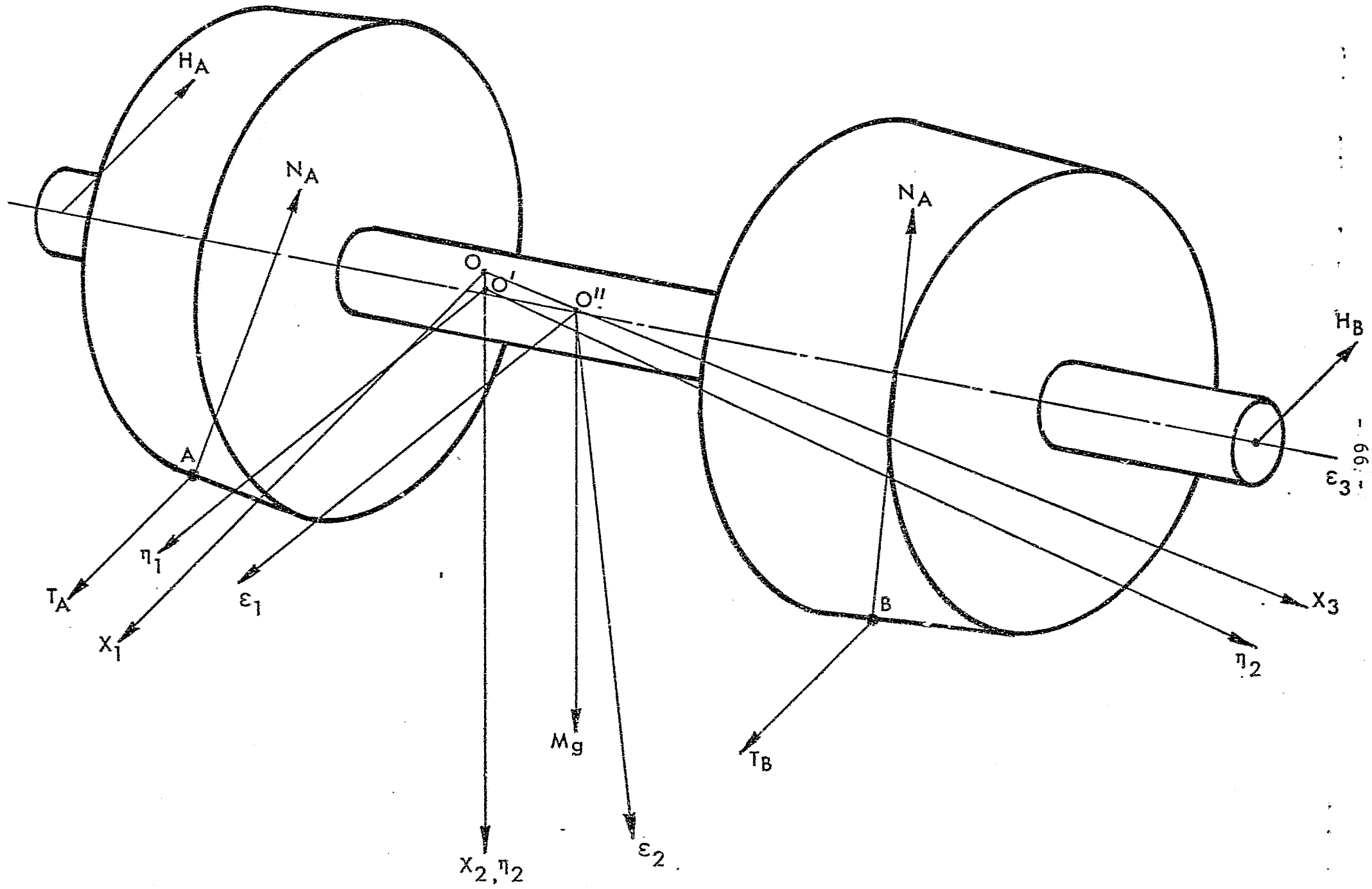

FIGURE 5.7 WHEELPAIR IN PERSPECTIVE AS A FREEBODY DIAGRAM TO SHOW THE FORCES ACTING ON IT

the dicone at the points of contact and the tractive forces which are in the direction of the rails. The points of application and the directions in which these forces act are shown in figure 5.7.

5.8.2 The spring forces

Ideally, the horizontal restraint imposed on the dicone to resist the tractive forces due to the rails would be exerted by springs acting in two separate planes parallel to the Ox_1x_2 plane on either side of the dicone, and in addition, these forces would always act in a horizontal direction.

As a practical alternative, long horizontal tension springs would be attached to sleeves able to slide freely along the dicone shaft; in other words, to all intents and purposes, the spring tension forces act in planes parallel to the Ox_1x_2 plane, and distant $\pm$ B from it.

As the dicone tilts, the springs deviate from their horizontal direction, but the vertical movement is small compared to the length of the springs. To avoid further complications, it will be assumed that the direction of the spring forces is always horizontal. In the light of this assumption, tilting has no effect on the spring forces (in practice, the effect would be negligible). Yawing and the forward movement of the dicone would cause the left- and right-hand spring forces to bo, respectively:

$-k(x_1-BTan\phi)$ and $-k(x_1+BTan\phi)$

5.8.3 Components of the normal forces

The components of the normal forces in the $O'\eta_1\eta_2\eta_3$ coordinate axes frame are shown in Figure 4.7 to be:

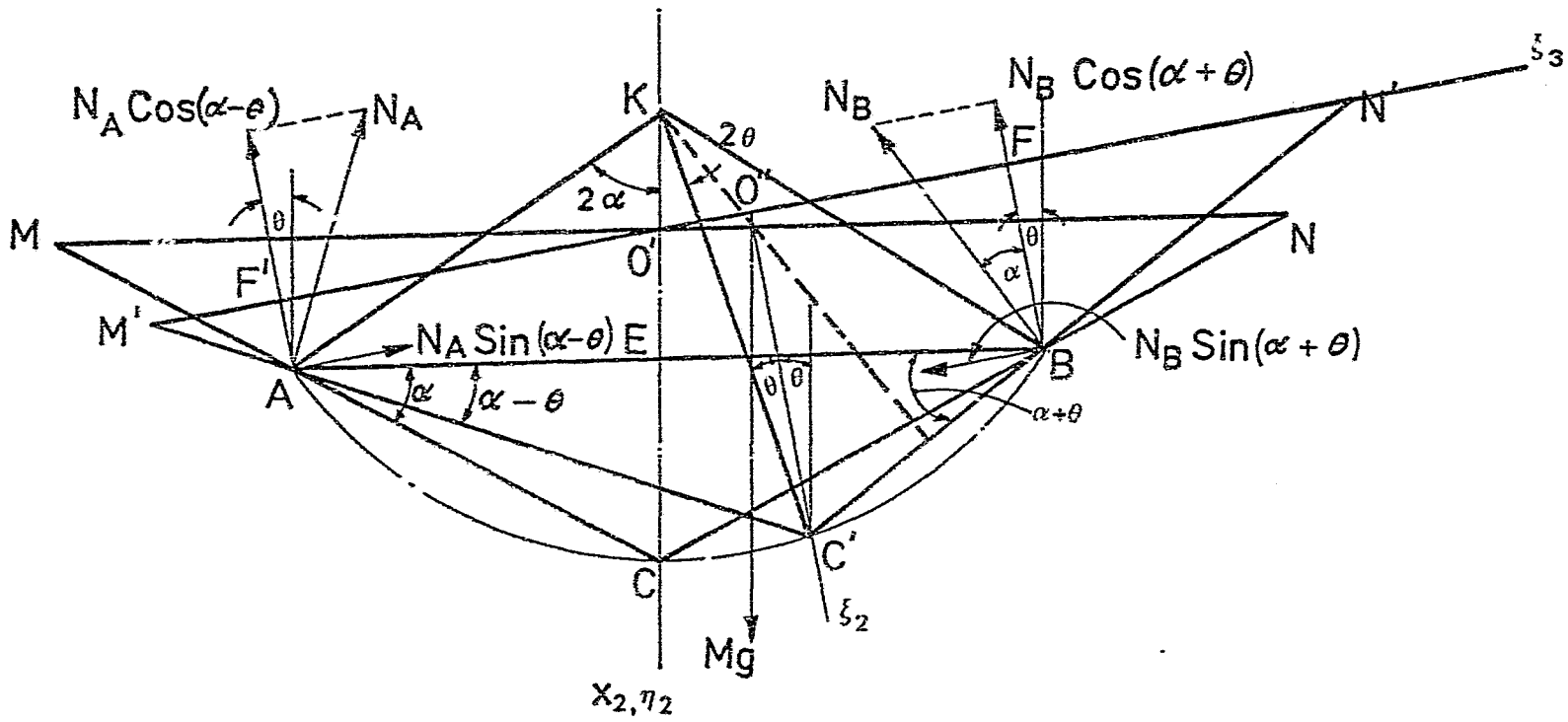

Figure 5.8: THE NORMAL FORCES WITH THEIR COMPONENTS AT THE POINTS OF CONTACT

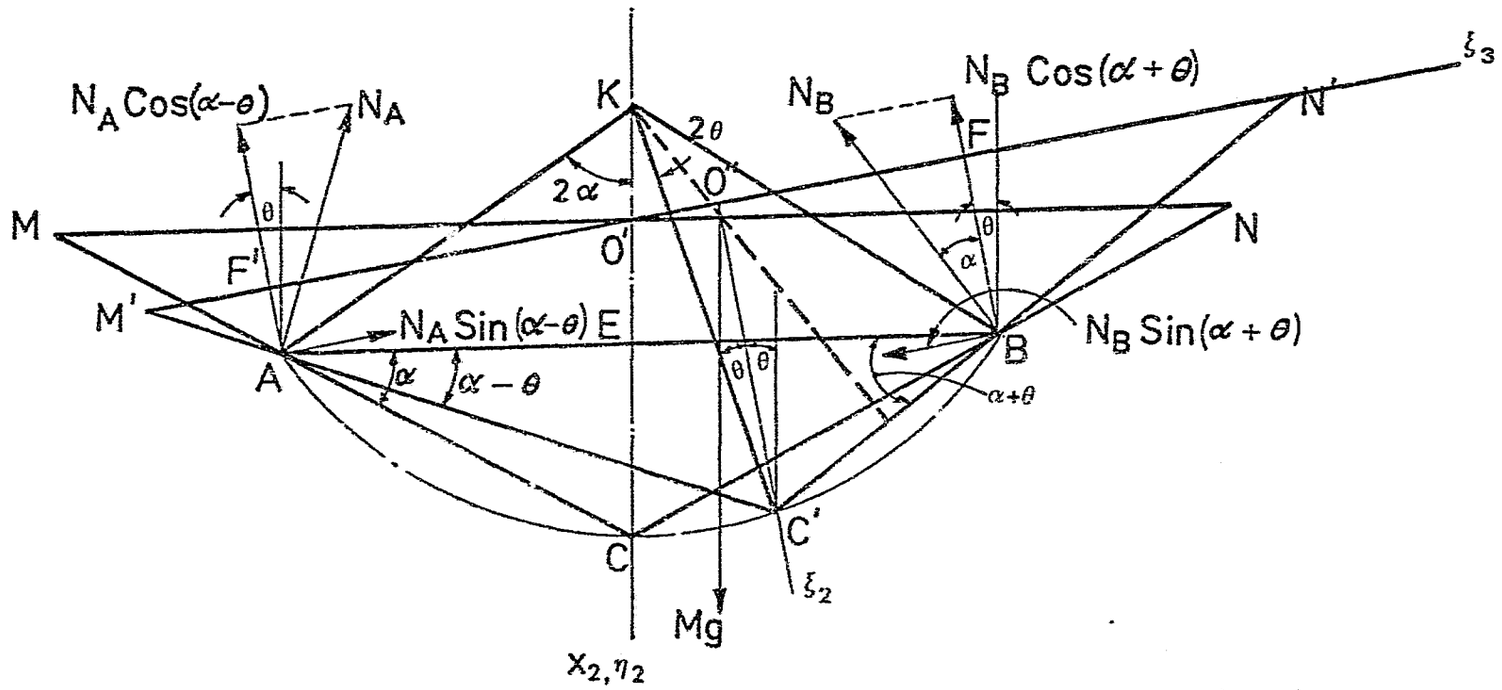

Figure 5.8: THE NORMAL FORCES WITH THEIR COMPONENTS AT THE POINTS OF CONTACT

$$\begin{bmatrix} 0 \\ -N_A\mathrm{Cos}(\alpha-\theta) - N_B\mathrm{Cos}(\alpha+\theta) \\ N_A\mathrm{Sin}(\alpha+\theta) - N_B\mathrm{Sin}(\alpha-\theta) \end{bmatrix}$$

The components of the normal forces in the $Ox_1x_2x_3$ coordinate axes frame are:

$$\begin{bmatrix} \mathrm{Cos}\phi & 0 & \mathrm{Sin}\phi \\ 0 & 1 & 0 \\ -\mathrm{Sin}\phi & 0 & \mathrm{Cos}\phi \end{bmatrix} \begin{bmatrix} 0 \\ -\{(N_A+N_B)\mathrm{Cos}\alpha\mathrm{Cos}\theta+(N_A-N_B)\mathrm{Sin}\alpha\mathrm{Sin}\theta\} \\ (N_A-N_B)\mathrm{Sin}\alpha\mathrm{Cos}\theta-(N_A+N_B)\mathrm{Cos}\alpha\mathrm{Sin}\theta \end{bmatrix}$$

$$= \begin{bmatrix} \{(N_A-N_B)\mathrm{Sin}\alpha\mathrm{Cos}\theta-(N_A+N_B)\mathrm{Cos}\alpha\mathrm{Sin}\theta\}\mathrm{Sin}\phi \\ -\{(N_A+N_B)\mathrm{Cos}\alpha\mathrm{Cos}\theta+(N_A-N_B)\mathrm{Sin}\alpha\mathrm{Sin}\theta\} \\ \{(N_A-N_B)\mathrm{Sin}\alpha\mathrm{Cos}\theta-(N_A+N_B)\mathrm{Cos}\alpha\mathrm{Sin}\theta\}\mathrm{Cos}\phi \end{bmatrix}$$

5.8.4 The tangential forces at the points of contact between the dicone and the rails

In the $Ox_1x_2x_3$ coordinate axes frame, the tangential forces at the left- and right-hand points of contact are represented by:

$$\bar{T}_{A_x} = \{T_A \quad 0 \quad 0\} \quad \text{and} \quad \{\bar{T}_{B_x} = T_B \quad 0 \quad 0\}$$

If sliding occurs at each contact point (and it has been concluded that such is the case), the tractive force at each contact point between the rails and the wheels is that determined by limiting friction. The Coulomb law relationship between the limiting frictional force and the

normal force at the point of contact is probably the most satisfactory assumption regarding the magnitudes of the forces at the contact points; that is,

$T_A = \mu N_A$ and $T_B = \mu N_B$

(where, hopefully, the coefficient of friction, or the constant of proportionality between the limiting frictional force and the normal force, is the same for both points of contact).

Since friction would reduce the spin velocity, it is a possible deduction that the rail velocity is greater than the velocities of the dicone surface at the points of contact at all stages of the oscillatory motion and that therefore the tractive forces exerted by the rails on the wheels are in the same direction as that in which the belts are moving.

5.9 THE LINEAR EQUATIONS OF MOTION

5.9.1 The matrix form of the linear equations of motion

From Newton II,

$$\Sigma \bar{F}_x = M\ddot{a}_{g_x}$$

where

$$\Sigma \bar{F}_x = \begin{bmatrix} (T_A+T_B-2kx_1)-\{(N_A+N_B)\mathrm{Cos}\alpha\mathrm{Sin}\theta-(N_A-N_B)\mathrm{Sin}\alpha\mathrm{Cos}\theta\}\mathrm{Sin}\phi \\ -\{(N_A+N_B)\mathrm{Cos}\alpha\mathrm{Cos}\theta+(N_A-N_B)\mathrm{Sin}\alpha\mathrm{Sin}\theta\}+Mg \\ \{-(N_A+N_B)\mathrm{Cos}\alpha\mathrm{Sin}\theta+(N_A-N_B)\mathrm{Sin}\alpha\mathrm{Cos}\theta\} \end{bmatrix}$$

5.9.2 Expansion of the separate lines of the matrix form

Taking each line of the matrix for the linear equations of

motion in turn,

$$(T_A+T_B-2kx_1) - \{(N_A+N_B)\cos\alpha\sin\theta-(N_A-N_B)\sin\alpha\cos\theta\}\sin\phi$$

$$= M\{\ddot{x}_1+(b\,\mathrm{cosec}2\alpha\sec^2\phi\sin2\theta-R\cos\phi\sin\theta)\ddot{\phi} + (R\sin\phi\sin\theta$$

$$+2b\,\mathrm{Cosec}2\alpha\sec^2\phi\tan\phi\sin2\theta)\dot{\phi}^2 + 2(2b\,\mathrm{Cosec}2\alpha\sec^2\phi\cos2\theta-R\cos\phi$$

$$\times\cos\theta)\dot{\phi}\dot{\theta} + (R\sin\phi\sin\theta-4b\,\mathrm{Cosec}2\alpha\tan\phi\sin2\theta)\dot{\theta}^2 +$$

$$+ (2b\,\mathrm{Cosec}2\alpha\tan\phi\cos2\theta - R\sin\phi\cos\theta)\ddot{\theta} \qquad \text{----------} \quad (A)$$

$$-(N_A+N_B)\cos\alpha\cos\theta - (N_A-N_B)\sin\alpha\sin\theta$$

$$= M[-g+b\ddot{\phi}\sec\phi\tan\phi(\tan\alpha-2\,\mathrm{Cosec}2\alpha\sin^2\ ) + b\dot{\phi}^2\sec\phi(\sec^2\phi +$$

$$\tan^2\phi)(\tan\alpha-2\,\mathrm{Cosec}2\alpha\sin^2\theta) - 4b\,\mathrm{Cosec}2\alpha\sec\phi\tan\phi\sin2\theta\dot{\phi}\dot{\theta}$$

$$+(R\cos\theta-4b\,\mathrm{Cosec}2\alpha\sec\phi\cos2\theta)\dot{\theta}^2 + (R\sin\theta-2b\,\mathrm{Cosec}2\alpha\sec\phi$$

$$\times \sin2\theta)\ddot{\theta}] \qquad \text{----------} \quad (B)$$

$$\{-(N_A+N_B)\cos\alpha\sin\theta + (N_A-N_B)\sin\alpha\cos\theta\}\cos\phi$$

$$= M[R\sin\phi\sin\theta\ddot{\phi} + R\cos\phi\sin\theta\dot{\phi}^2 + 2R\sin\phi\cos\theta\dot{\phi}\dot{\theta} + (R\cos\phi\sin\theta$$

$$-4b\,\mathrm{Cosec}2\alpha\sin2\theta)\dot{\theta}^2 + (2b\,\mathrm{Cosec}2\alpha\cos2\theta - R\cos\phi\cos\theta)\ddot{\theta}]$$

$$\text{----------} \quad (C)$$

5.9.3. Separation of (N_A+N_B) and (N_A-N_B) terms

Multiplying equation (B) by $-\text{Cos}\theta$ and adding it to equation (C) multiplied by $-\text{Sec}\phi\text{Sin}\theta$ gives:

$$(N_A+N_B)\text{Cos}\alpha = M[g\text{Cos}\theta-\text{Tan}\phi\{R\text{Sin}^2\theta+b\text{Sec}\phi\text{Cos}\theta(\text{Tan}\alpha$$

$$-2\text{Cosec}2\alpha\text{Sin}^2\theta)\}\ddot{\theta}-\{R\text{Sin}^2\theta+b\text{Sec}\phi\text{Cos}\theta(\text{Sec}^2\phi+\text{Tan}^2\phi)(\text{Tan}\alpha$$

$$-2\text{Cosec}2\alpha\text{Sin}^2\theta)\}\dot{\phi}^2-2\text{Tan}\phi(R\text{Sin}\theta\text{Cos}\theta-2b\text{Cosec}2\alpha\text{Sec}\phi\text{Cos}\theta$$

$$\times\text{Sin}2\theta)\dot{\phi}\dot{\theta}-(R-4b\text{Cosec}2\alpha\text{Sec}\phi\text{Cos}\theta)\dot{\theta}^2+2b\text{Cosec}2\alpha\text{Sec}\phi\text{Sin}\theta\ddot{\theta}]$$

Multiplying equation (C) $\text{Sec}\phi\text{Cos}\theta$ and subtracting from it equation (B) multiplied by $\text{Sin}\theta$ gives:

$$(N_A-N_B)\text{Sin}\alpha = M[g\text{Sin}\theta+\text{Tan}\phi\{R\text{Sin}\theta\text{Cos}\theta-b\text{Sec}\phi\text{Sin}\theta(\text{Tan}\alpha-2\text{Cosec}2\alpha$$

$$\times\text{Sin}^2\theta)\}\ddot{\phi}+\{R\text{Sin}\theta\text{Cos}\theta-b\text{Sec}\phi\text{Sin}\theta(\text{Sec}^2\phi+\text{Tan}^2\phi)(\text{Tan}\alpha-2\text{Cosec}2\alpha$$

$$\times\text{Sin}^2\theta)\}\dot{\phi}^2+2\text{Tan}\phi(R\text{Cos}^2\theta+2b\text{Cosec}2\alpha\text{Sec}\phi\text{Sin}\theta\text{Sin}2\theta)\dot{\phi}\dot{\theta}-$$

$$4b\text{Cosec}2\alpha\text{Sec}\phi\text{Sin}\theta\dot{\theta}^2-(R-2b\text{Cosec}2\alpha\text{Sec}\phi\text{Cos}\theta)\ddot{\theta}]$$

5.9.4 The equation of motion for the linear dicone movement in the direction of the rails

The first line of the equations of motion derived in Section 5.9.2 reads as follows:

$$(T_A+T_B-2kx_1)-\{(N_A+N_B)\text{Cos}\alpha\text{Sin}\theta-(N_A-N_B)\text{Sin}\alpha\text{Cos}\theta\}\text{Sin}\phi$$

$$=M\ddot{x}_1+\ldots/73$$

$$= M\{\ddot{x}_1 + (b\,Cosec2\alpha\,Sec^2\phi\,Sin2\theta - R\,Cos\phi\,Sin\theta)\ddot{\phi} + (R\,Sin\phi\,Sin\theta + 2b\,Cosec2\alpha\,Sec^2\phi\,Tan\phi\,Sin2\theta)\dot{\phi}^2 + 2(2b\,Cosec2\alpha\,Sec^2\phi\,Cos2\theta - R\,Cos\phi\,Cos\theta)\dot{\phi}\dot{\theta} + (R\,Sin\phi\,Sin\theta - 4b\,Cosec2\alpha\,Tan\phi\,Sin2\theta)\dot{\theta}^2 + (2b\,Cosec2\alpha\,Tan\phi\,Cos2\theta - R\,Sin\phi\,Cos\theta)\ddot{\theta}\}$$

Now

$$\frac{1}{M}\{(N_A+N_B)\,Cos\alpha\,Sin\theta - (N_A-N_B)\,Sin\alpha\,Cos\theta\}$$

$$= Sin\theta[g\,Cos\theta - Tan\phi\{R\,Sin^2\theta + b\,Sec\phi\,Cos\theta\,(Tan\alpha - 2\,Cosec2\alpha\,Sin^2\theta)\}\ddot{\phi} - \{R\,Sin^2\theta + b\,Sec\phi\,Cos\theta\,(Sec^2\phi + Tan^2\phi)\,(Tan\alpha - 2\,Cosec2\alpha\,Sin^2\theta)\}\dot{\phi}^2 - 2\,Tan\phi\,(R\,Sin\theta\,Cos\theta - 2b\,Cosec2\alpha\,Sec\phi\,Cos\theta\,Sin2\theta)\dot{\phi}\dot{\theta} - (R - 4b\,Cosec2\alpha\,Sec\phi\,Cos\theta)\dot{\theta}^2 + 2b\,Cosec2\alpha\,Sec\phi\,Sin\theta\ddot{\theta}] - Cos\theta[g\,Sin\theta + Tan\phi\{R\,Sin\theta\,Cos\theta - b\,Sec\phi\,Sin\theta\,(Tan\alpha - 2\,Cosec2\alpha\,Sin^2\theta)\}\ddot{\phi} + \{R\,Sin\theta\,Cos\theta - b\,Sec\phi\,Sin\theta\,(Sec^2\phi + Tan^2\phi)\,(Tan\alpha - 2\,Cosec2\alpha\,Sin^2\theta)\dot{\phi}^2 + 2\,Tan\phi\,(R\,Cos^2\theta + 2b\,Cosec2\alpha\,Sec\phi\,Sin\theta\,Sin2\theta)\dot{\phi}\dot{\theta} - 4b\,Cosec2\alpha\,Sec\phi\,Sin\theta\dot{\theta}^2 - (R - 2b\,Cosec2\alpha\,Sec\phi\,Cos\theta)\ddot{\theta}]$$

$$= -Tan\phi\{R\,Sin\theta\,(Sin^2\theta + Cos^2\theta) + b\,Sec\phi\,(Tan\alpha - 2\,Cosec2\alpha\,Sin^2\theta)\,(Sin\theta\,Cos\theta - Sin\theta\,Cos\theta)\}\ddot{\phi} - \{R\,Sin\theta\,(Sin^2\theta + Cos^2\theta) + b\,Sec\phi\,(Sec^2\phi + Tan^2\phi)\,(Tan\alpha - 2\,Cosec2\alpha\,Sin^2\theta)\,(Sin\theta\,Cos\theta - Sin\theta\,Cos\theta)\}\dot{\phi}^2 - 2\,Tan\phi\{R\,Cos\theta\,(Sin^2\theta + Cos^2\theta) - 2b\,Cosec2\alpha\,Sec\phi\,Sin2\theta\,(Sin\theta\,Cos\theta - Sin\theta\,Cos\theta)\}\dot{\phi}\dot{\theta} - \{R\,Sin\theta - 4b\,Cosec2\alpha\,Sec\phi\,(Sin\theta\,Cos\theta + Sin\theta\,Cos\theta)\}\dot{\theta}^2 + \{R\,Cos\theta + 2b\,Cosec2\alpha\,Sec\phi$$

($Sin^2\theta$.../ Page 74

$(\mathrm{Sin}^2\theta-\mathrm{Cos}^2\theta)\}\ddot{\theta} = -R\mathrm{Tan}\phi\mathrm{Sin}\theta\ddot{\phi}-R\mathrm{Sin}\theta\dot{\phi}^2-2R\mathrm{Tan}\phi\mathrm{Cos}\theta\dot{\phi}\dot{\theta}-(R\mathrm{Sin}\theta-4b\mathrm{Cosec}2\alpha\mathrm{Sec}\phi\mathrm{Sin}2\theta)\dot{\theta}^2+(R\mathrm{Cos}\theta-2b\mathrm{Cosec}2\alpha\mathrm{Sec}\phi\mathrm{Cos}2\theta)\ddot{\theta}$

Hence

$\ddot{x}_1+\frac{2k}{M}x_1-(R\mathrm{Cos}\phi\mathrm{Sin}\theta-b\mathrm{Cosec}2\alpha\mathrm{Sec}^2\phi\mathrm{Sin}2\theta)\ddot{\phi}+(R\mathrm{Sin}\phi\mathrm{Sin}\theta+2b\mathrm{Cosec}2\alpha\mathrm{Sec}^2\phi\mathrm{Tan}\phi\mathrm{Sin}2\theta)\dot{\phi}^2-2(R\mathrm{Cos}\phi\mathrm{Cos}\theta-2b\mathrm{Cosec}2\alpha\mathrm{Sec}^2\phi\mathrm{Cos}2\theta)\dot{\phi}\dot{\theta}+(R\mathrm{Sin}\phi\mathrm{Sin}\theta-4b\mathrm{Cosec}2\alpha\mathrm{Tan}\phi\mathrm{Sin}2\theta)\dot{\theta}^2-(R\mathrm{Sin}\phi\mathrm{Cos}\theta-2b\mathrm{Cosec}2\alpha\mathrm{Tan}\phi\mathrm{Cos}2\theta)\ddot{\theta}$

$-R\mathrm{Tan}\phi\mathrm{Sin}\phi\mathrm{Sin}\theta\ddot{\phi}-R\mathrm{Sin}\phi\mathrm{Sin}\theta\dot{\phi}^2-2R\mathrm{Tan}\phi\mathrm{Sin}\phi\mathrm{Cos}\theta\dot{\phi}\dot{\theta}-(R\mathrm{Sin}\theta-4b\mathrm{Cosec}2\alpha\mathrm{Sec}\phi\mathrm{Sin}2\theta)\mathrm{Sin}\phi\dot{\theta}^2+(R\mathrm{Cos}\theta-2b\mathrm{Cosec}2\alpha\mathrm{Sec}\phi\mathrm{Cos}2\theta)\mathrm{Sin}\phi\ddot{\theta}$

$-\mu\mathrm{Sec}\alpha[g\mathrm{Cos}\theta-\mathrm{Tan}\phi\{R\mathrm{Sin}^2\theta+b\mathrm{Sec}\phi\mathrm{Cos}\theta(\mathrm{Tan}\alpha-2\mathrm{Cosec}2\alpha\mathrm{Sin}^2\theta)\}\ddot{\phi}-\{R\mathrm{Sin}^2\theta+b\mathrm{Sec}\phi\mathrm{Cos}\theta(\mathrm{Sec}^2\phi+\mathrm{Tan}^2\phi)(\mathrm{Tan}\alpha-2\mathrm{Cosec}2\alpha\mathrm{Sin}^2\theta)\}\dot{\phi}^2-2\mathrm{Tan}\phi(R\mathrm{Sin}\theta\mathrm{Cos}\theta-2b\mathrm{Cosec}2\alpha\mathrm{Sec}\phi\mathrm{Cos}\ \mathrm{in}2\theta)\dot{\phi}\dot{\theta}-(R-4b\mathrm{Cosec}2\alpha\mathrm{Sec}\phi\mathrm{Cos}\theta)\dot{\theta}^2+2b\mathrm{Cosec}2\alpha\mathrm{Sec}\phi\mathrm{Sin}\theta\ddot{\theta} = 0$

$\ddot{x}_1+\frac{2k}{M}x_1-\mu g\mathrm{Sec}\alpha\mathrm{Cos}\theta+\{R\mathrm{Sin}\theta(-\mathrm{Cos}\phi-\mathrm{Tan}\phi\mathrm{Sin}\phi)+b\mathrm{Cosec}2\alpha\mathrm{Sec}^2\phi\mathrm{Sin}2\theta+\mu R\mathrm{Sec}\alpha\mathrm{Sin}^2\theta+\mu b\mathrm{Sec}\alpha\mathrm{Sec}\phi\mathrm{Cos}\theta(\mathrm{Tan}\alpha-2\mathrm{Cosec}2\alpha\mathrm{Sin}^2\theta)\}\ddot{\phi}+\{R(\mathrm{Sin}\phi\mathrm{Sin}\theta-\mathrm{Sin}\phi\mathrm{Sin}\theta)+\mu R\mathrm{Sec}\alpha\mathrm{Tan}\phi\mathrm{Sin}^2\theta+2b\mathrm{Cosec}2\alpha\mathrm{Sec}^2\phi\mathrm{Tan}\phi\mathrm{Sin}2\theta+\mu b\mathrm{Sec}\alpha\mathrm{Sec}\phi\mathrm{Cos}\theta(\mathrm{Sec}^2\phi+\mathrm{Tan}^2\phi)(\mathrm{Tan}\alpha-2\mathrm{Cosec}2\alpha\mathrm{Sin}^2\theta)\}\dot{\phi}^2$

-2{RCosθ.../Page 75

$$-2\{R\cos\theta(\cos\phi+\tan\phi\sin\phi)+\mu R\sec\alpha\tan\phi\sin\theta\cos\theta-2b\operatorname{cosec}2\alpha\sec^2\phi\cos2\theta$$

$$-2\mu b\sec\alpha\operatorname{cosec}2\alpha\sec\phi\cos\theta\sin2\theta\}\dot{\phi}\dot{\theta}+\{R(\sin\phi\sin\theta-\sin\phi\sin\theta)$$

$$+\mu R\sec\alpha-4b\operatorname{cosec}2\alpha\tan\phi\sin2\theta-4\mu b\operatorname{cosec}2\alpha\sec\alpha\sec\phi\cos\theta\}\dot{\theta}^2$$

$$-\{R(\sin\phi\cos\theta-\sin\phi\cos\theta)-2b\operatorname{cosec}2\alpha(\tan\phi-\sec\phi\sin\phi)\cos2\theta$$

$$-2\mu b\operatorname{cosec}2\alpha\sec\alpha\sec\phi\sin\theta\}\ddot{\theta} = 0$$

$$\ddot{x}_1+\frac{2k}{M}x_1-\mu g\sec\alpha\cos\theta+\{R\sin\theta(\mu\sec\alpha\sin\theta-\sec\phi)+\mu b\sec\alpha\tan\alpha\sec\phi\cos\theta+$$

$$b\operatorname{cosec}2\alpha\sec\phi\sin2\theta(\sec\phi-\mu\sec\alpha\sin\theta)\}\ddot{\phi}+\{\mu R\sec\alpha\sin^2\theta+2b\operatorname{cosec}2\alpha\times$$

$$\sec^2\phi\tan\phi\sin2\theta+\mu b\sec\alpha\sec\phi\cos\theta(\sec^2\phi+\tan^2\phi)(\tan\alpha-2\operatorname{cosec}2\alpha\times$$

$$\sin^2\theta)\}\dot{\phi}^2-2\{R\sec\phi\cos\theta(1+\mu\sec\alpha\sin\phi\sin\theta)-2b\operatorname{cosec}2\alpha\sec\phi(\sec\phi\cos2\theta+$$

$$\mu\sec\alpha\cos\theta\sin2\theta)\}\dot{\phi}\dot{\theta}+\{\mu R\sec\alpha-4b\operatorname{cosec}2\alpha(\tan\phi\sin2\theta+\sec\alpha\sec\phi\cos\theta)\}\dot{\theta}^2-$$

$$2\mu b\operatorname{cosec}2\alpha\sec\alpha\sin\theta\ddot{\theta} = 0$$

5.10 THE MOMENTS OF THE FORCES ACTING ON THE DICONE ABOUT ITS CENTRE OF MASS

5.10.1 Introduction

In order that the equations of the angular motion of the dicone can be established, it is required that the moments of the various forces acting on the dicone about its centre of mass should be known. The coordinates of these moments will be measured in the $O''\xi_1\xi_2\xi_3$ coordinate axes frame.

5.10.2 The moments of the spring forces about the centre of mass of the dicone

The spring forces acting on the dicone were found in Section 5.8.2 to be

$-k(x_1-B\text{Tan}\phi)$ and $-k(x_1+B\text{Tan}\phi)$

for the left- and right-hand springs respectively. Since the spring forces have been assumed to act in the horizontal direction, the moments of the forces can be considered to be acting in the $O'\eta_1\eta_2\eta_3$ coordinate axes frame. The centre of mass of the dicone, after it has tilted through the angle θ, has been displaced along the $O'\eta_3$ axis through the distance

$b\text{Cosec}2\alpha\text{Sec}\phi\text{Sin}2\theta - R\text{Sin}\theta$.

The spring forces therefore have a moment about the $O'\eta_2$ axis given by:

$$k(x_1-B\text{Tan}\phi)\{B+(b\text{Cosec}2\alpha\text{Sec}\phi\text{Sin}2\theta-R\text{Sin}\theta)\text{Cos}\phi\}$$

$$-k(x_1+B\text{Tan}\phi)\{B-(b\text{Cosec}2\alpha\text{Sec}\phi\text{Sin}2\theta-R\text{Sin}\theta)\text{Cos}\phi\}$$

$$= 2k\{x_1\text{Cos}\phi(b\text{Cosec}2\alpha\text{Sec}\phi\text{Sin}2\theta-R\text{Sin}\theta)-B^2\text{Tan}\phi\}$$

In the $O''\xi_1\xi_2\xi_3$ coordinate axes frame, this moment would have components:

$$2k\text{Sin}\theta\{x_1\text{Cos}\phi(b\text{Cosec}2\alpha\text{Sec}\phi\text{Sin}2\theta-R\text{Sin}\theta)-B^2\text{Tan}\phi\}$$

along the $O''\xi_1$ axis, and

$$2k\text{Cos}\theta\{x_1\text{Cos}\phi(b\text{Cosec}2\alpha\text{Sec}\phi\text{Sin}2\theta-R\text{Sin}\theta)-B^2\text{Tan}\phi\}$$

along the $O''\xi_2$ axis.

5.10.3 Moments of the normal forces about the centre of mass of the dicone

The normal forces at the contact points were found in Section 5.8.3 to be:

$$\bar{N}_A = \{0 \quad -N_A\text{Cos}\theta \quad N_A\text{Sin}\theta\} \quad \text{and} \quad \{0 \quad -N_B\text{Cos}\alpha \quad -N_B\text{Sin}\alpha\}$$

The position vectors of the contact points with respect to the centre of mass are $\underset{\sim}{a}$ and $\underset{\sim}{b}$, where

$$\bar{a} = \begin{bmatrix} a_1 \\ a_2 \\ a_3 \end{bmatrix} = \begin{bmatrix} 0 \\ R-b\text{Sec}\phi(\text{Tan}\alpha\text{Cos}\theta+\text{Sin}\theta) \\ -b\text{Sec}\phi(\text{Cos}\theta+\text{Cot}\alpha\text{Sin}\theta) \end{bmatrix}, \bar{b} = \begin{bmatrix} b_1 \\ b_2 \\ b_3 \end{bmatrix} = \begin{bmatrix} 0 \\ R-b\text{Sec}\phi(\text{Tan}\alpha\text{Cos}\theta-\text{Sin}\theta) \\ b\text{Sec}\phi(\text{Cos}\theta-\text{Cot}\alpha\text{Sin}\theta) \end{bmatrix}$$

so that some of the moments $\bar{g}_N^*$ is given by

$$\bar{g}_N^* = \begin{bmatrix} g_1 \\ g_2 \\ g_3 \end{bmatrix} = \begin{bmatrix} 0 & -a_3 & a_2 \\ a_3 & 0 & -a_1 \\ -a_2 & a_1 & 0 \end{bmatrix} \begin{bmatrix} 0 \\ -N_A\text{Cos}\alpha \\ +N_A\text{Sin}\alpha \end{bmatrix} + \begin{bmatrix} 0 & -b_3 & b_2 \\ b_3 & 0 & -b_1 \\ -b_2 & b_1 & 0 \end{bmatrix} \begin{bmatrix} 0 \\ -N_B\text{Cos}\alpha \\ -N_B\text{Sin}\alpha \end{bmatrix}$$

$$= \begin{bmatrix} a_3N_A\text{Cos}\alpha+a_2N_A\text{Sin}\alpha+b_3N_B\text{Cos}\alpha-b_2N_B\text{Sin}\alpha \\ -a_1N_A\text{Sin}\alpha+b_1N_B\text{Sin}\alpha \\ -a_1N_A\text{Cos}\alpha-b_1N_B\text{Cos}\alpha \end{bmatrix}$$

$$= \begin{bmatrix} (a_3N_A+b_3N_B)\text{Cos}\alpha+(a_2N_A-b_2N_B)\text{Sin}\alpha \\ 0 \\ 0 \end{bmatrix}$$

since $a_1 = b_1 = 0$

The first line becomes:

$$-b\text{Cos}\alpha\text{Sec}\phi\{N_A(\text{Cos}\theta+\text{Cot}\alpha\text{Sin}\theta) - N_B(\text{Cos}\theta-\text{Cot}\alpha\text{Sin}\theta)\} +$$

$$\text{Sin}\alpha[N_A\{R-b\text{Sec}\phi(\text{Tan}\alpha\text{Cos}\theta+\text{Sin}\theta)\}-N_B\{R-b\text{Sec}\phi(\text{Tan}\alpha\text{Cos}\theta-\text{Sin}\theta)\}]$$

$$= (N_A-N_B)R\text{Sin}\alpha-b\text{Sec}\phi\{(N_A-N_B)(\text{Cos}\alpha+\text{Tan}\alpha\text{Sin}\alpha)\text{Cos}\theta$$

$$+(N_A+N_B)(\text{Cot}\alpha\text{Cos}\alpha+\text{Sin}\alpha)\text{Sin}\theta\}$$

$$= R(N_A-N_B)\text{Sin}\alpha-2b\text{Cosec}2\alpha\text{Sec}\phi\{(N_A-N_B)\text{Sin}\alpha\text{Cos}\theta+(N_A+N_B)\text{Cos}\alpha\text{Sin}\theta\}$$

$$\therefore \frac{1}{M}g^*_{N_1} = \frac{1}{M}[R(N_A-N_B)\text{Sin}\alpha-2b\text{Cosec}2\alpha\{(N_A-N_B)\text{Sin}\alpha\text{Cos}\theta$$

$$+ (N_A+N_B)\text{Cos}\alpha\text{Sin}\theta\}]$$

$$= R[g\text{Sin}\theta+\text{Tan}\phi\{R\text{Sin}\theta\text{Cos}\theta-b\text{Sec}\phi\text{Sin}\theta(\text{Tan}\alpha-2\text{Cosec}2\alpha\text{Sin}^2\theta)\}\ddot{\phi}+$$

$$\{R\text{Sin}\theta\text{Cos}\theta-b\text{Sec}\phi\text{Sin}\theta(\text{Sec}^2\phi+\text{Tan}^2\phi)(\text{Tan}\alpha-2\text{Cosec}2\alpha\text{Sin}^2\theta)\}\dot{\phi}^2+$$

$$2\text{Tan}\phi(R\text{Cos}^2\theta+2b\text{Cosec}2\alpha\text{Sec}\phi\text{Sin}\theta\text{Sin}2\theta)\dot{\phi}\dot{\theta}-4b\text{Cosec}2\alpha\text{Sec}\phi\text{Sin}\theta\dot{\theta}^2-$$

$$(R-2b\text{Cosec}2\alpha\text{Sec}\phi\text{Cos}\theta)\ddot{\theta}]-2b\text{Cosec}2\alpha\text{Sec}\phi\Big[[g\text{Sin}\theta+\text{Tan}\phi\{R\text{Sin}\theta\text{Cos}\theta-$$

$$b\text{Sec}\phi\text{Sin}\theta(\text{Tan}\alpha-2\text{Cosec}2\alpha\text{Sin}^2\theta)\}\ddot{\phi}+\{R\text{Sin}\theta\text{Cos}\theta-b\text{Sec}\phi\text{Sin}\theta(\text{Sec}^2\phi+$$

$$\text{Tan}^2\phi)(\text{Tan}\alpha-2\text{Cosec}2\alpha\text{Sin}^2\theta)\}\dot{\phi}^2+2\text{Tan}\phi(R\text{Cos}^2\theta+2b\text{Cosec}2\alpha\text{Sec}\phi\text{Sin}\theta\text{Sin}2\theta)\dot{\phi}\dot{\theta}-$$

4bCosec2α.../ 79 |

$$4b\text{Cosec}2\alpha\text{Sec}\phi\text{Sin}\theta\dot{\theta}^2-(R-2b\text{Cosec}2\alpha\text{Sec}\phi\text{Cos}\theta)\ddot{\theta}]\text{Cos}\theta+[g\text{Sin}\theta-$$

$$\text{Tan}\phi\{R\text{Sin}^2\theta+b\text{Sec}\phi\text{Cos}\theta(\text{Tan}\alpha-2\text{Cosec}2\alpha\text{Sin}^2\theta)\}\ddot{\phi}-\{R\text{Sin}^2\theta+$$

$$b\text{Sec}\phi\text{Cos}\theta(\text{Sec}^2\phi+\text{Tan}^2\phi)(\text{Tan}\alpha-2\text{Cosec}2\alpha\text{Sin}^2\theta)\}\dot{\phi}^2-2\text{Tan}\phi$$

$$(R\text{Sin}\theta\text{Cos}\theta-2b\text{Cosec}2\alpha\text{Sec}\phi\text{Cos}\theta\text{Sin}2\theta)\dot{\phi}\dot{\theta}-(R-4b\text{Cosec}2\alpha\text{Sec}\phi\text{Cos}\theta)\dot{\theta}^2+$$

$$2b\text{Cosec}2\alpha\text{Sec}\phi\text{Sin}\theta\ddot{\theta}]\text{Sin}\theta\Big] = g(R\text{Sin}\theta-2b\text{Cosec}2\alpha\text{Sec}\phi\text{Sin}2\theta) +$$

$$[R\text{Tan}\phi\{R\text{Sin}\theta\text{Cos}\theta-b\text{Sec}\phi\text{Sin}\theta(\text{Tan}\alpha-2\text{Cosec}2\alpha\text{Sin}^2\theta)\}+2b\text{Cosec}2\alpha\times$$

$$\times\text{Sec}\phi\text{Tan}\phi\{-R\text{Sin}\theta\text{Cos}^2\theta+R\text{Sin}^3\theta+b\text{Sec}\phi(\text{Tan}\alpha-2\text{Cosec}2\alpha\text{Sin}^2\theta)$$

$$(\text{Sin}\theta\text{Cos}\theta+\text{Sin}\theta\text{Cos}\theta)\}]\ddot{\phi}+[R\{R\text{Sin}\theta\text{Cos}\theta-b\text{Sec}\phi\text{Sin}\theta(\text{Sec}^2\phi+\text{Tan}^2\phi)$$

$$(\text{Tan}\alpha-2\text{Cosec}2\alpha\text{Sin}^2\theta)\}+2b\text{Cosec}2\alpha\text{Sec}\phi\{-R\text{Sin}\theta\text{Cos}^2\theta+R\text{Sin}^3\theta+$$

$$b\text{Sec}\phi(\text{Sec}^2\phi+\text{Tan}^2\phi)(\text{Tan}\alpha-2\text{Cosec}2\alpha\text{Sin}^2\theta)(\text{Sin}\theta\text{Cos}\theta+\text{Sin}\theta\text{Cos}\theta)\}]\dot{\phi}^2+$$

$$2\text{Tan}\phi[R(R\text{Cos}^2\theta+2b\text{Cosec}2\alpha\text{Sec}\phi\text{Sin}\theta\text{Sin}2\theta)+4b\text{Cosec}2\alpha\text{Sec}\phi\{-R\text{Cos}^3\theta+$$

$$R\text{Sin}^2\theta\text{Cos}\theta-2b\text{Cosec}2\alpha\text{Sec}\phi\text{Sin}2\theta(\text{Sin}\theta\text{Cos}\theta+\text{Sin}\theta\text{Cos}\theta)]\dot{\phi}\dot{\theta}+$$

$$[-4Rb\text{Cosec}2\alpha\text{Sec}\phi\text{Sin}\theta+2b\text{Cosec}2\alpha\text{Sec}\phi\{4b\text{Cosec}2\alpha\text{Sec}\phi(\text{Sin}\theta\text{Cos}\theta-$$

$$\text{Sin}\theta\text{Cos}\theta)+R\text{Sin}\theta]\dot{\theta}^2+[-R^2+2Rb\text{Cosec}2\alpha\text{Sec}\phi\text{Cos}\theta+2Rb\text{Cosec}2\alpha\text{Sec}\phi\text{Cos}\theta-$$

$$4b^2\text{Cosec}^2 2\alpha\text{Sec}^2\phi(\text{Cos}^2\theta+\text{Sin}^2\theta)]\ddot{\theta} = g(R\text{Sin}\theta-2b\text{Cosec}2\alpha\text{Sec}\phi\text{Sin}2\theta)+$$

$$\text{Tan}\phi[R^2\text{Sin}\theta\text{Cos}\theta-Rb\text{Sec}\phi\{\text{Tan}\alpha-2\text{Cosec}2\alpha\text{Sin}\theta(3\text{Sin}^2\theta-1)\}+$$

$$2b^2\text{Cosec}2\alpha\text{Soc}^2\phi\text{Sin}2\theta(\text{Tan}\alpha-2\text{Cosec}2\alpha\text{Sin}^2\theta)]\ddot{\phi}+[R^2\text{Sin}\theta\text{Cos}\theta-$$

$$Rb\text{Sec}\phi\{\text{Sin}\theta(\text{Sec}^2\phi+\text{Tan}^2\phi)(\text{Tan}\alpha-2\text{Cosec}2\alpha\text{Sin}^2\theta)+2\text{Cosec}2\alpha\text{Tan}\phi$$

Sinθ.../ 80

$$\mathrm{Sin}\theta\mathrm{Cos}2\theta\} + 2b^2\mathrm{Cosec}2\alpha\mathrm{Sec}^2\phi\mathrm{Sin}2\theta(\mathrm{Tan}\alpha - 2\mathrm{Cosec}2\alpha\mathrm{Sin}^2\theta)(\mathrm{Sec}^2\phi + \mathrm{Tan}^2\phi)]\dot{\phi}^2 + 2\mathrm{Tan}\phi[R^2\mathrm{Cos}^2\theta + 2Rb\mathrm{Cosec}2\alpha\mathrm{Sec}\phi\mathrm{Cos}\theta(4\mathrm{Sin}^2\theta - 1) + 4b^2\mathrm{Cosec}^2 2\alpha\mathrm{Sec}^2\phi\mathrm{Sin}^2 2\theta]\dot{\phi}\dot{\theta} - 2Rb\mathrm{Cosec}2\alpha\mathrm{Sec}\phi\mathrm{Sin}\theta\dot{\theta}^2 - (R^2 - 4Rb\mathrm{Cosec}2\alpha\mathrm{Sec}\phi\mathrm{Cos}\theta + 4b^2\mathrm{Cosec}^2 2\alpha\mathrm{Sec}^2\phi)\ddot{\theta}$$

5.10.4 Moments of the tangential forces at the points of contact about the centre of mass of the dicone

From Section 4.8.4,

$$\bar{T}_{A_x} = \{T_A \quad 0 \quad 0\} \quad \text{and} \quad \bar{T}_{B_x} = \{T_B \quad 0 \quad 0\}$$

The tangential tractive force at the left-hand point of contact then has components in the $O''\xi_1\xi_2\xi_3$ coordinate axes frame:

$$\bar{T}_{A_\xi} = \begin{bmatrix} \mathrm{Cos}\phi & 0 & -\mathrm{Sin}\theta \\ \mathrm{Sin}\phi\mathrm{Sin}\theta & \mathrm{Cos}\theta & \mathrm{Cos}\phi\mathrm{Sin}\theta \\ \mathrm{Sin}\phi\mathrm{Cos}\theta & -\mathrm{Sin}\theta & \mathrm{Cos}\phi\mathrm{Cos}\theta \end{bmatrix} \begin{bmatrix} T_A \\ 0 \\ 0 \end{bmatrix} = \begin{bmatrix} T_A\mathrm{Cos}\phi \\ T_A\mathrm{Sin}\phi\mathrm{Sin}\theta \\ T_A\mathrm{Sin}\phi\mathrm{Cos}\theta \end{bmatrix}$$

Similarly, the tangential tractive force at the right-hand point of contact in the $O''\xi_1\xi_2\xi_3$ coordinate axes frame is the column vector

$$\bar{T}_{B_\xi} = \{T_B\mathrm{Cos}\phi \quad T_B\mathrm{Sin}\phi\mathrm{Sin}\theta \quad T_B\mathrm{Sin}\phi\mathrm{Cos}\theta\}$$

Hence the sum of the moments of the tangential tractive forces about the centre of mass of the dicone is given by:

$$\bar{g}_T^* = \begin{bmatrix} 0 & -a_3 & a_2 \\ a_3 & 0 & -a_1 \\ -a_2 & a_1 & 0 \end{bmatrix} \begin{bmatrix} T_A\text{Cos}\phi \\ T_A\text{Sin}\phi\text{Sin}\theta \\ T_A\text{Sin}\phi\text{Cos}\theta \end{bmatrix} + \begin{bmatrix} 0 & -b_3 & b_2 \\ b_3 & 0 & -b_1 \\ -b_2 & b_1 & 0 \end{bmatrix} \begin{bmatrix} T_B\text{Cos}\phi \\ T_B\text{Sin}\phi\text{Sin}\theta \\ T_B\text{Sin}\phi\text{Cos}\theta \end{bmatrix}$$

$$= \begin{bmatrix} T_A\text{Sin}\phi(a_2\text{Cos}\theta - a_3\text{Sin}\theta) + T_B\text{Sin}\phi(b_2\text{Cos}\theta - b_3\text{Sin}\theta) \\ \text{Cos}\phi(T_A a_3 + T_B b_3) \\ -\text{Cos}\phi(T_A a_2 + T_B b_2) \end{bmatrix}$$

where $a_1 = b_1 = 0$

$$\bar{g}_T^* = \begin{bmatrix} \text{Sin}\phi[\text{Cos}\theta[T_A\{R - b\text{Sec}\phi(\text{Tan}\alpha\text{Cos}\theta + \text{Sin}\theta)\} + T_B\{R - b\text{Sec}\phi(\text{Tan}\alpha\text{Cos}\theta \\ \text{Cos}\phi\{-T_A b\text{Sec}\phi(\text{Cos}\theta + \text{Cot}\alpha\text{Sin}\theta) + T_B b\text{Sec}\phi(\text{Cos}\theta\text{Cot}\alpha\text{Sin}\theta)\} \\ -\text{Cos}\phi[T_A\{R - b\text{Sec}\phi(\text{Tan}\alpha\text{Cos}\theta + \text{Sin}\theta)\} + T_B\{R - b\text{Sec}\phi(\text{Tan}\alpha\text{Cos}\theta - \text{Sin}\theta)\}] \end{bmatrix}$$

$$\begin{bmatrix} -\text{Sin}\theta)\}] - b\text{Sec}\phi\text{Sin}\theta\{-T_A(\text{Cos}\theta + \text{Cot}\alpha\text{Sin}\theta) + T_B(\text{Cos}\theta - \text{Cot}\alpha\text{Sin}\theta)\}] \end{bmatrix}$$

$$= \begin{bmatrix} (T_A + T_B)(R\text{Sin}\phi\text{Cos}\theta + 2b\text{Cosec}2\alpha\text{Sin}\overline{\alpha+\theta}\text{Sin}\overline{\alpha-\theta}\text{Tan}\phi) \\ -b\{(T_A + T_B)\text{Cot}\alpha\text{Sin}\theta + (T_A - T_B)\text{Cos}\theta\} \\ -R(T_A + T_B)\text{Cos}\phi + b\{(T_A + T_B)\text{Tan}\alpha\text{Cos}\theta + (T_A - T_B)\text{Sin}\theta\} \end{bmatrix}$$

$$= \mu \begin{bmatrix} (N_A + N_B)(R\text{Sin}\phi\text{Cos}\theta + 2b\text{Cosec}2\alpha\text{Sin}\overline{\alpha+\theta}\text{Sin}\overline{\alpha-\theta}\text{Tan}\phi) \\ -b\{(N_A + N_B)\text{Cot}\alpha\text{Sin}\theta + (N_A - N_B)\text{Cos}\theta\} \\ -R(N_A + N_B)\text{Cos}\phi + b\{(N_A + N_B)\text{Tan}\alpha\text{Cos}\theta + (N_A - N_B)\text{Sin}\theta\} \end{bmatrix}$$

Taking each line in turn,

$$g^*_{T_1} = \mu M [g\mathrm{Cos}\theta - \mathrm{Tan}\phi\{R\mathrm{Sin}^2\theta + b\mathrm{Sec}\phi\mathrm{Cos}\theta(\mathrm{Tan}\alpha - 2\mathrm{Cosec}2\alpha\mathrm{Sin}^2\theta)\}\ddot{\phi} -$$

$$\{R\mathrm{Sin}^2\theta + b\mathrm{Sec}\phi\mathrm{Cos}\theta(\mathrm{Sec}^2\phi + \mathrm{Tan}^2\phi)(\mathrm{Tan}\alpha - 2\mathrm{Cosec}2\alpha\mathrm{Sin}^2\theta)\}\dot{\phi}^2 -$$

$$2\mathrm{Tan}\phi(R\mathrm{Sin}\theta\mathrm{Cos}\theta - 2b\mathrm{Cosec}2\alpha\mathrm{Sec}\phi\mathrm{Cos}\theta\mathrm{Sin}2\theta)\dot{\phi}\dot{\theta} - (R - 4b\mathrm{Cosec}2\alpha \times$$

$$\mathrm{Sin}2\theta)\dot{\theta}^2 + 2b\mathrm{Cosec}2\alpha\mathrm{Sec}\phi\mathrm{Sin}\theta\ddot{\theta}](R\mathrm{Sin}\phi\mathrm{Cos}\theta + 2\mathrm{Cosec}2\alpha\mathrm{Sin}\overline{\alpha+\theta}$$

$$\mathrm{Sin}\overline{\alpha-\theta}\mathrm{Tan}\phi)\mathrm{Sec}\alpha$$

$$g^*_{T_2} = -\mu b\{(N_A+N_B)\mathrm{Cot}\alpha\mathrm{Sin}\theta + (N_A-N_B)\mathrm{Cos}\theta\}$$

$$= -\mu b\mathrm{Cosec}\alpha\{(N_A+N_B)\mathrm{Cos}\alpha\mathrm{Sin}\theta + (N_A-N_B)\mathrm{Sin}\alpha\mathrm{Cos}\theta\}$$

Now

$$\frac{1}{M}\{(N_A+N_B)\mathrm{Cos}\alpha\mathrm{Sin}\theta + (N_A-N_B)\mathrm{Sin}\alpha\mathrm{Cos}\theta\}$$

$$= \mathrm{Sin}\theta[g\mathrm{Cos}\theta - \mathrm{Tan}\phi\{R\mathrm{Sin}^2\theta + b\mathrm{Sec}\phi\mathrm{Cos}\theta(\mathrm{Tan}\alpha - 2\mathrm{Cosec}2\alpha\mathrm{Sin}^2\theta)\}\ddot{\phi} -$$

$$\{R\mathrm{Sin}^2\theta + b\mathrm{Sec}\phi\mathrm{Cos}\theta(\mathrm{Sec}^2\phi + \mathrm{Tan}^2\phi)(\mathrm{Tan}\alpha - 2\mathrm{Cosec}2\alpha\mathrm{Sin}^2\theta)\}\dot{\phi}^2 -$$

$$2\mathrm{Tan}\phi(R\mathrm{Sin}\theta\mathrm{Cos}\theta - 2b\mathrm{Cosec}2\alpha\mathrm{Sec}\phi\mathrm{Cos}\theta\mathrm{Sin}2\theta)\dot{\phi}\dot{\theta} - (R - 4b\mathrm{Cosec}2\alpha \times$$

$$\mathrm{Sec}\phi\mathrm{Cos}\theta)\dot{\theta}^2 + 2b\mathrm{Cosec}2\alpha\mathrm{Sec}\phi\mathrm{Sin}\theta\ddot{\theta}] + \mathrm{Cos}\theta[g\mathrm{Sin}\theta + \mathrm{Tan}\phi\{R\mathrm{Sin}\theta\mathrm{Cos}\theta -$$

$$b\mathrm{Sec}\phi\mathrm{Sin}\theta(\mathrm{Tan}\alpha - 2\mathrm{Cosec}2\alpha\mathrm{Sin}^2\theta)\}\ddot{\phi} + \{R\mathrm{Sin}\theta\mathrm{Cos}\theta - b\mathrm{Sec}\phi\mathrm{Sin}\theta(\mathrm{Sec}^2\phi +$$

$$\mathrm{Tan}^2\phi)(\mathrm{Tan}\alpha - 2\mathrm{Cosec}2\alpha\mathrm{Sin}^2\theta)\}\dot{\phi}^2 + 2\mathrm{Tan}\phi(R\mathrm{Cos}^2\theta + 2b\mathrm{Cosec}2\alpha\mathrm{Sec}\phi \times$$

$$\mathrm{Sin}\theta\mathrm{Sin}2\theta)\dot{\phi}\dot{\theta} - 4b\mathrm{Cosec}2\alpha\mathrm{Sec}\phi\mathrm{Sin}\theta\dot{\theta}^2 - (R - 2b\mathrm{Cosec}2\alpha\mathrm{Sec}\phi\mathrm{Cos}\theta)\ddot{\theta}]$$

so

$$g^*_{T_2} = -\mu bM\,\mathrm{Cosec}\alpha[\,g\mathrm{Sin}2\theta+\mathrm{Tan}\phi\{R\mathrm{Sin}\theta\mathrm{Ccs}2\theta-b\mathrm{Sec}\phi\mathrm{Sin}\theta(\mathrm{Tan}\alpha-2\mathrm{Cosec}2\alpha\mathrm{Sin}^2\theta)\ddot{\phi}+\{R\mathrm{Sin}\theta\mathrm{Cos}2\theta-b\mathrm{Sec}\phi\mathrm{Sin}2\theta(\mathrm{Tan}\alpha-2\mathrm{Cosec}2\alpha\mathrm{Sin}^2\theta)\times(\mathrm{Sec}^2\phi+\mathrm{Tan}^2\phi)\}\dot{\phi}^2-2\mathrm{Tan}\phi(R\mathrm{Cos}\theta\mathrm{Cos}2\theta-2b\mathrm{Cosec}2\alpha\mathrm{Sec}\phi\mathrm{Sin}^2 2\theta)\dot{\phi}\dot{\theta}-R\mathrm{Sin}\theta\dot{\theta}^2-(R\mathrm{Cos}\theta-2b\mathrm{Cosec}2\alpha\mathrm{Sec}\phi)\ddot{\theta}]$$

$$g^*_{T_3} = -\mu[R(N_A+N_B)\mathrm{Cos}\phi-b\{(N_A+N_B)\mathrm{Tan}\alpha\,\mathrm{Cos}\theta+(N_A-B_B)\mathrm{Sin}\theta\}]$$

$$= -\mu MR\mathrm{Sec}\alpha\mathrm{Cos}\phi[\,g\mathrm{Cos}\theta-\mathrm{Tan}\phi\{R\mathrm{Sin}^2\theta+b\mathrm{Sec}\phi\mathrm{Cos}\theta(\mathrm{Tan}\alpha-2\mathrm{Cosec}2\alpha\mathrm{Sin}^2\theta)\}\ddot{\phi}-\{R\mathrm{Sin}^2\theta+b\mathrm{Sec}\phi\mathrm{Cos}\theta(\mathrm{Sec}^2\phi+\mathrm{Tan}^2\phi)(\mathrm{Tan}\alpha-2\mathrm{Cosec}2\alpha\mathrm{Sin}^2\theta)\}\dot{\phi}^2-2\mathrm{Tan}\phi(R\mathrm{Sin}\theta\mathrm{Cos}\theta-2b\mathrm{Cosec}2\alpha\mathrm{Sec}\phi\mathrm{Cos}\theta\mathrm{Sin}2\theta)\dot{\phi}\dot{\theta}-(R-4b\mathrm{Cosec}2\alpha\mathrm{Sec}\phi\mathrm{Cos}\theta)\dot{\theta}^2+2b\mathrm{Cosec}2\alpha\mathrm{Sec}\phi\mathrm{Sin}\theta\ddot{\theta}]+\mu Mb[\mathrm{Tan}\alpha\,\mathrm{Sec}\alpha\times\mathrm{Cos}\theta[\,g\mathrm{Cos}\theta-\mathrm{Tan}\phi\{R\mathrm{Sin}^2\theta+b\mathrm{Sec}\phi\mathrm{Cos}\theta(\mathrm{Tan}\alpha-2\mathrm{Cosec}2\alpha\mathrm{Sin}^2\theta)\}\ddot{\phi}-\{R\mathrm{Sin}^2\theta+b\mathrm{Sec}\phi\mathrm{Cos}\theta(\mathrm{Sec}^2\phi+\mathrm{Tan}^2\phi)(\mathrm{Tan}\alpha-2\mathrm{Cosec}2\alpha\mathrm{Sin}^2\theta)\}\dot{\phi}^2-2\mathrm{Tan}\phi(R\mathrm{Sin}\theta\mathrm{Cos}\theta-2b\mathrm{Cosec}2\alpha\mathrm{Sec}\phi\mathrm{Cos}\theta\mathrm{Sin}2\theta)\dot{\phi}\dot{\theta}-(R-4b\mathrm{Cosec}2\alpha\times\mathrm{Sec}\phi\mathrm{Cos}\theta)\dot{\theta}^2+2b\mathrm{Cosec}2\alpha\mathrm{Sec}\phi\mathrm{Sin}\theta\ddot{\theta}]+\mathrm{Cosec}\alpha\mathrm{Sin}\theta[\,g\mathrm{Sin}\theta+\mathrm{Tan}\phi\times\{R\mathrm{Sin}\theta\mathrm{Cos}\theta-b\mathrm{Sec}\phi\mathrm{Sin}\theta(\mathrm{Tan}\alpha-2\mathrm{Cosec}2\alpha\mathrm{Sin}^2\theta)\}\ddot{\phi}+\{R\mathrm{Sin}\theta\mathrm{Cos}\theta-b\mathrm{Sec}\phi\mathrm{Sin}\theta(\mathrm{Sec}^2\phi+\mathrm{Tan}^2\phi)(\mathrm{Tan}\alpha-2\mathrm{Cosec}2\alpha\mathrm{Sin}^2\theta)\}\dot{\phi}^2+2\mathrm{Tan}\phi(R\mathrm{Cos}^2\theta+2b\mathrm{Cosec}2\alpha\mathrm{Sec}\phi\mathrm{Sin}\theta\mathrm{Sin}2\theta)\dot{\phi}\dot{\theta}-4b\mathrm{Cosec}2\alpha\mathrm{Sec}\phi\mathrm{Sin}\theta\dot{\theta}^2-(R-2b\mathrm{Cosec}2\alpha\mathrm{Sec}\phi\mathrm{Cos}\theta)\ddot{\theta}]]$$

$$g_{T_3} = \mu M[g\{-R\mathrm{Sec}\alpha\mathrm{Cos}\phi\mathrm{Cos}\theta+b(\mathrm{Tan}\alpha\mathrm{Sec}\alpha\mathrm{Cos}^2\theta+\mathrm{Cosec}\alpha\mathrm{Sin}^2\theta)+$$

$$\mathrm{Tan}\phi\{R^2\mathrm{Sec}\alpha\mathrm{Cos}\phi\mathrm{Sin}^2\theta+Rb\mathrm{Sec}\alpha\mathrm{Cos}\theta(\mathrm{Tan}\alpha-2\mathrm{Cosec}2\alpha\mathrm{Sin}^2\theta)+$$

$$Rb\mathrm{Sin}^2\theta\mathrm{Cos}\theta(\mathrm{Cosec}\alpha-\mathrm{Tan}\alpha\mathrm{Sec}\alpha)-b^2\mathrm{Sec}\phi(\mathrm{Tan}\alpha-2\mathrm{Cosec}2\alpha\mathrm{Sin}^2\theta)\times$$

$$(\mathrm{Tan}\alpha\mathrm{Sec}\alpha\mathrm{Cos}^2\theta+\mathrm{Cosec}\alpha\mathrm{Sin}^2\theta)\}\ddot{\phi}+\{R^2\mathrm{Sec}\alpha\mathrm{Cos}\phi\mathrm{Sin}^2\theta+Rb\mathrm{Sec}\alpha\mathrm{Cos}\theta\times$$

$$(\mathrm{Sec}^2\phi+\mathrm{Tan}^2\phi)(\mathrm{Tan}\alpha-2\mathrm{Cosec}2\alpha\mathrm{Sin}^2\theta)+Rb\mathrm{Sin}^2\theta\mathrm{Cos}\theta(\mathrm{Cosec}\alpha-\mathrm{Tan}\alpha\mathrm{Sec}\alpha)-$$

$$b^2\mathrm{Sec}\phi(\mathrm{Tan}\alpha-2\mathrm{Cosec}2\alpha\mathrm{Sin}^2\theta)(\mathrm{Tan}\alpha\mathrm{Sec}\alpha\mathrm{Cos}^2\theta+\mathrm{Cosec}\alpha\mathrm{Sin}^2\theta)\}\dot{\phi}^2+$$

$$2\mathrm{Tan}\phi\{R^2\mathrm{Sec}\alpha\mathrm{Cos}\phi\mathrm{Sin}\theta\mathrm{Cos}\theta-2Rb\mathrm{Cosec}2\alpha\mathrm{Sec}\alpha\mathrm{Cos}\theta\mathrm{Sin}2\theta+2Rb(\mathrm{Cosec}\alpha-$$

$$\mathrm{Tan}\alpha\mathrm{Sec}\alpha)\mathrm{Sin}\theta\mathrm{Cos}^2\theta+2b^2\mathrm{Cosec}2\alpha\mathrm{Sec}\phi\mathrm{Sin}2\theta(\mathrm{Tan}\alpha\mathrm{Sec}\alpha\mathrm{Cos}^2\theta+$$

$$\mathrm{Cosec}\alpha\mathrm{Sin}^2\theta)\}\dot{\phi}\dot{\theta}+\{R^2\mathrm{Sec}\alpha\mathrm{Cos}\phi-4Rb\mathrm{Cosec}2\alpha\mathrm{Sec}\alpha\mathrm{Cos}\theta-Rb\mathrm{Tan}\alpha\mathrm{Sec}\alpha\mathrm{Cos}\theta+$$

$$4b^2\mathrm{Cosec}2\alpha\mathrm{Sec}\phi(\mathrm{Sec}\alpha\mathrm{Tan}\alpha\mathrm{Cos}^2\theta-\mathrm{Cosec}\alpha\mathrm{Sin}^2\theta)\}\dot{\theta}^2-b\{R\mathrm{Sin}\theta(2\mathrm{Cosec}2\alpha\times$$

$$\mathrm{Sec}\alpha+\mathrm{Cosec}\alpha)-2b\mathrm{Cosec}2\alpha\mathrm{Sec}\phi\mathrm{Sin}\theta\mathrm{Cos}\theta(\mathrm{Tan}\alpha\mathrm{Sec}\alpha+\mathrm{Cosec}\alpha)\}\ddot{\theta}]$$

$$= \mu M[g\{b(\mathrm{Cosec}\alpha-2\mathrm{Sec}\alpha\mathrm{Cot}2\alpha\mathrm{Cos}^2\theta)-R\mathrm{Sec}\alpha\mathrm{Cos}\phi\mathrm{Cos}\theta\}+\mathrm{Tan}\phi\{R^2\mathrm{Sec}\alpha\times$$

$$\mathrm{Cos}\phi\mathrm{Sin}^2\theta+Rb\mathrm{Sec}\alpha\mathrm{Tan}\alpha\mathrm{Cos}\theta\mathrm{Cos}2\theta-b^2\mathrm{Sec}\phi(\mathrm{Tan}\alpha-2\mathrm{Cosec}2\alpha\mathrm{Sin}^2\theta)\times$$

$$(\mathrm{Tan}\alpha\mathrm{Sec}\alpha\mathrm{Cos}^2\theta+\mathrm{Cosec}\alpha\mathrm{Sin}^2\theta)\}\ddot{\phi}+\{R^2\mathrm{Sec}\alpha\mathrm{Cos}\phi\mathrm{Sin}^2\theta+Rb\mathrm{Sec}\alpha\mathrm{Cos}\theta\times$$

$$(\mathrm{Sec}^2\phi+\mathrm{Tan}^2\phi)(\mathrm{Tan}\alpha-2\mathrm{Cosec}2\alpha\mathrm{Sin}^2\theta)+Rb\mathrm{Sec}\alpha\mathrm{Cot}2\alpha\mathrm{Sin}^2\theta\mathrm{Cos}\theta-$$

$$b^2\mathrm{Sec}\phi(\mathrm{Tan}\alpha-2\mathrm{Cosec}2\alpha\mathrm{Sin}^2\theta)(\mathrm{Tan}\alpha\mathrm{Sec}\alpha\mathrm{Cos}^2\theta+\mathrm{Cosec}\alpha\mathrm{Sin}^2\theta)\}\dot{\phi}^2+$$

$$2\mathrm{Tan}\phi\{R^2\mathrm{Sec}\alpha\mathrm{Cos}\phi\mathrm{Sin}\theta\mathrm{Cos}\theta-4Rb\mathrm{Sec}\alpha\mathrm{Tan}\alpha\mathrm{Sin}\theta\mathrm{Cos}^2\theta+2b^2\mathrm{Cosec}2\alpha\times$$

$\mathrm{Sec}\alpha\mathrm{Cos}\theta.../85$

$$\mathrm{Sec}\alpha\mathrm{Cos}\theta\mathrm{Sin}2\theta(\mathrm{Tan}\alpha\mathrm{Sec}\alpha\mathrm{Cos}^2\theta+\mathrm{Cosec}\alpha\mathrm{Sin}^2\theta)\}\dot{\phi}\dot{\theta}+\{R^2\mathrm{Sec}\alpha\mathrm{Cos}\theta-$$

$$Rb\mathrm{Sec}\alpha\mathrm{Cos}\theta(4\mathrm{Cosec}2\alpha-\mathrm{Tan}\alpha)+8b^2\mathrm{Cosec}2\alpha\mathrm{Sec}\alpha\mathrm{Sin}\overline{\alpha+\vartheta}\mathrm{Sin}\overline{\alpha-\theta}\}\dot{\theta}^2-$$

$$b\{R\mathrm{sin}\theta(2b\mathrm{Cosec}2\alpha\mathrm{Sec}\alpha+\mathrm{Cosec}\alpha)-4b\mathrm{Cosec}^2 2\alpha\mathrm{Sec}\alpha\mathrm{Sec}\phi\mathrm{Sin}\theta\mathrm{Cos}\theta\}\ddot{\theta}]$$

Again, these equations will be used to complete the equations of angular motion.

5.11 THE EQUATIONS OF ANGULAR MOTION

5.11.1 Derivations of the equations of angular motion

The angular velocity of the $O''\xi_1\xi_2\xi_3$ coordinate axes frame was given in Section 5.6.3 as the column vector

$$\bar{\omega}_{\varepsilon\,\mathrm{frame}} = \{\dot{\theta} \quad \dot{\phi}\mathrm{Cos}\theta \quad -\dot{\phi}\mathrm{Sin}\theta\}$$

The column vector for the dicone angular velocity was

$$\bar{\omega}_{\varepsilon\,\mathrm{dicone}} = \{\dot{\theta} \quad \dot{\phi}\mathrm{Cos}\theta \quad n-\dot{\phi}\mathrm{Sin}\theta\}$$

The moment of momentum of the dicone, $\bar{h}$, is then given by:

$$\bar{h} = \bar{\bar{J}}\bar{\omega}_{\varepsilon\,\mathrm{dicone}} = \begin{bmatrix} J_1 & 0 & 0 \\ 0 & J_2 & 0 \\ 0 & 0 & J_3 \end{bmatrix} \begin{bmatrix} \dot{\theta} \\ \dot{\phi}\mathrm{Cos}\theta \\ n-\dot{\phi}\mathrm{Sin}\theta \end{bmatrix} \cdot \begin{bmatrix} J_1\dot{\theta} \\ J_2\dot{\phi}\mathrm{Cos}\theta \\ J_3(n-\dot{\phi}\mathrm{Sin}\theta) \end{bmatrix}$$

The sum of the moments of the forces applied to the dicone about its centre of mass equals the time rate of change of its moment of momentum, that is,

$$\bar{g}^* = \dot{\bar{h}} = \frac{d}{dt}(\bar{\bar{J}}\bar{\omega})$$

$$= \bar{\bar{J}}\dot{\bar{\omega}} + \bar{\bar{\Omega}}\bar{\bar{J}}\bar{\omega}$$

where

$$\bar{g}^* = \bar{\bar{\Sigma}}\bar{g}_i$$

$\bar{g}_i$ is the moment of the ith force applied to the dicone about its centre of mass and where

$$\bar{\bar{\Omega}} = \begin{bmatrix} 0 & -\omega_3 & \omega_2 \\ \omega_3 &) & -\omega_1 \\ & & 0 \end{bmatrix} = \begin{bmatrix} 0 & \dot{\phi}\mathrm{Sin}\theta & \dot{\phi}\mathrm{Cos}\theta \\ -\dot{\phi}\mathrm{Sin}\theta & 0 & -\dot{\theta} \\ -\dot{\phi}\mathrm{Cos}\theta & \dot{\theta} & 0 \end{bmatrix}$$

$$\bar{g}^* = \begin{bmatrix} J_1 & 0 & 0 \\ 0 & J_2 & 0 \\ 0 & 0 & J_3 \end{bmatrix} \begin{bmatrix} \ddot{\theta} \\ \ddot{\phi}\mathrm{Cos}\theta - \dot{\phi}\dot{\theta}\mathrm{Sin}\theta \\ \dot{n} - \ddot{\phi}\mathrm{Sin}\theta - \dot{\phi}\dot{\theta}\mathrm{Cos}\theta \end{bmatrix} +$$

$$= \begin{bmatrix} 0 & \dot{\phi}\mathrm{Sin}\theta & \dot{\phi}\mathrm{Cos}\theta \\ -\dot{\phi}\mathrm{Sin}\theta & 0 & \dot{\theta} \\ -\phi\mathrm{Cos}\theta & \dot{\theta} & 0 \end{bmatrix} \begin{bmatrix} J_1\dot{\theta} \\ J_2\dot{\phi}\mathrm{Cos}\theta \\ J_3(n - \dot{\phi}\mathrm{Sin}\theta) \end{bmatrix}$$

$$= \begin{bmatrix} J_1\ddot{\theta} + \ldots \end{bmatrix} /2$$

$$= \begin{bmatrix} J_1\ddot{\theta}+(J_2-J_3)\dot{\phi}^2\mathrm{Sin}\theta\mathrm{Cos}\theta+J_3n\dot{\phi}\mathrm{Cos}\theta \\ J_2\ddot{\phi}\mathrm{Cos}\theta+(J_3-J_2-J_1)\dot{\phi}\dot{\theta}\mathrm{Sin}\theta-J_3n\dot{\theta} \\ J_3\dot{n}-J_3\ddot{\phi}\mathrm{Sin}\theta-J_3\dot{\phi}\dot{\theta}\mathrm{Cos}\theta+(J_2-J_1)\dot{\phi}\dot{\theta}\mathrm{Cos}\theta \end{bmatrix}$$

$$= \begin{bmatrix} J_1\ddot{\theta}+(J_1-J_3)\dot{\phi}^2\mathrm{Sin}\theta\mathrm{Cos}\theta+J_3n\dot{\phi}\mathrm{Cos}\theta \\ J_2\ddot{\theta}\mathrm{Cos}\theta+(J_3-2J_1)\dot{\phi}\dot{\theta}\mathrm{Sin}\theta-J_3n\dot{\theta} \\ J_3(\dot{n}-\ddot{\phi}\mathrm{Sin}\theta-\dot{\phi}\dot{\theta}\mathrm{Cos}\theta) \end{bmatrix}$$

where, because of the symmetry of the dicone about its major axis,

$J_2 = J_1$

5.11.2 The development of the equations of angular motion

The first line of the matrix equation is

$$\frac{1}{M}\{J_1\ddot{\theta}+(J_1-J_3)\dot{\phi}^2\mathrm{Sin}\theta\mathrm{Cos}\theta+J_3n\dot{\phi}\mathrm{Cos}\theta\}$$

$$= g(R\mathrm{Sin}\theta-2b\mathrm{Cosec}2\alpha\mathrm{Sec}\phi\mathrm{Sin}2\theta)+\mathrm{Tan}\alpha[R^2\mathrm{Sin}\theta\mathrm{Cos}\theta-Rb\mathrm{Sec}\phi\times$$

$$\{\mathrm{Tan}\alpha-2\mathrm{Cosec}2\alpha\mathrm{Sin}\theta(3\mathrm{Sin}^2\theta-1)\}+2b^2\mathrm{Cosec}2\alpha\mathrm{Sec}^2\phi\mathrm{Sin}2\theta(\mathrm{Tan}\alpha-$$

$$2\mathrm{Cosec}2\alpha\mathrm{Sin}^2\theta)]\ddot{\phi}+[R^2\mathrm{Sin}\theta\mathrm{Cos}\theta-Rb\mathrm{Sec}\phi\{2\mathrm{Cosec}2\alpha\mathrm{Tan}\phi\mathrm{Sin}\theta\mathrm{Cos}2\theta+$$

$$\mathrm{Sin}\theta(\mathrm{Sec}^2\phi+\mathrm{Tan}^2\phi)(\mathrm{Tan}\alpha-2\mathrm{Cosec}2\alpha\mathrm{Sin}^2\theta)\}+2b^2\mathrm{Cosec}2\alpha\mathrm{Sec}^2\phi\mathrm{Sin}2\theta\times$$

(Tanα-.../89

$(\mathrm{Tan}\alpha-2\mathrm{Cosec}2\alpha\mathrm{Sin}^2\theta)(\mathrm{Sec}^2\phi+\mathrm{Tan}^2\phi)[\dot{\phi}^2+2\mathrm{Tan}\phi[R^2\mathrm{Cos}^2\theta+$

$2Rb\mathrm{Cosec}2\alpha\mathrm{Sec}\phi\mathrm{Cos}\theta(4\mathrm{Sin}^2\theta-1)+4b^2\mathrm{Cosec}^2 2\alpha\mathrm{Sec}^2\phi\mathrm{Sin}^2 2\theta]\dot{\phi}\dot{\theta}-$

$2Rb\mathrm{Cosec}2\alpha\mathrm{Sec}\phi\mathrm{Sin}\theta\dot{\theta}^2-(R^2-4Rb\mathrm{Cosec}2\alpha\mathrm{Sec}\phi\mathrm{Cos}\theta+4b^2\mathrm{Cosec}^2 2\alpha\times$

$\mathrm{Sec}^2\phi)\ddot{\theta}+\mu\mathrm{Sec}\alpha[g\mathrm{Cos}\theta-\mathrm{Tan}\phi\{R\mathrm{Sin}^2\theta+b\mathrm{Sec}\phi\mathrm{Cos}\theta(\mathrm{Tan}\alpha-2\mathrm{Cosec}2\alpha\mathrm{Sin}^2\theta)\}\ddot{\phi}-$

$\{R\mathrm{Sin}^2\theta+b\mathrm{Sec}\phi\mathrm{Cos}\theta(\mathrm{Sec}^2\phi+\mathrm{Tan}^2\phi)(\mathrm{Tan}\alpha-2\mathrm{Cosec}2\alpha\mathrm{Sin}^2\theta)\}\dot{\phi}^2-$

$2\mathrm{Tan}\phi(R\mathrm{Sin}\theta\mathrm{Cos}\theta-2b\mathrm{Cosec}2\alpha\mathrm{Sec}\phi\mathrm{Cos}\theta\mathrm{Sin}2\theta)\dot{\phi}\dot{\theta}-(R-4b\mathrm{Cosec}2\alpha\mathrm{Sin}2\theta)\dot{\theta}^2+$

$2b\mathrm{Cosec}2\alpha\mathrm{Sec}\phi\mathrm{Sin}\theta\ddot{\theta}](R\mathrm{Sin}\phi\mathrm{Cos}\theta+2b\mathrm{Cosec}2\alpha\mathrm{Sin}\overline{\alpha+\theta}\mathrm{Sin}\overline{\alpha-\theta}\mathrm{Tan}\phi)+$

$2k\mathrm{Sin}\theta\{x_1\mathrm{Cos}\phi(b\mathrm{Cosec}2\alpha\mathrm{Sec}\phi\mathrm{Sin}2\theta-R\mathrm{Sin}\theta)-B^2\mathrm{Tan}\phi\}\frac{1}{M}.$

The second line of the matrix equation is

$\frac{1}{I}\{J_2\ddot{\phi}\mathrm{Cos}\theta+(J_3-2J_1)\dot{\phi}\dot{\theta}\mathrm{Sin}\theta-J_3n\dot{\theta}\}$

$= -\mu b\mathrm{Cosec}\alpha[g\mathrm{Sin}2\theta+\mathrm{Tan}\phi\{R\mathrm{Sin}\theta\mathrm{Cos}2\theta-b\mathrm{Sec}\phi\mathrm{Sin}2\theta(\mathrm{Tan}\alpha-$

$2\mathrm{Cosec}2\alpha\mathrm{Sin}^2\theta)\ddot{\phi}+\{R\mathrm{Sin}\theta\mathrm{Cos}2\theta-b\mathrm{Sec}\phi\mathrm{Sin}2\theta(\mathrm{Tan}\alpha-2\mathrm{Cosec}2\alpha\mathrm{Sin}^2\theta)\times$

$(\mathrm{Sec}^2\phi+\mathrm{Tan}^2\phi)\}\dot{\phi}^2-2\mathrm{Tan}\phi(R\mathrm{Cos}\theta\mathrm{Cos}2\theta-2b\mathrm{Cosec}2\alpha\mathrm{Sec}\phi\mathrm{Sin}^2 2\theta)\dot{\phi}\dot{\theta}-$

$R\mathrm{Sin}\theta\dot{\theta}^2-(R\mathrm{Cos}\theta-2b\mathrm{Cosec}2\alpha\mathrm{Sec}\phi)\ddot{\theta}]+\frac{2k}{M}\{x_1\mathrm{Cos}\phi(b\mathrm{Cosec}2\alpha\mathrm{Sec}\phi\mathrm{Sin}2\theta-$

$R\mathrm{Sin}\theta)-B^2\mathrm{Tan}\phi\}$

The last line of the matrix equation is as follows:

$\frac{J_3}{M}(\dot{n}-\ddot{\phi}\mathrm{Sin}\theta-\dot{\phi}\dot{\theta}\mathrm{Cos}\theta)$

$=\mu[g\{b(\mathrm{Cosec}$ .../89

$$= \mu[g\{b(\mathrm{Cosec}\alpha - 2\mathrm{Sec}\alpha\mathrm{Cot}2\alpha\mathrm{Cos}^2\theta) - R\mathrm{Sec}\alpha\mathrm{Cos}\phi\mathrm{Cos}\theta\} + \mathrm{Tan}\phi\{R^2\mathrm{Sec}\alpha \times$$

$$\mathrm{Cos}\phi\mathrm{Sin}^2\theta + Rb\mathrm{Sec}\alpha\mathrm{Tan}\alpha\mathrm{Cos}\theta\mathrm{Cos}2\theta - b^2\mathrm{Sec}\phi(\mathrm{Tan}\alpha - 2\mathrm{Cosec}2\alpha\mathrm{Sin}^2\theta) \times$$

$$(\mathrm{Tan}\alpha\mathrm{Sec}\alpha\mathrm{Cos}^2\theta + \mathrm{Cosec}\alpha\mathrm{Sin}^2\theta)\}\ddot{\phi} + \{R^2\mathrm{Sec}\alpha\mathrm{Cos}\phi\mathrm{Sin}^2\theta + Rb\mathrm{Sec}\alpha\mathrm{Cos}\theta \times$$

$$(\mathrm{Sec}^2\phi + \mathrm{Tan}^2\phi)(\mathrm{Tan}\alpha - 2\mathrm{Cosec}2\alpha\mathrm{Sin}^2\theta) + Rb\mathrm{Sec}\alpha\mathrm{Cot}2\alpha\mathrm{Sin}^2\theta\mathrm{Cos}\theta -$$

$$b^2\mathrm{Sec}^2\phi(\mathrm{Tan}\alpha - 2\mathrm{Cosec}2\alpha\mathrm{Sin}^2\theta)(\quad\alpha\mathrm{Cos}\alpha\mathrm{Cos}^2\theta + \mathrm{Cosec}\alpha\mathrm{Sin}^2\theta)\}\dot{\phi}^2 +$$

$$2\mathrm{Tan}\phi\{R^2\mathrm{Sec}\alpha\mathrm{Cos}\phi\mathrm{Sin}\theta\mathrm{Cos}\theta - 4Rb\mathrm{Sec}\alpha\mathrm{Tan}\alpha\mathrm{Sin}\theta\mathrm{Cos}^2\theta + 2b^2\mathrm{Cosec}2\alpha$$

$$\mathrm{Sec}\alpha\mathrm{Cos}\quad\mathrm{Sin}2\theta(\mathrm{Tan}\alpha\mathrm{Sec}\alpha\mathrm{Cos}^2\theta + \mathrm{Cosec}\alpha\mathrm{Sin}^2\theta)\}\dot{\phi}\dot{\theta} + \mathrm{Sec}\alpha\{R^2\mathrm{Cos}\theta -$$

$$Rb\mathrm{Cos}\theta(4\mathrm{Cosec}2\alpha - \mathrm{Tan}\alpha) + 8b^2\mathrm{Cosec}2\alpha\mathrm{Sin}\overline{\alpha+\theta}\mathrm{Sin}\overline{\alpha-\theta}\}\dot{\theta}^2 - b\mathrm{Sec}\alpha\mathrm{Sin}\theta \times$$

$$\{R(2b\mathrm{Cosec}2\alpha\mathrm{Sec}\alpha + \mathrm{Cosec}\alpha) - 4b\mathrm{Cosec}^2 2\alpha\mathrm{Sec}\phi\mathrm{Cos}\theta\}\ddot{\theta}]$$

These equations will be discussed in the succeding sections.

5.12 THE FREQUENCY OR CHARACTERISTIC EQUATIONS FOR THE DICONE-RAILS-RESTRAINING SPRINGS DYNAMIC SYSTEM.

5.12.1 The linearising of the equations of motion

The equations of motion which have been derived are lengthy and involved functions of the three variables and the various derivatives of these variables. These variables are x_1, ϕ and θ. In an attempt to derive appropriate meaning from these equations, it is pertinent to investigate the behaviour of the system when these variables are small and whose first order changes in magnitude are regarded

as being of much greater significance than quantities of second and higher order in smallness of magnitude. If only first order changes of magnitude are allowed for, the three equations of angular motion reduce to (taking into account that $J_2 = J_1$):

$$\frac{J_1}{M}\ddot{\theta} + \frac{J_3}{M}n\dot{\phi} = g(R-4b\,\mathrm{Cosec}2\alpha)\theta - (R-2b\,\mathrm{Cosec}2\alpha)^2\ddot{\theta}$$

$$+ \mu g\,\mathrm{Sec}\alpha(R+b\,\mathrm{Tan}\alpha)\phi$$

$$\frac{J_1}{M}\ddot{\phi} - \frac{J_3}{M}n\dot{\theta} = -2\mu gb\,\mathrm{Cosec}\alpha\theta + \mu b\,\mathrm{Cosec}\alpha(R-2b\,\mathrm{Cosec}2\alpha)\ddot{\theta}$$

$$- \frac{2k}{M}B^2\phi$$

$$\frac{J_3}{M}\dot{n} = \mu g\,\mathrm{Sec}\alpha\{(\mathrm{Cot}\alpha - 2\mathrm{Cot}2\alpha)b - R\}$$

The remaining equation is that for the linear movement of the dicone in the directions of the rails. This reduces to:

$$\ddot{x}_1 + \frac{2k}{M}x = \mu g\,\mathrm{Sec}\alpha$$

5.12.2 The characteristic equations of the system

In their linearized form, the equations of motion show that there is no coupling between the linear motion of the dicone and the angular motion; that is, the linear movement of the dicone along the track is not affected by the rotary movement of the dicone, and that the converse is also true. The first two equations for the angular movement relate to the two degrees of rotary freedom of the system (that is, the ability of the dicone to tilt

and to yaw), while the last of the equations for the angular movement shows that, in the linearized form, the rate of change of the dicone speed is independent of the yawing and tilting movements. Since the amount of change of spin speed would be a first order variable in smallness, this change does not alter the linearized forms of the first two equations. To resolve these equations, suppose that

$$\theta = \Theta e^{st} \quad \text{and} \quad \phi = \Phi e^{st}$$

The first two equations for angular movement can then be written in matrix form follows:

$$\begin{bmatrix} \{\frac{J_1}{M} + (R-2b\text{Cosec}2\alpha)^2\}s^2 + g(4b\text{Cosec}2\alpha - R) & \frac{J_3}{M}ns - \mu g\text{Sec}\alpha(R+b\text{Tan}\alpha) \\ \mu b\text{Cosec}\alpha(R-2b\text{Cosec}2\alpha)s^2 - \frac{J_3}{M}ns + 2\mu gb\text{Cosec}\alpha & \frac{J_1}{M}s^2 + \frac{2k}{M}B^2 \end{bmatrix} \begin{bmatrix} \Theta \\ \Phi \end{bmatrix} = \begin{bmatrix} 0 \\ 0 \end{bmatrix}$$

It is convenient to designate the term $2b\text{Cosec}2\alpha - R$ as R^* [1] and likewise the expression

$$J_1 + M(R-2b\text{Cosec}2\alpha)^2 \; (= J_1 + M(-R^*)^2)$$

as J_1^*. The characteristic determinant for the equations of angular motion is

$$\begin{vmatrix} \frac{J_1^*}{M}s^2 + g(2b\text{Cosec}2\alpha + R^*) & \frac{J_3}{M}ns - \mu g\text{Sec}\alpha(R+b\text{Tan}\alpha) \\ -\mu bR^*\text{Cosec}\alpha s^2 - \frac{J_3}{M}ns + 2\mu gb\text{Cosec}\alpha & \frac{J_1}{M}s^2 + \frac{2kB^2}{M} \end{vmatrix} = 0$$

---

(1) This form of R^* has been adopted since $2b\text{Cosec}2\alpha > R$.

so that the characteristic equation is then:

$$\frac{J_1 J_1^*}{M^2}s^4 + \frac{J_3}{M}n\mu bR^*\mathrm{Cosec}\alpha s^3 + \{\frac{J_1}{M}g(2b\mathrm{Cosec}2\alpha+R^*) + \frac{2J_1^*kB^2}{M^2}$$

$$+ (\frac{J_3 n}{M})^2 - 2\mu^2 bR^*\mathrm{Cosec}2\alpha(R+b\mathrm{Tan}\alpha)\}s^2 - \frac{J_3}{M}\mu ng\{R\mathrm{Sec}$$

$$+ b\mathrm{Cosec}\alpha(1+\mathrm{Sec}^2\alpha)\}s + \frac{2kB^2}{M}g(2b\mathrm{Cosec}2\alpha+R^*)$$

$$+ 4\mu^2 g^2 b\mathrm{Cosec}2\alpha(R+b\mathrm{Tan}\alpha) = 0$$

The characteristic equation has been used in Appendix A2 to determine the theoretical frequencies for the system on which the experimental work was done in order that a comparison could be made between the theoretical and experimental values.

CHAPTER 6

DESIGN OF THE TEST RIG (WITH A DESCRIPTION OF SUBSEQUENT MODIFICATIONS)

6.1 INTRODUCTION

In an ideal experimental arrangement, a wheelpair would be caused to t avel along a pair of equidistant, uniform and parallel straight rails. The behaviour of the wheelpair as it travelled along the track would be observed, and this method was actually used by Davies [25] in 1939. A model four-wheeled vehicle was caused to travel an 18,3 m long track with the rails spaced at 24,5 mm. The model was either pulled along the track with a length of string or propelled forward by a rubber rope catapult, with sufficient slope on the track for the vehicle to maintain its speed. Since the path followed by the model was traced by a stylus on waxed paper laid between the rails, this experimental method is reminiscent of the use of a Fletcher's Trolley to demonstrate the acceleration of a falling weight. These model tests were followed by full scale tests which were conducted on a specially built standard gauge, 182,9 m long track, where the path followed by a single wheel pair, or a bogie, was traced onto a board (fixed outside the rails) by a small spring loaded recording wheel. Since the control of the wheelpair possible in such an experimental procedure was far from ideal, it was soon abandoned. Whereas the results

from the two kinds of experiment, model and full-scale, were similar, it was not feasible to lay the full scale track with the accuracy possible for the model test so that inequalities showed up in the full scale tests.

The kinematic equivalent to letting the wheelpair roll along the rails is to restrain it and to let the rails move instead. A problem then arises as to how the rails are to be satisfactorily simulated. Over the past twenty-five years, the accepted method of simulating the rails has been to use roller rigs, whose *modus operandi* is shown in Figure 6.1, which is taken from Althammer [26]. This article describes the latest plant at Munich and compares it with various other installations. Photographs of a relatively small test rig

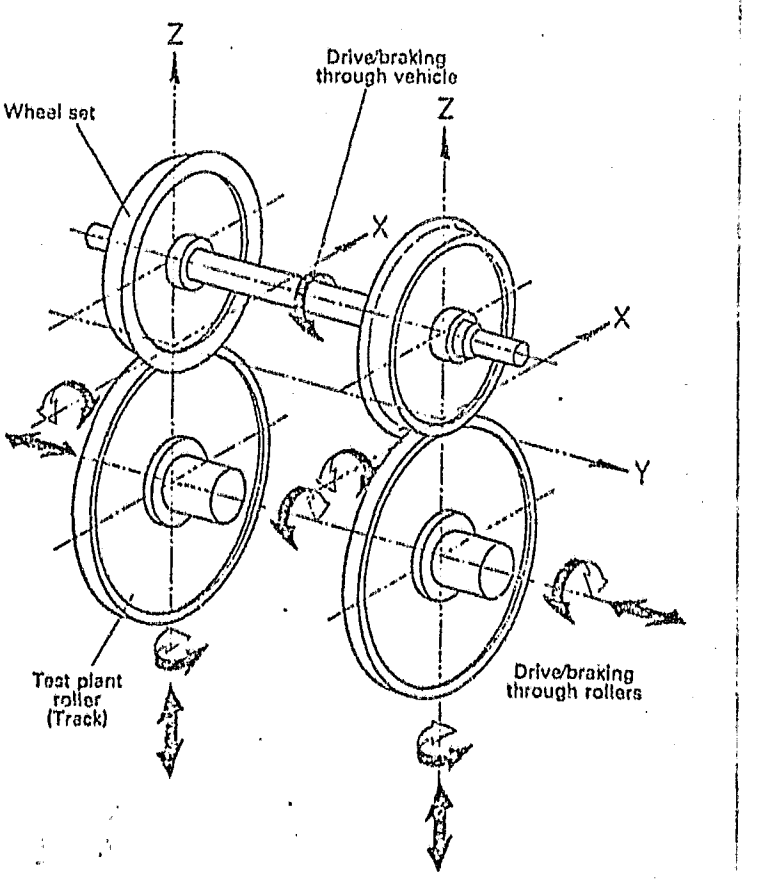

Figure 6.1: POSSIBLE DEGREES OF FREEDOM OF ONE TEST PLANT ROLLER UNIT

and of a full scale test rig are shown in Figure 6.2 and Figure 6.3 respectively.

Roller rigs are a form of environmental testing, regarding which Grootenhuis in his preface to Salter [37] says:

> The assessment of the dynamic responses of every part of the system, however, is very much more difficult and uncertain than its counterpart, static stressing. ... A way out of this impasse is to observe the behaviour of the system during a dynamic test and much of environmental engineering is concerned with testing systems under simulated service conditions. However, does the observer really understand what he is observing and how can he be guided to make the right deductions?

Salter adds to this:

> There is a large range of equipment, extending from micro-miniature components to major sections of spacecraft, which it has become fashionable to subject to a 'vibration-test' at some stage in its design or production.

He then proceeds to discuss how it is possible to misinterpret what one sees and adds:

> We may see some grounds for the disrepute into which certain methods of vibration-tests have fallen.

It is apparent from these discussions on environmental testing that any form of such testing should ensure that the model envisaged during the test corresponds to the reality it is attempting to reproduce. Comments were made towards the end of Chapter 1 that the manner in which the wheelpair moves on a roller rig is different from the straight path which it would follow if it were travelling along rails. There has been some disquiet among railway engineers about roller rigs; thus various types of test rigs were discussed at the International Railways Congress in 1969 and it was

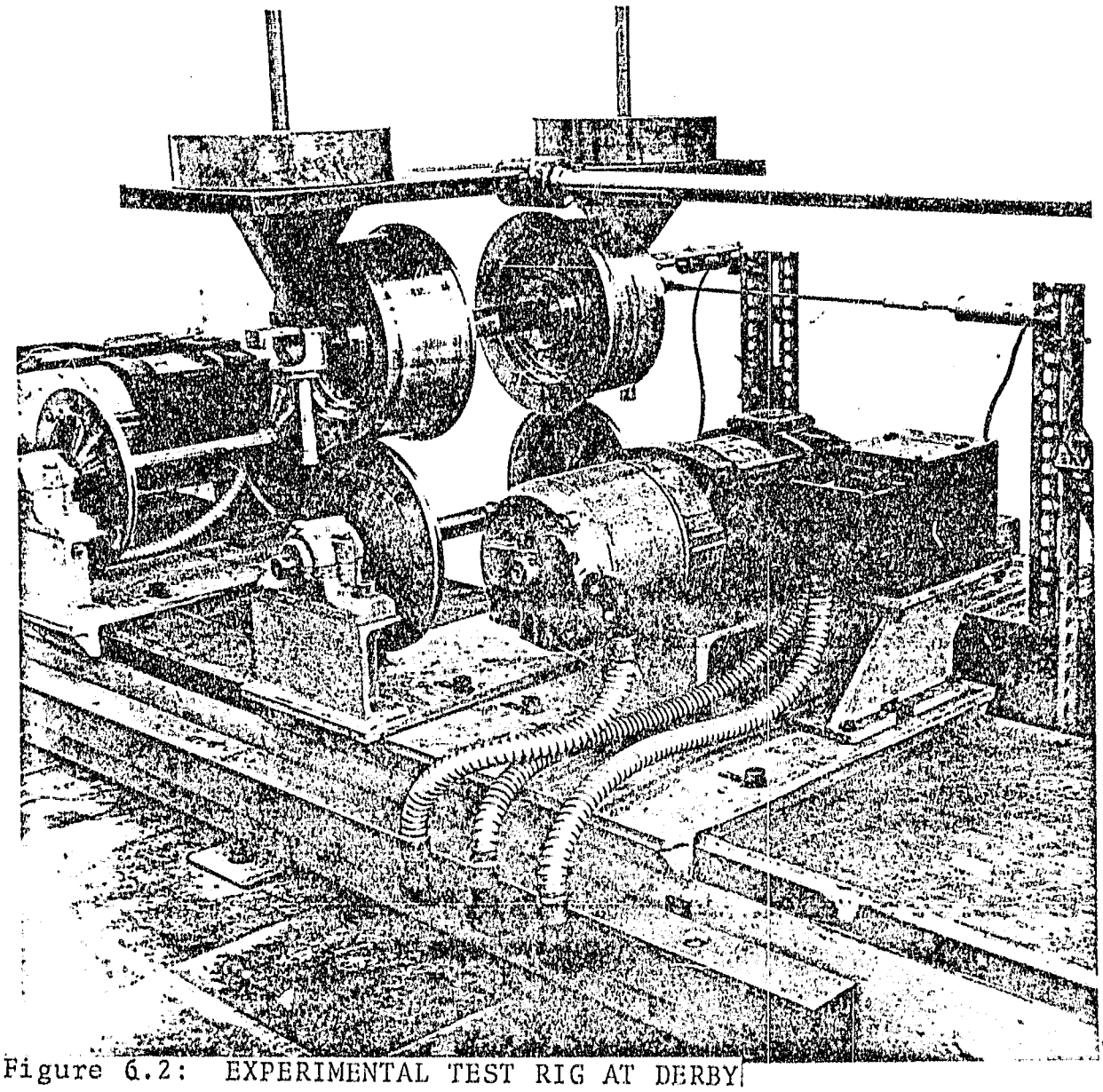

Figure 6.2: EXPERIMENTAL TEST RIG AT DERBY

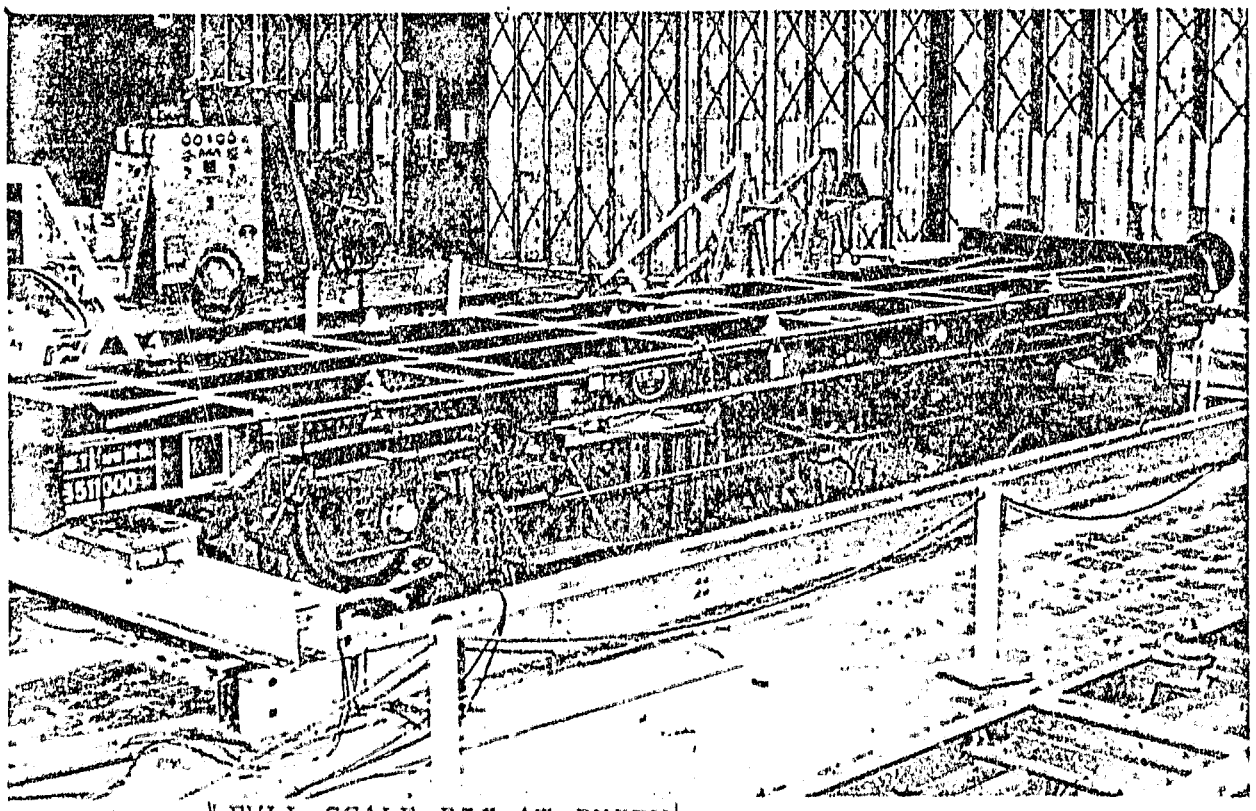

Figure 6.3: FULL SCALE RIG AT DERBY

then stated in a report [38] that

> Generated data that has no meaningful counterpart in the real world is useless and misleading.

What is possible is that in the minds of the users of these rigs, a different form of motion is envisaged and for that reason the details of the experimental rig shown in Figure 6.2 (as given by Wickens [8]) calls for examination:

> The figure shows a one-fifth model elastically restrained wheelset. The wheelset has coned wheels with a wheel tread circle radius of 10.2 cm* and a taper ratio of 0.05. The elastic restraint is provided by a light alloy tube 3.91 m long, which is pivotted at one end and attached to the wheelset at the other. The wheelset is supported on a roller which is driven by a constant speed electric motor through an electro-magnetic induction coupling.

The description of the test rig is tantalizingly brief - indeed it may be thought to be incomplete. It would appear that the axis of the pivot on the elastic restraint is vertical, so that the wheelpair rotates about a point which is 38½ times the wheel tread circle radius distant from the axis of the wheelpair. As a consequence of this method of constraint, the possible angle of yaw which could be experienced by the wheelset is minimal, and for all practical purposes, the motion of the wheelpair is confined to the vertical plane passing through the points of contact. Further, it would seem that it has been reasoned that the single spring force exerted in the direction of the aluminium alloy tube could replace the elastic restraint normally applied to the wheelpair by restraining springs acting on bearings on the wheelpair shaft situated on the outer sides of the wheels. This ignores the fact that the two separate forces which act on

---

*Metric substitutions for the original Imperial units have been made.

the bearings not only provide a resultant in the direction of the track on which the wheelpairs rest but also provide a restraining couple controlling the yaw of the wheelpair.

6.2 DESIGN REQUIREMENTS

It was decided that the approach to the experimental work should, quite deliberately, be different from the procedure followed elsewhere. First of all, the problem to be investigated was to be reduced to its basic minimum; for example, the wheelpair was to have no gravity force other than its own weight imposed on it. The rail simulating surfaces were required to travel in straight lines in the region of contact between the wheels and the corresponding rail simulating surfaces. Forces imposed on the wheelpair shaft in the direction of the rails would resist the forces at the contact points between the wheelpair and the rail simulating surfaces. These forces would also together exercise control over the angular movement of the wheelpair, but unlike the Derby rig, the possible angular movement would not be confined to a small angle of yaw.

6.2.1 Determination of the initial equipment parameters

Before designing a suitable apparatus, it was necessary to decide what cone taper angle should be used. It was thought that the use of a large taper angle of 30° would exaggerate possible hunting tendencies, but the subsequent tests showed that this decision was unwise as such a dicone entirely refused to hunt. Nevertheless, this behaviour is explicable in the light of the theory set out in Chapter 4, and in this way its response was a confirmation of the theory which had been developed.

It was at first thought desirable to attempt to minimise the dicone spin variation and that this end could be achieved through the flywheel effect of a heavy dicone. Royer's theory of shaft energy storage appeared at that stage to be a possible cause of hunting so it was decided that two heavy cast iron cones (which together made up the dicone) would each be clamped to a fairly flexible wheel-pair shaft so as to exaggerate any possible spring energy storage effect in the shaft. The cones were kept in the correct position relative to one another by fitting a clamping ring into grooves machined in each cone base. This ring also offset the possibility that the shaft would bend under the weight of the cones.

12 mm wide steel strips cut to the correct length were to be welded into continuous loops which were wrapped around two sets of 30 cm diameter pulleys to make up the rail simulating surfaces. Only one of the pulleys in each set was to be driven while the other would be an idler which could be moved relative to the driven pulley so that the belt tension could be adjusted. Further requirements were that the steel strip would require support in the region of contact between the strip and the dicone and that some form of horizontal restraint would have to be imposed on the dicone shaft.

6.3 DESIGN AND DEVELOPMENT OF THE FIRST TEST RIG

Before discussing the various details of the design, it is useful to indicate the appearance of the completed rig, which is shown in Figure 6.4(a) without the dicone in position. Since it was planned that the rail simulating surfaces (that is, the steel strip) should make line contac with the sides of the dicone, the pulleys supporting

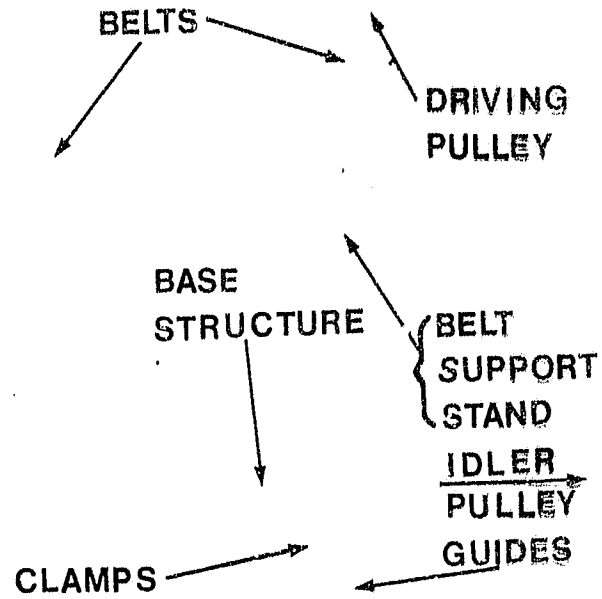
BELTS
DRIVING PULLEY
BASE STRUCTURE
BELT SUPPORT STAND
IDLER PULLEY
GUIDES
CLAMPS

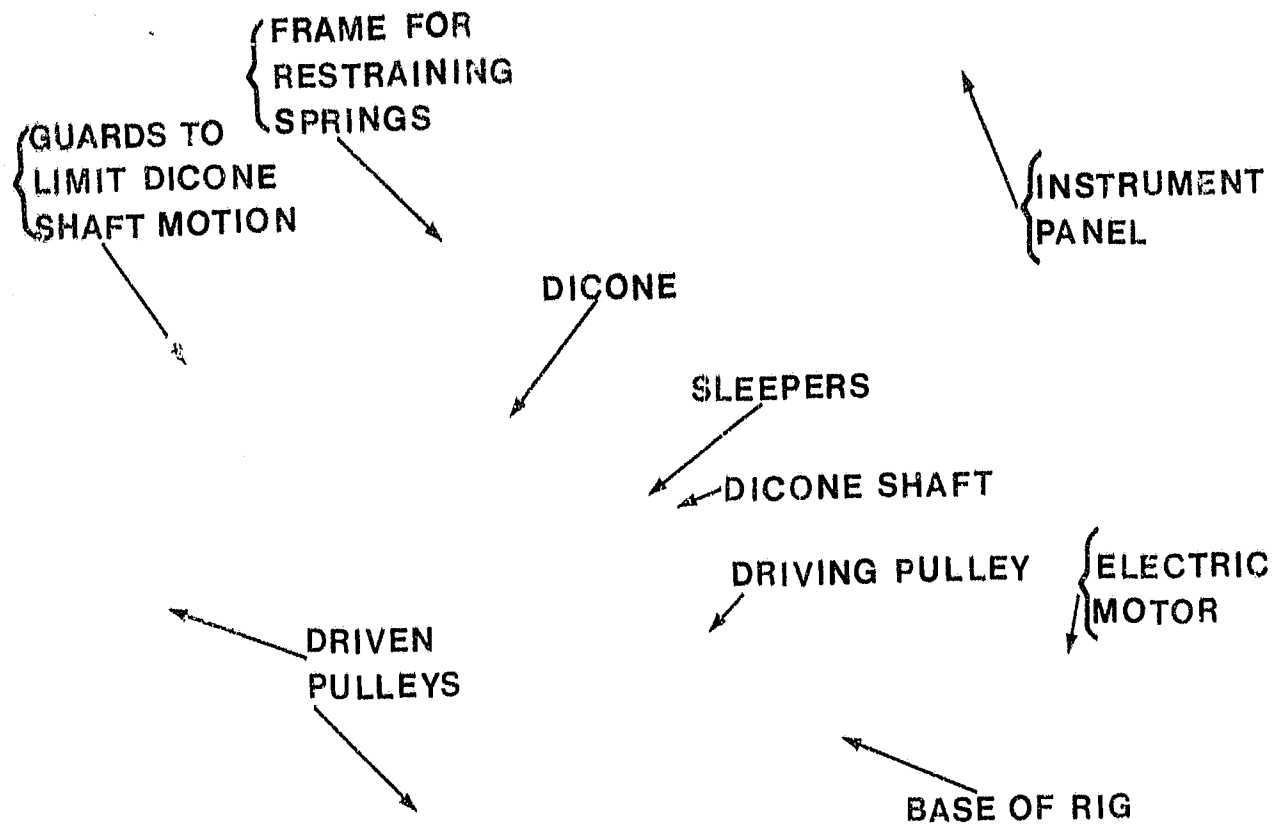
FRAME FOR RESTRAINING SPRINGS
GUARDS TO LIMIT DICONE SHAFT MOTION
INSTRUMENT PANEL
DICONE
SLEEPERS
DICONE SHAFT
DRIVING PULLEY
ELECTRIC MOTOR
DRIVEN PULLEYS
BASE OF RIG

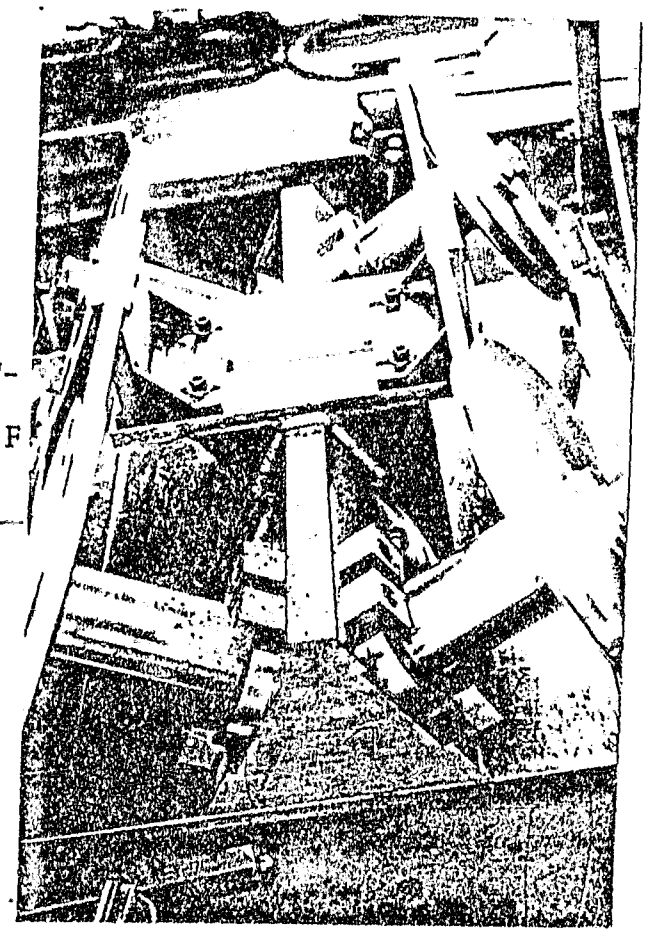

Figure 6.4(a):

WITHOUT DICONE IN POSITION, SHOWING BELTS (OF TRACK) NOTE THE TEFLON STRIPS BELOW THE CENTRE OF THE BELT WHICH CARRY THE WEIGHT OF THE DICONE

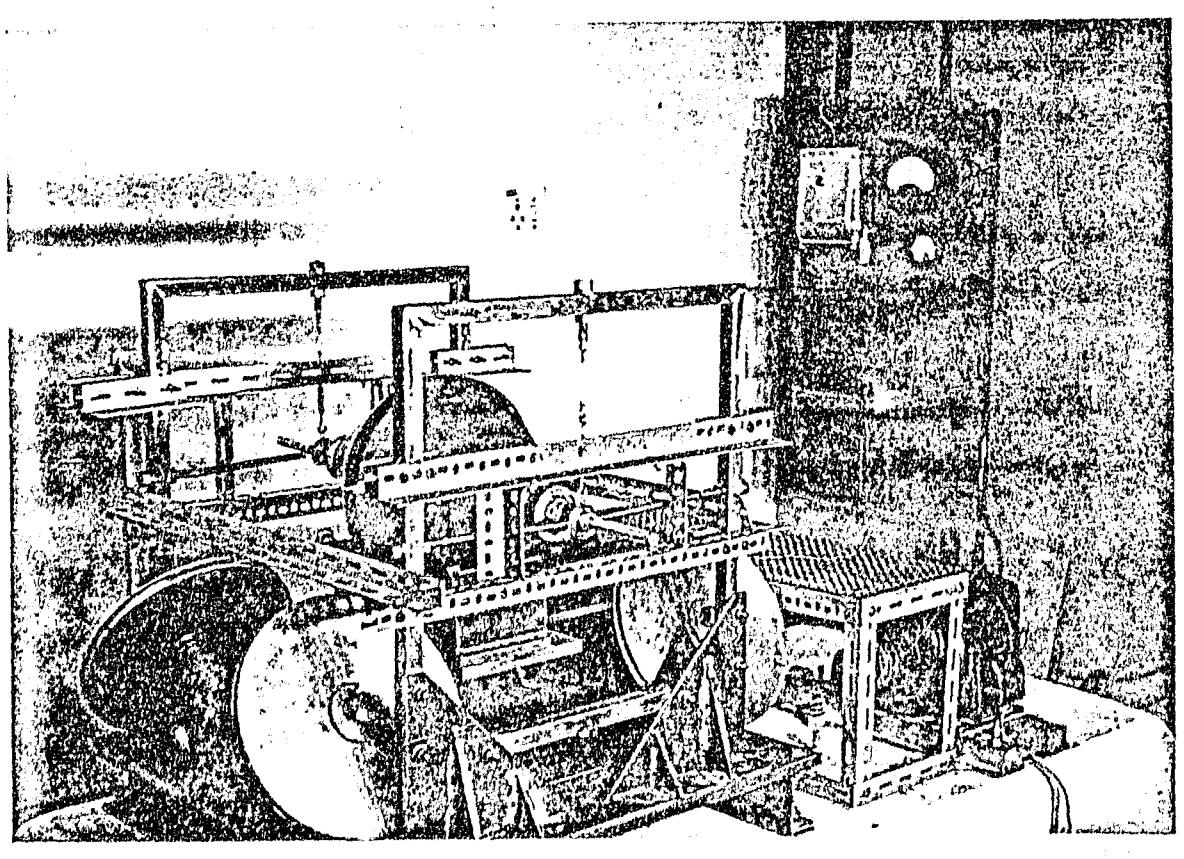

Figure 6.4(b): THE DICONE APPARATUS CAN BE SEEN ON THE BELT WHILE THE DRIVING MOTOR AND ITS INSTRUMENT PANEL IS ON THE RIGHT HAND SIDE

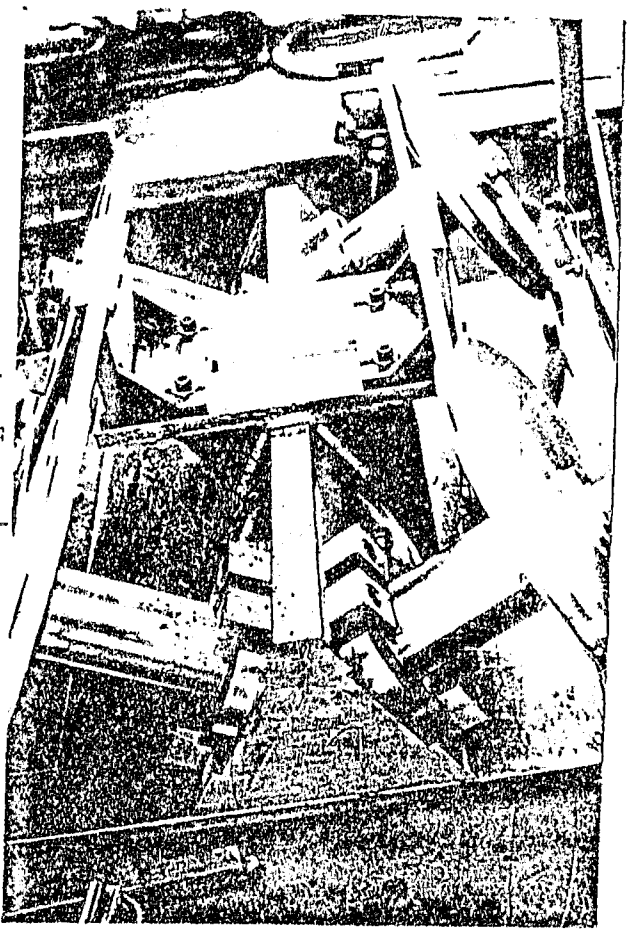

Figure 6.4(a):

WITHOUT DICONE IN POSITION, SHOWING BELTS (OR TRACK) NOTE THE TEFLON STRIPS BELOW THE CENTRE OF THE BELT WHICH CARRY THE WEIGHT OF THE DICONE

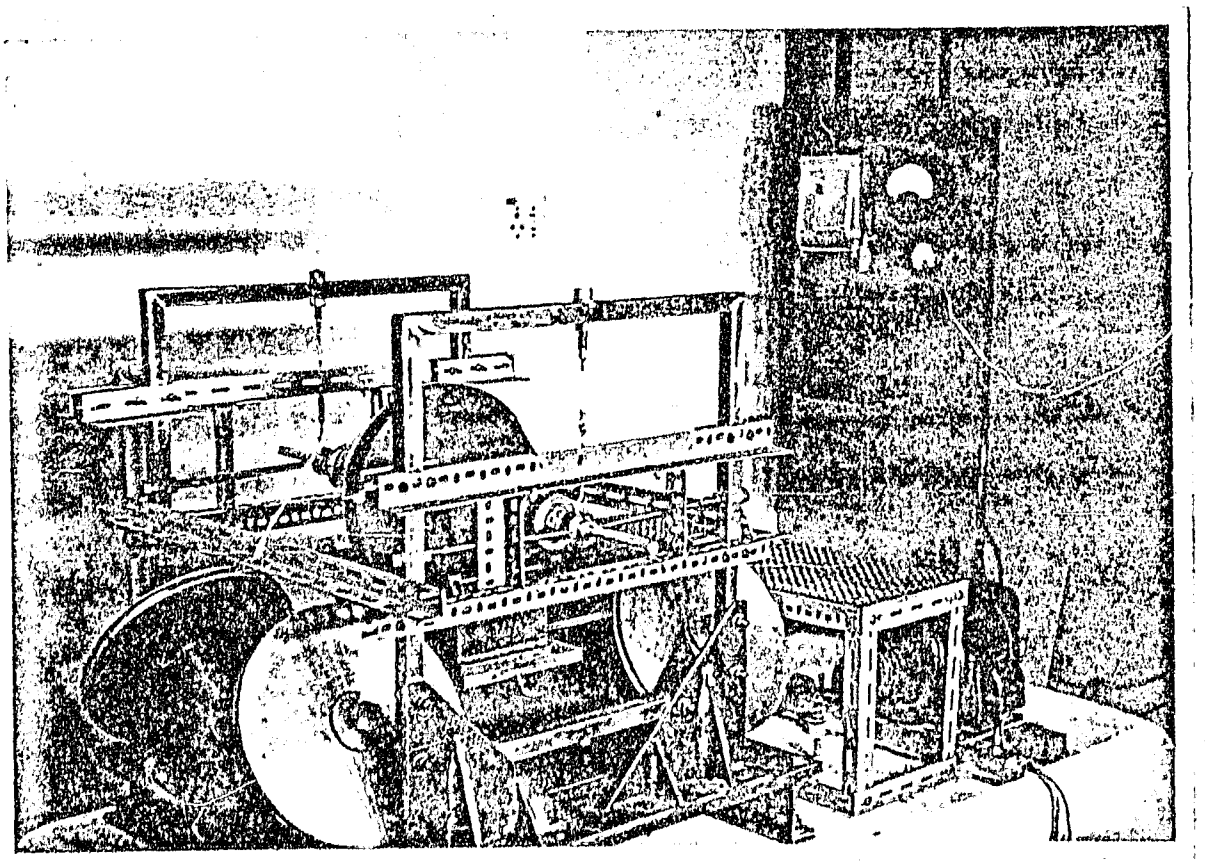

Figure 6.4(b): THE DICONE APPARATUS CAN BE SEEN ON THE BELT WHILE THE DRIVING MOTOR AND ITS INSTRUMENT PANEL IS ON THE RIGHT HAND SIDE

the loops were placed so that the plane of the pulleys was at 30° to the vertical. The steel strip loops fitted to the driving and idler pulleys can be seen in position in the photograph. Figure 6.4(b) shows a side view of the complete rig with the dicone in position and also shows the concrete block on which the rig was mounted, the electric driving motor and the switch board by which the motor was controlled. Details of the design of this rig are given in the following section.

6.3.1 Detailed designs

The square frames made up of square cross-section tubing, which are seen on either side of the rig in Figure 6.4(b), were used to hold the spring points to which the outer end of each restraining spring, which was attached to the dicone shaft sleeve at the other end of the spring, was fastened. These sleeves, which were designed to slide freely along the wheelpair shaft, are shown in Figure 6.5(a). The Dexion angles shown in Figure 6.4(b) were added afterwards to the square frames as a safety measure to restrain the dicone in the event of derailment. An assembled dicone is shown in Figure 6.5(b).

Since the planes of the pulleys were inclined, the pulley drives on the base structure supporting the pulleys had to be designed in accordance with this requirement. An isometric drawing of this part of the rig is shown in Figure 6.6. Fastened to the 13 mm thick steel base plate is a vee-shaped structure which runs the full length of the base. At one end of the vee-structure was an opening through which the drive shaft passed. At the inner end of the drive shaft was a bevel gear which meshed with the bevel fitted to one end of the driven pulley shaft. The

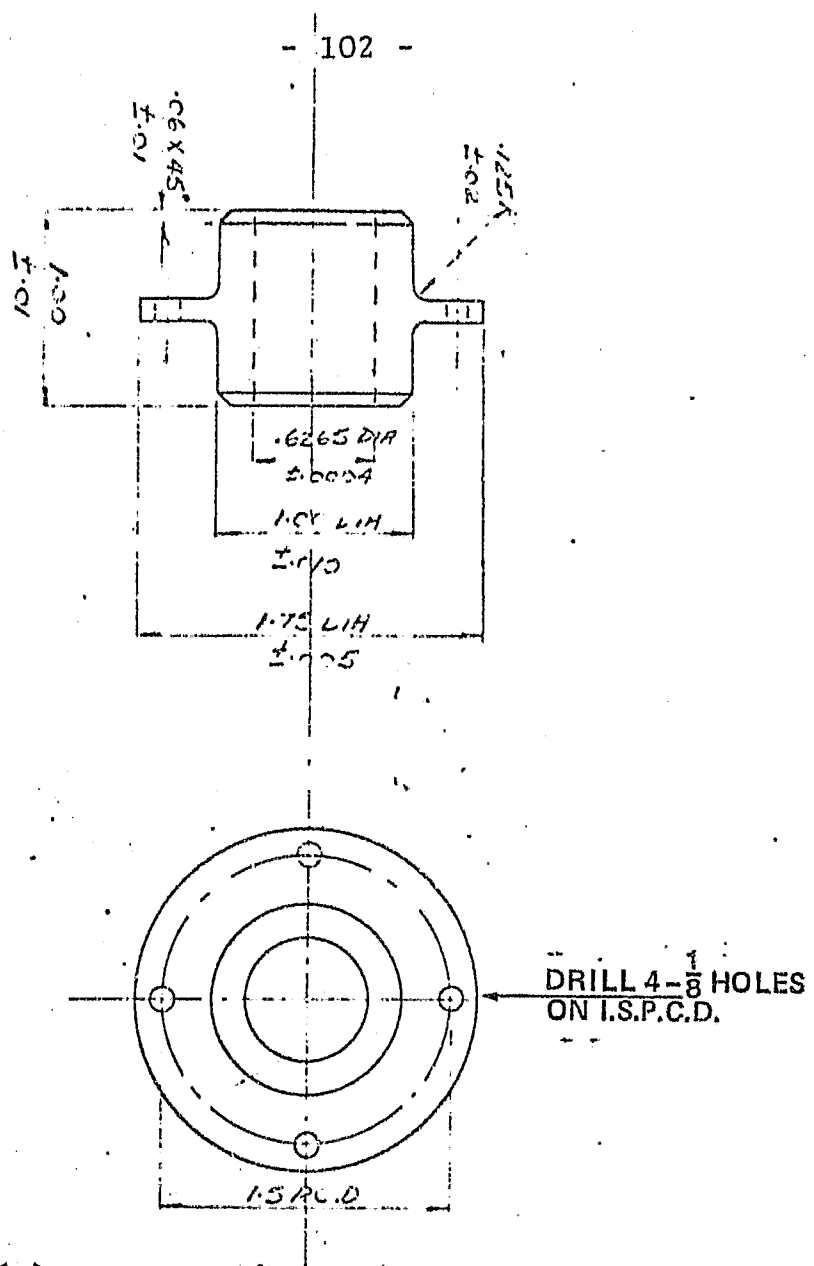

Figure 6.5(a): DICONE SHAFT SLEEVE

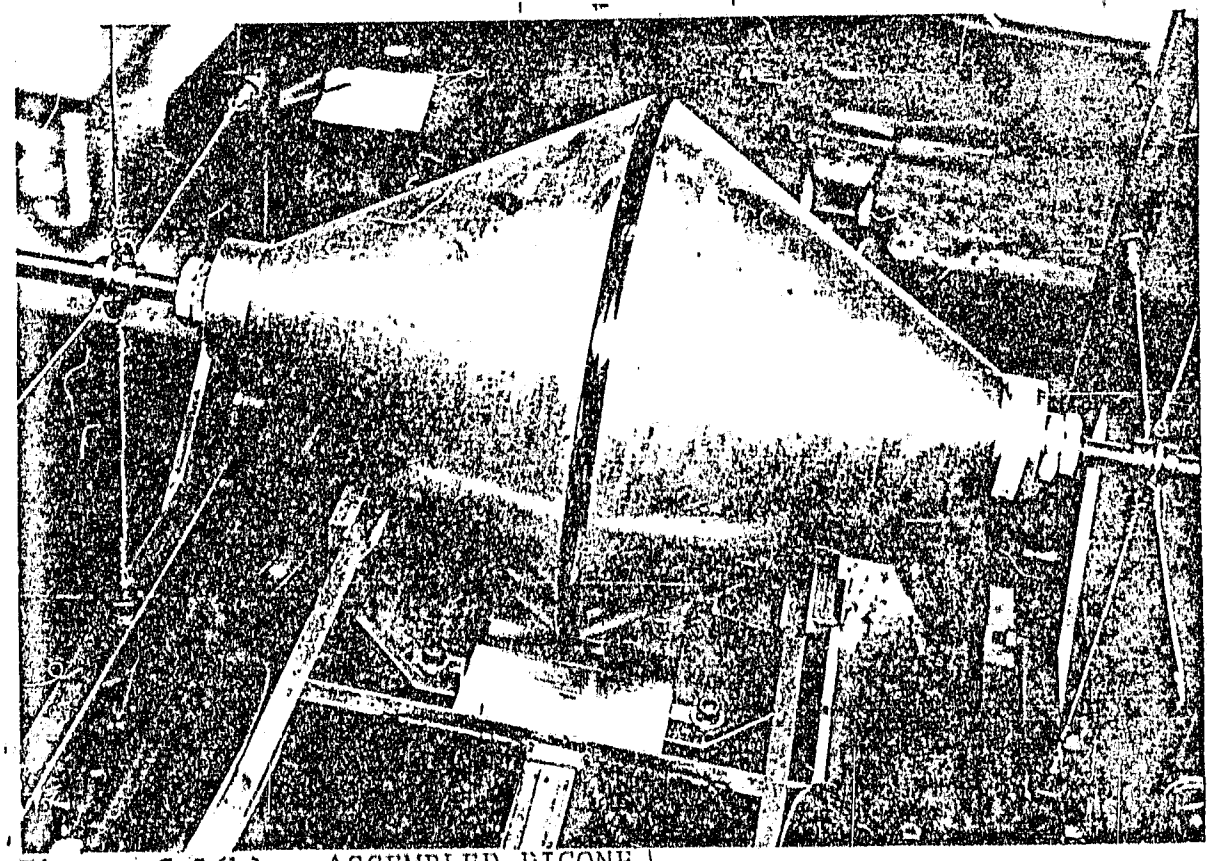

Figure 6.5(b): ASSEMBLED DICONE

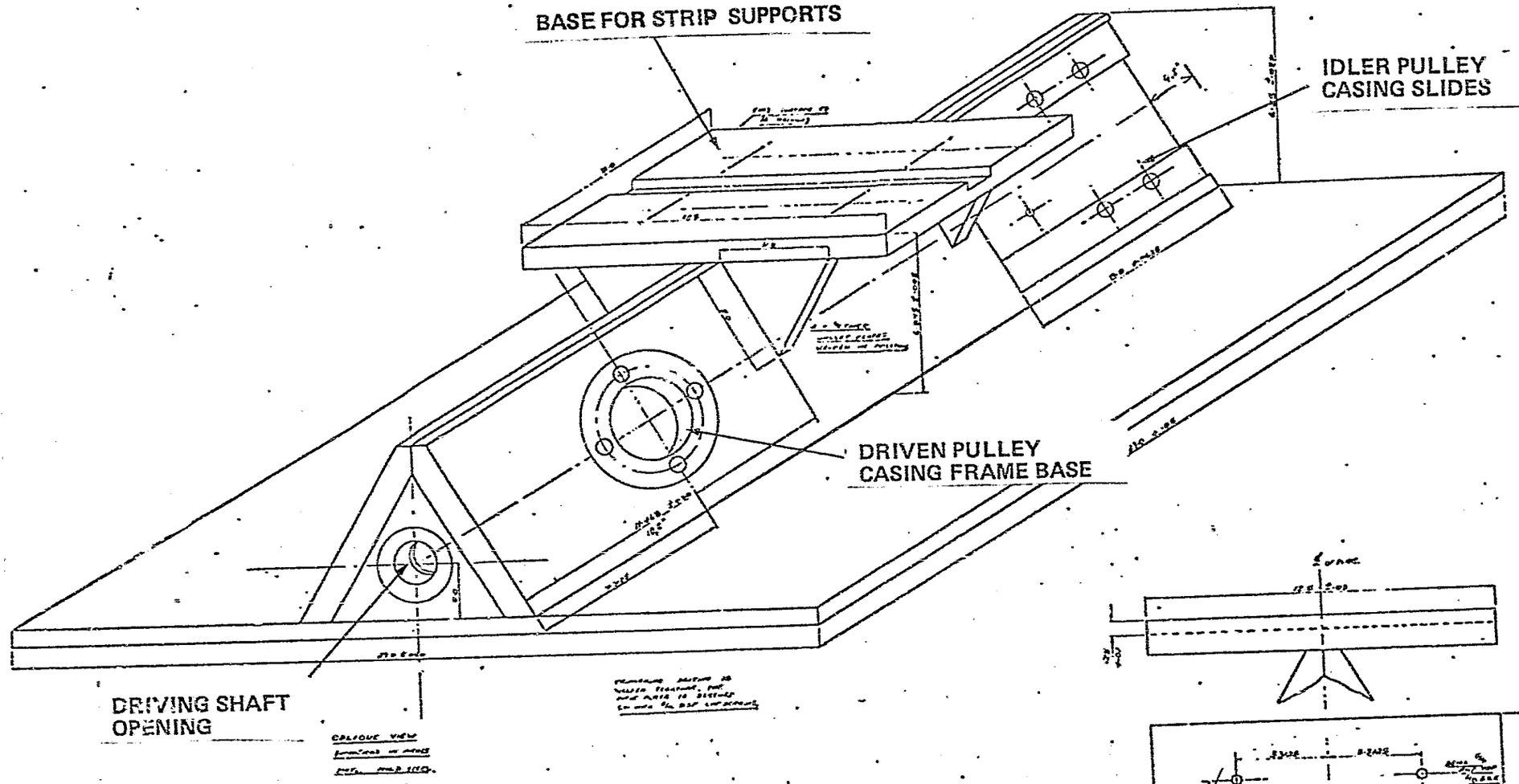

Figure 6.6: ISOMETRIC VIEW OF BASE

assembly of the driven pulley and its shaft and casing (the latter fitting into the base) is shown in Figure 6.7(a). At the end of the base furthest from the drive shaft were the slides for the idler pulley casing.

Figure 6.7(b) shows the design of the machined cast iron cones. The two cones which make up the dicone were mounted on the dicone shaft by means of ball bearings fitted to the apex and mounted inside a cover in the base of the cone. The central table on the top of the vee-structure seen in Figure 6.6 served as the base for the two supports required to correctly position the rail simulating surfaces in the contact area with the dicone. Details of these supports, showing how the Teflon strips used to minimise friction on the lower faces of the steel strips were gripped can be seen in Figure 6.8. Vee-belt drives were used between the 1 kW DC electric motor, which was used to drive the rig, and a variable speed gear box, and also between the gear box and the drive shaft of the rig. Table 6.1 gives particulars of the driving arrangements.

Table 6.1: DETAILS OF THE DRIVE PARTICULARS

Bevel gear reduction	0.17:1
Pulley diameter reduction (drive shaft to gear box)	0.522:1
Pulley diameter reduction (gear box to motor)	0.404:1
Overall speed reduction (ignoring gear box)	0.161:1
Maximum motor speed	2 800 r/min
Maximum belt spee'	13.4 m/s

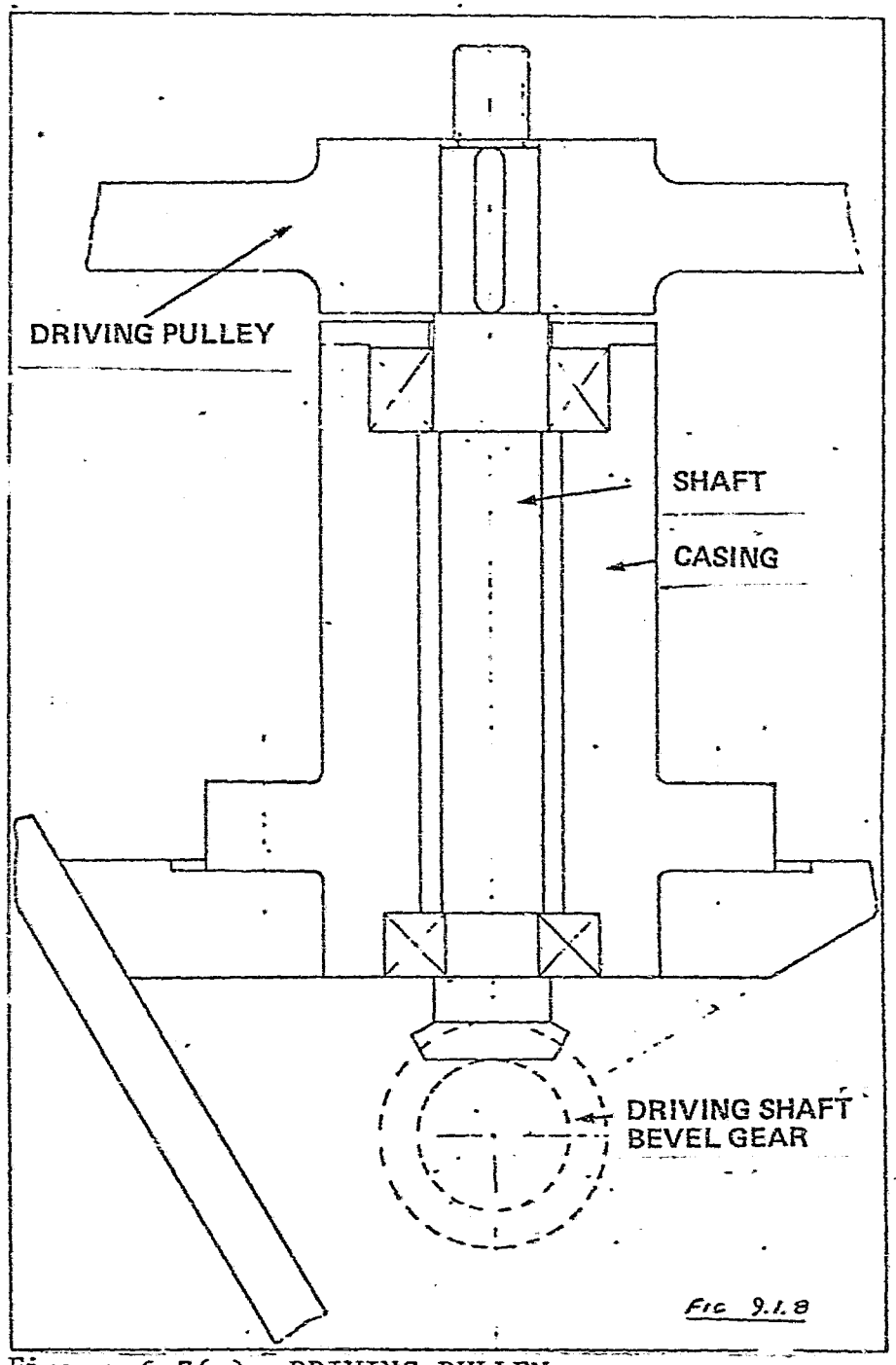

Figure 6.7(a): DRIVING PULLEY SHAFT ASSEMBLEY

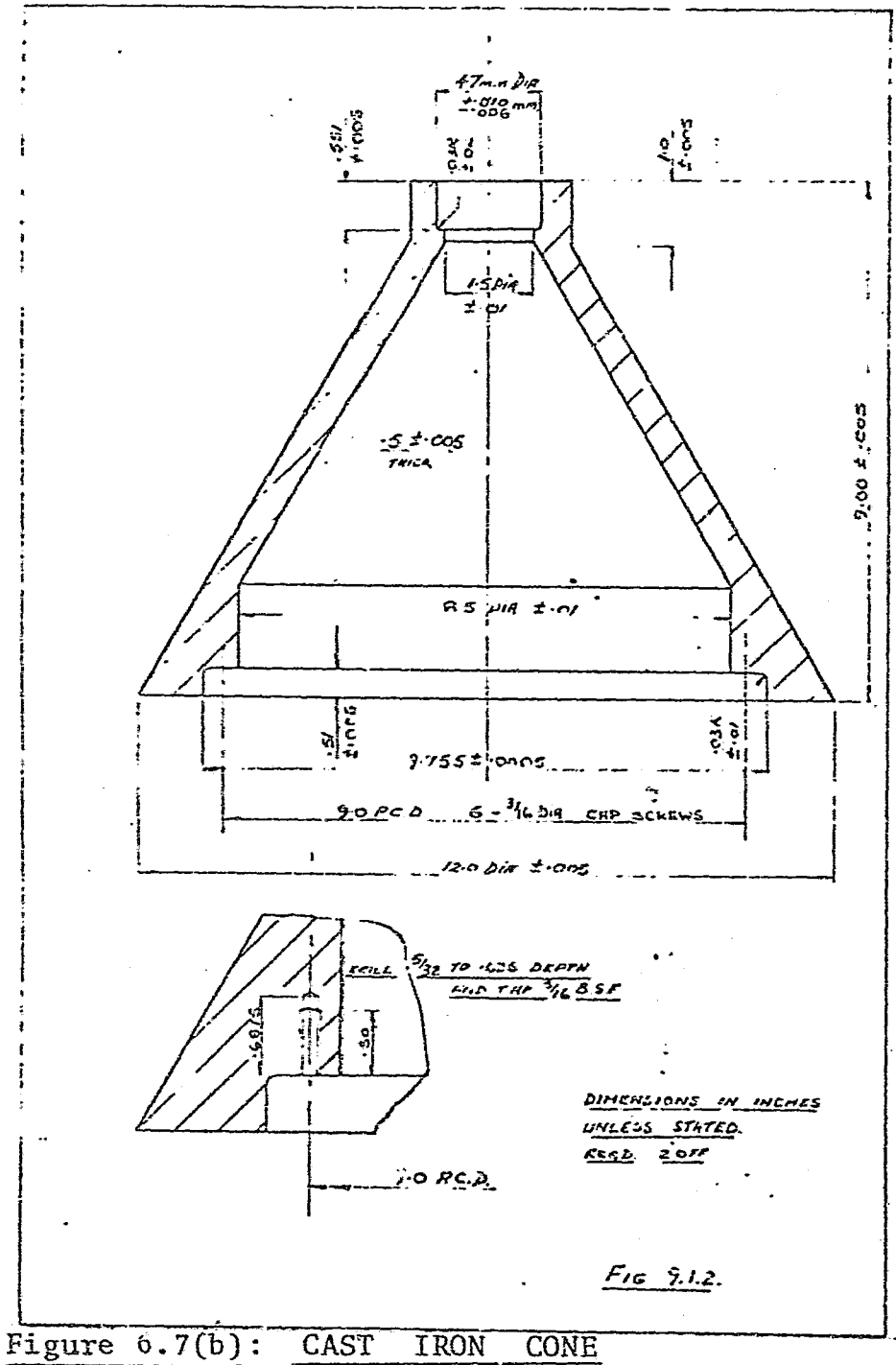

Figure 6.7(b): CAST IRON CONE

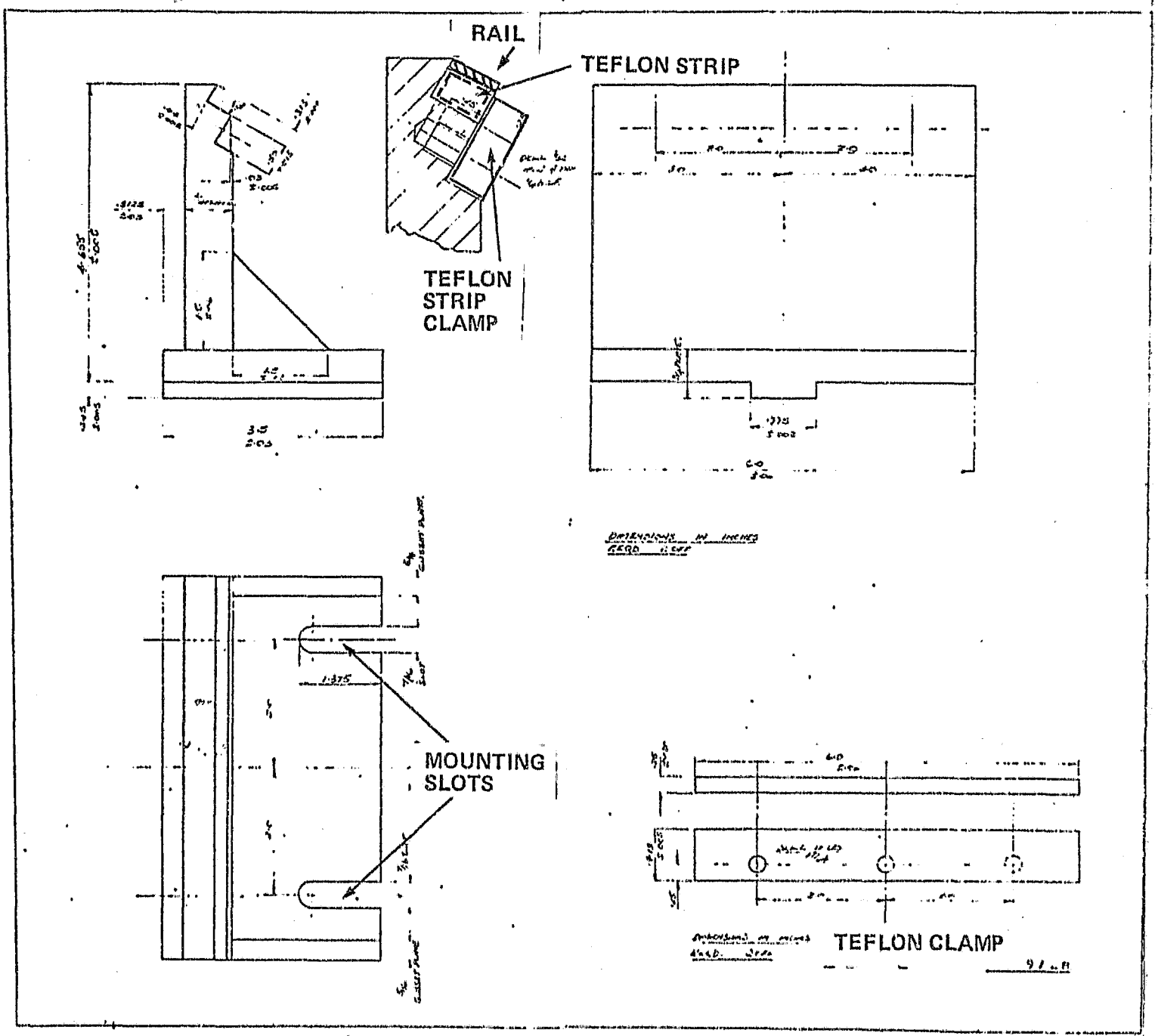

Figure 6.8: RAIL SUPPORT

6.3.2 Initial test rig modifications

On testing the rig as described, it was found that there was too much whip in the dicone shaft, so it was necessary to replace it by a stiffer shaft. After reassembly, the dicone was again balanced. No provision had been made in the original design to prevent the steel strip from being moved sideways in the contact region between the dicone and the strip, and the trial tests quickly showed that it was necessary to take steps to control this movement. However, how to achieve adequate guidance to prevent lateral displacement of the strip continued to be a problem until it was finally overcome in the last modifications to the rig. Since the mass of the dicone after assembly was 54 kg, its inertia was considerable, producing a marked back lash in the bevel gears if its spin speed altered at all; furthermore, the Teflon strips wore rapidly and it was thought that this was caused by excessive loading because of the mass of the dicone. Although the dicone showed some oscillatory tendencies at a belt speed of 6.8 m/s, the test runs showed that the operation of this dicone was remarkably stable, particularly at higher speeds.

Of great interest in these tests was the wear pattern on the steel bands used in the test runs: the outer parts of the belt surface were shiny and bright, with a contrasting thin dull central pattern. It had not been thought necessary at that stage to camber the steel strip bands in any way so that at any instant the full width of the strip would be in contact with the dicone surface. Since the surface velocities would coincide only in the central position, it was concluded that the shiny surface observed was brought about by rubbing movements between the dicone and the outer regions of the strip. This is relevant inasmuch as it shows how persistent the pure rolling motion was in

these tests. (In the subsequent tests where the wheelpair had a much reduced taper angle, the wheelpair could be caused to hunt, once a certain rail simulating surface speed had been exceeded, and since the wheels then slid over the rails, the particular wear pattern observed in this first series of tests was not repeated.)

6.3.3 Second test rig modifications

No theoretical explanation was available as to the cause of the refusal of the dicone to oscillate when the test runs were made on the rig referred to above. A decision was consequently called for as to the way in which the rig should be modified if further progress was to be achieved. After consideration, it was thought that the dicone refused to hunt because:

(a) The cone taper angle of 30° was far too large and that hunting would be more likely to occur if a more typical taper angle of, say, 5° were adopted.

(b) It was a disadvantage that the mass of the dicone was so large. (Not only would a light dicone be more easily handled, but the load on the rig would also be reduced.)

(c) Any tendency for the dicone to hunt might have been inhibited by the fact that the contact region between the steel strip and the dicone, which in these tests had extended over the full width of the strip, was excessive.

While it was not directly related to the hunting problem, it was felt that reliance on Royer's theory (namely, that the spring energy storage in the wheelpair axle was a

possible cause of hunting) should be abandoned, as the validity of the theory appeared by then to be increasingly unlikely. The use of a full dicone was also discontinued- instead, only those portions of the dicone surface likely to come into contact with the rail surfaces were retained. The redesigned wheel pair, as was the case with the dicone, had ball bearings fitted at each end, the inner races of which were in turn fixed to the wheelpair shaft. The movement of the shaft was controlled by the same dicone shaft sleeves and restraining springs which had been used in the original rig. The very much lighter wheelpair can be seen in operation in Figure 6.9(a).

The problem of avoiding an exessively wide contact region between the dicone and the rail simulating surface was not so easily overcome, and involved a trial-and-error process of testing a variety of different materials and configurations. This is an important issue in view of the emphasis placed by other workers on the material used in the wheelsets and supporting rollers. Wickens in the discussion following Matsudaira's paper [39] said:

> The question of dynamic similarity was considered ... . These considerations led to the use of aluminium alloy for both wheels and rollers which, at one-fifth full scale, preserved full dynamic similarity. In principle, the use of materials with very low moduli of elasticity, and of reasonable density, should enable dynamically similar models to be built at quite small scales.

However, as Matsudaira correctly pointed out in his reply to the discussion of his paper, the coefficient of friction between aluminium to aluminium surfaces is different to that between steel to steel surfaces. The conclusion from the work done here is that, while the coefficient of friction has an effect on the hunting frequency, that of the wheelpair

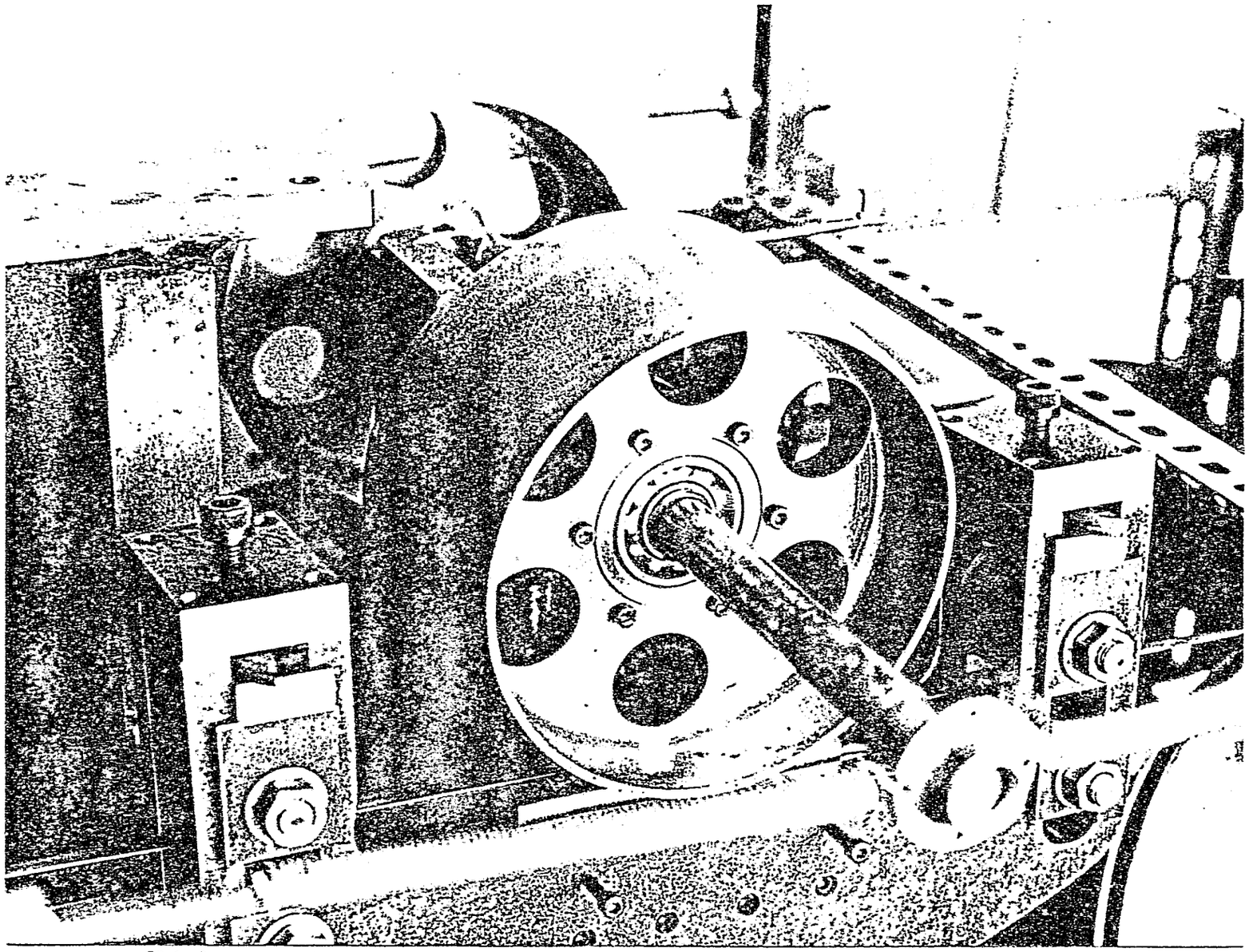

Figure 6.9(a): REDESIGNED WHEELPAIR

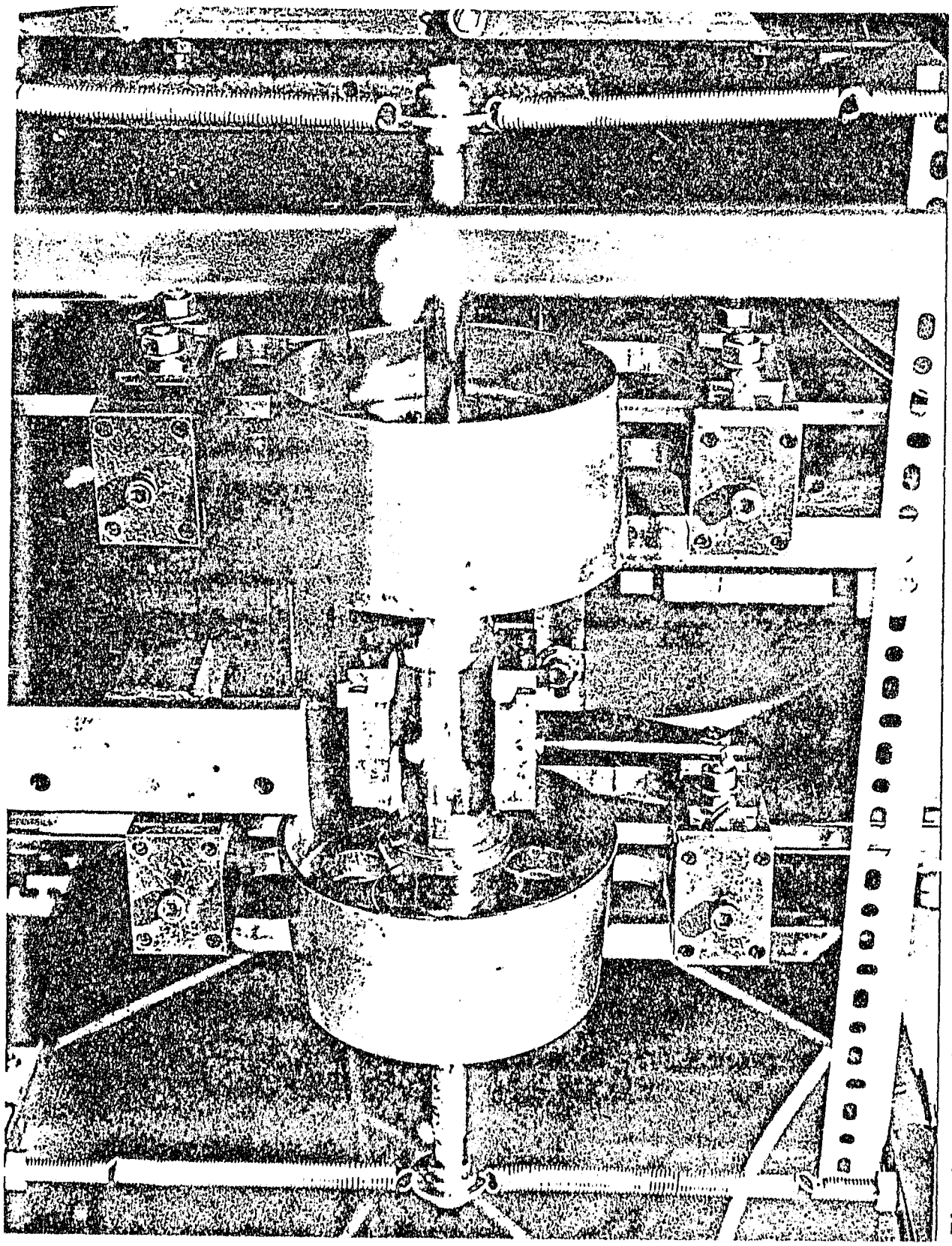

Fig 6.9(b): ANOTHER VIEW OF REDESIGNED WHEELPAIR

spin speed is far greater. (Not only was the kind of material used in the rail simulating surface found to be unimportant, but so was the surface texture; thus the wheelpair oscillated at the appropriate rail speed regardless of the fact that the rail simulating surface was close-coiled steel spring, steel strip or any of the other materials employed.)

The first new material to be used for the purpose of reducing the width of the contact between the wheelpair and the rails was high tensile steel wire. Since the wheelpair was now much lighter, it was expected that the tractive force needed to cause the wheelpair would be much reduced and that the tensile strength of the wire would not be exceeded. The butt welds needed to fabricate continuous loops of wire were, however, difficult to make and this caused rapid failure of the loops because of fatigue fractures at the welds, while mild steel loops were not much better. Eventually, 3,18 mm (1/8 inch) diameter close-coiled steel wire spring was used. Suitable lengths of this material was made into continuous loops by the use of connecting hooks formed at each end. This spring mat-rial (sometimes used as a domes rtain support) proved satisfactory in that a number sful test runs were made with little evidence that sence of the joints changed the motion of the wheelpair. Lateral displacement of the coiled springs was successfully overcome by means of suitably grooved bronze blocks placed under the coiled springs in the contact region with the wheelpair and by idler pulleys situated before and after the bronze blocks.

6.3.4 Third test rig modification

The test runs made on the rig as described in the previous section demonstrated that the linear and the angular

oscillatory modes were distinct and not coupled in any way. They could therefore be investigated separately as different, unconnected phenomena. Because the rotary motion was of far greater interest than the linear movement, it was decided that the linear movement of the wheelpair in the direction of the track should be eliminated by means of the dicone yoke shown in Figure 6.10. This yoke was placed on the rig in such a way that it could rotate freely about a vertical axis lying in the plane situated midway between the rails. Two double row angular contact bearings were used to fit the yoke into its housing so that high axial rigidity could be assured. The shaft housing of the wheelpair was held in position in the yoke between vertical hexagonal cross-section Teflon strips fitted into the inner sides of the yoke. In this way, the wheelpair was free to tilt and to yaw with the minimum of frictional resistance to such movement.

Although test runs had been successfully conducted with the close-coiled springs, the flexibility of this material was too great for it to be a satisfactory long term rail simulating material. An attempt was then made to use spliced steel wire loops but despite the care taken making the splices, some enlargement of the wire rope cross-section occurred in the region of the splices. It was possible to conduct successful tests with these loops but the likelihood that the enlargements in the splice region should prove to be significant led to a decision to reject these loops as a suitable rail simulating material. It was then decided that if steel strip were supported differently from that attempted previously, this material might yet prove to be satisfactory.

At this stage, a combined research effort undertaken by the author in collaboration with the South African Railways

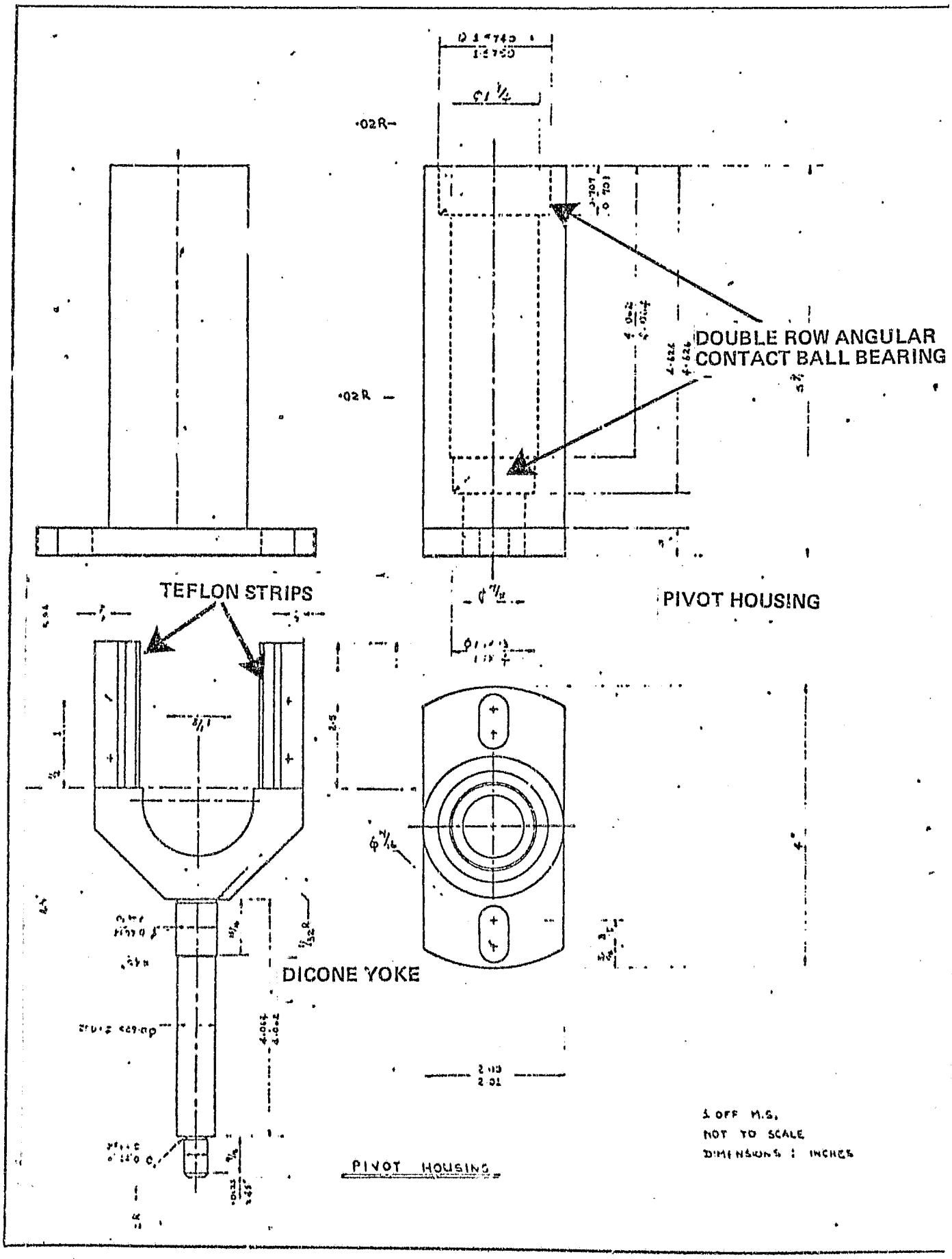

Figure 6.10: DICONE YOKE AND BEARING

(SAR) called for the construction of a special test rig to test profiled railway wheels. Some of the design features of the resulting rig, shown in plan and elevation in Figures 6.11 and 6.12 respectively, were subsequently helpful in suggesting how the design of the existing rig could be further improved. In the SAR rig, the steel strip was supported in the contact region between the wheelpair and the rails by means of the four rollers shown in Figure 6.13. Double flanged outer pulleys were used so as to control the sideways drift of the rails. Inevitably, even though it was slight, there was some sag in the strip in the region between the supporting rollers and it was apparent that the problem of how to support the strip in the contact region had not yet been adequately resolved. What was, however, a successful innovation in this rig was the adoption of camber in the rollers so as to produce a curved profile in the strip in the contact region between the wheels and the rails. Not only did the curved profile stiffen the strip but it also caused (as far as this was possible) point contact between the wheels and the supporting steel strip. On the grounds that the radius of curvature of the steel strip as it passed over the driving and idler pulleys affected the maximum tensile stress in the steel strip (and since this strip was already considered to be exessive), the diameters of these pulleys were increased from 29.6 cm in the original rig to 45.7 cm in the SAR Rig. Nevertheless these band breakages due to fatigue failure continued to be a troublesome feature, involving loss of working time as the bands were replaced. Despite this, the typical patterns of the wheelpair oscillatory motion was demonstrated in the ensuing test runs, it was possible for the SAR to acquire new information about profiled wheels and as far as this work was concerned, useful operating information for further development was obtained.

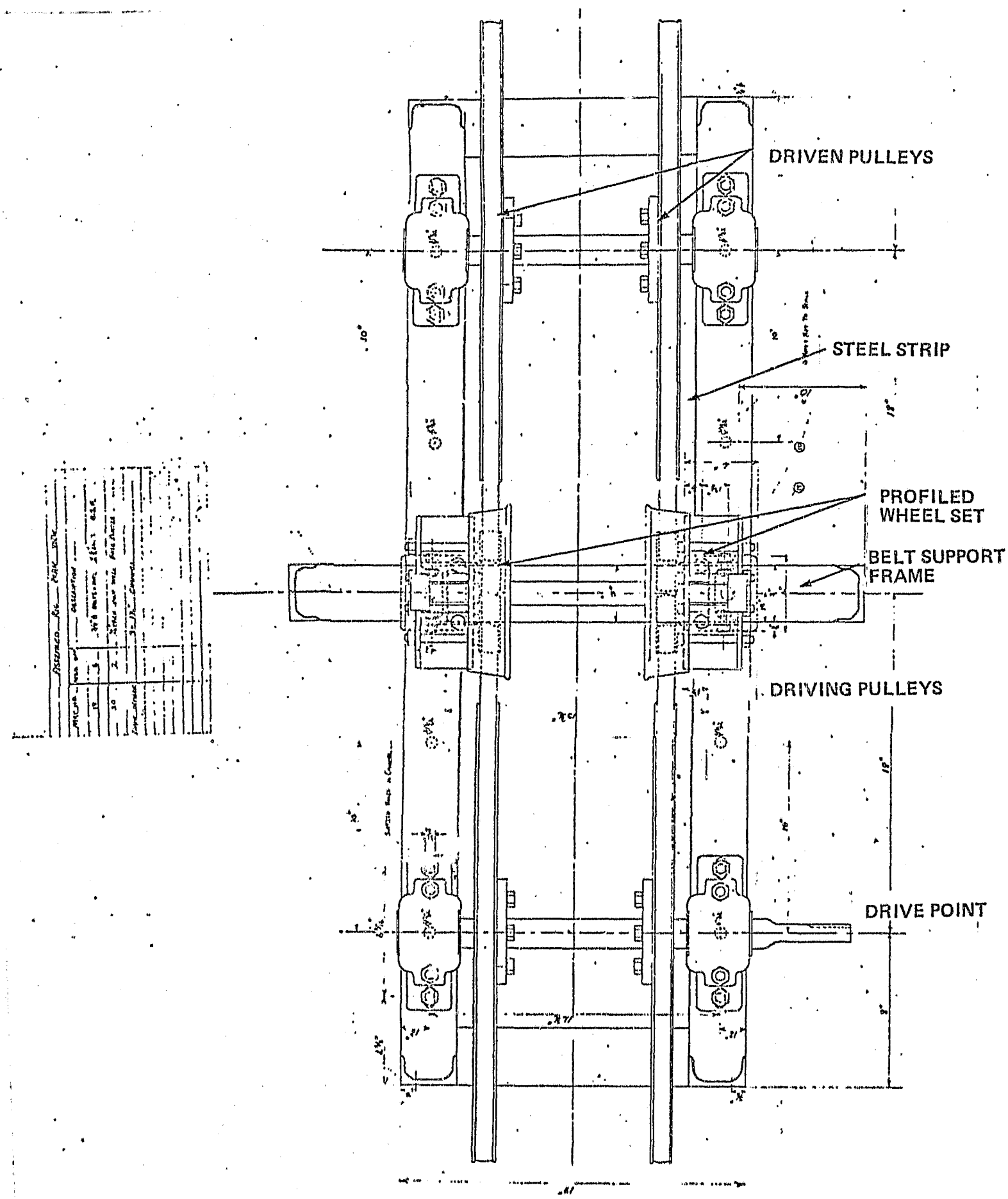

Figure 6.11: PLAN VIEW OF SAR TEST RIG

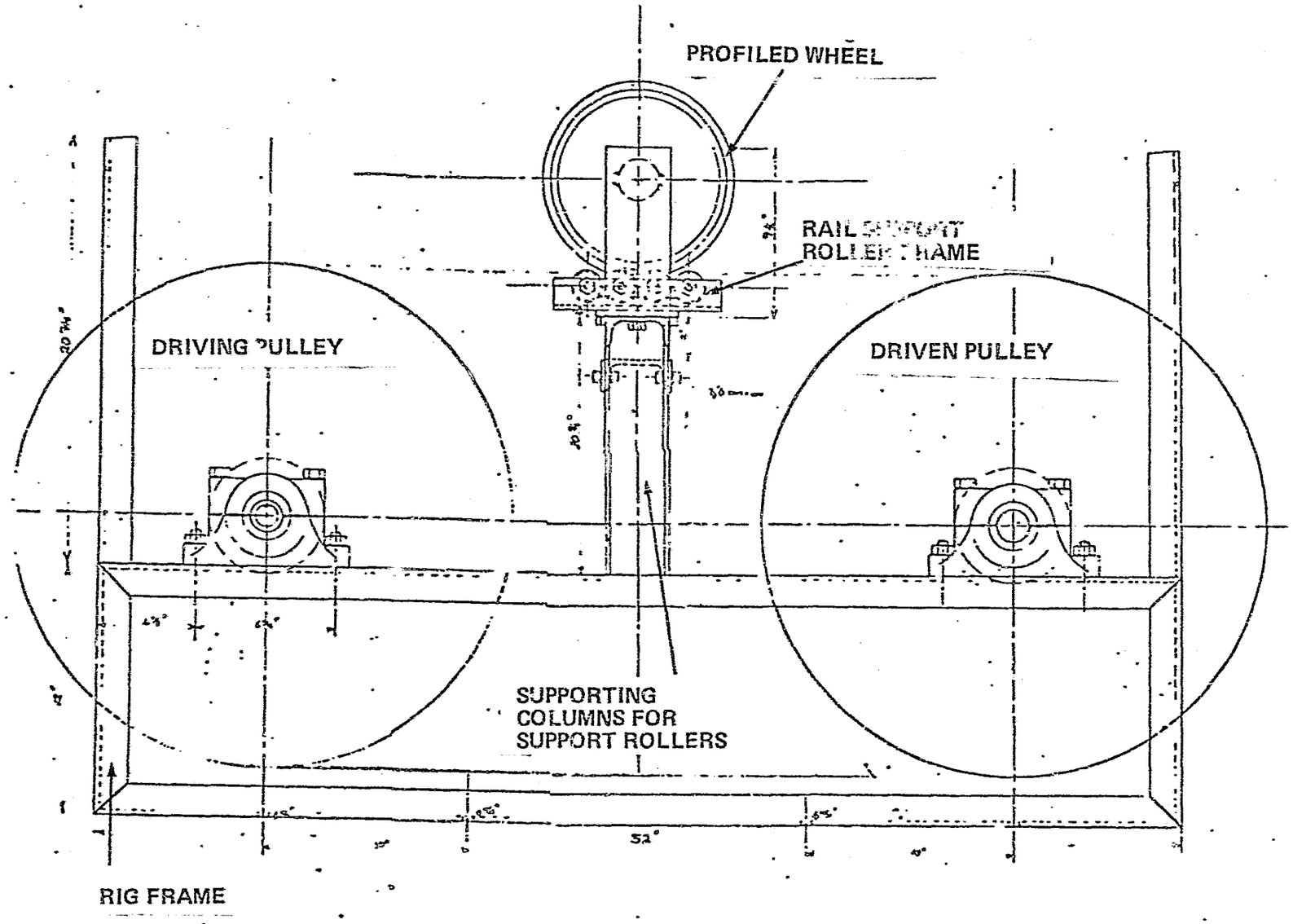

Figure 6.12: ELEVATION OF SAR TEST RIG

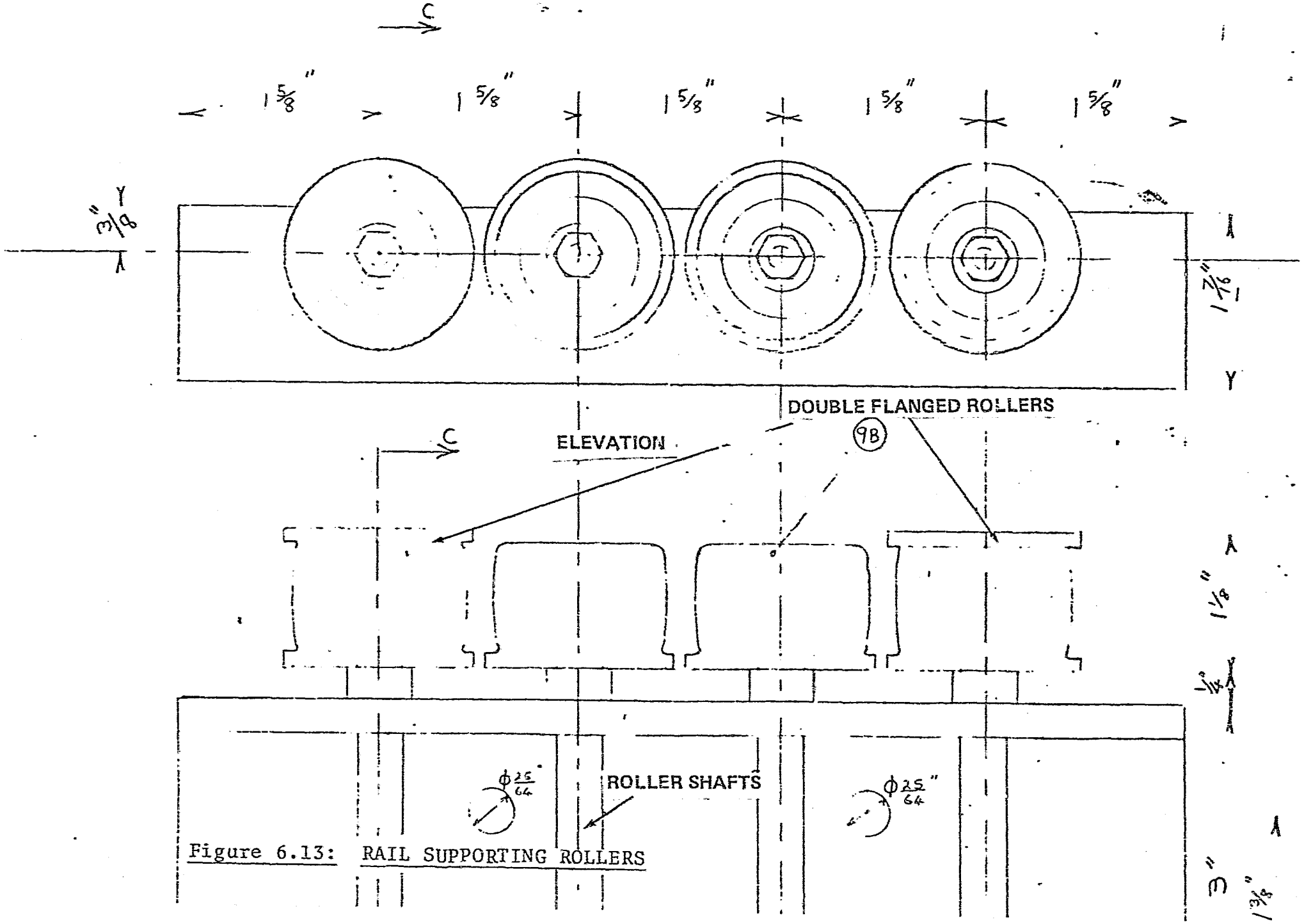

Figure 6.13: RAIL SUPPORTING ROLLERS

6.3.5 Final form of the test rig

Before embarking on the design of the final modifications to the rig, a careful review of the deficiencies previously encountered in the rig was made. It was decided that the main stumbling blocks to the successful functioning of the rig lay not only in the quality of the steel strip which had been used, but also in how the strip was guided through the contact region between the strip and the wheels, that is, the path of the strip had to be along a straight line and the lateral guidance given it in this vital region had to be adequate. (The modifications subsequently carried out proved to be highly successful and the rig in its final state is in fact suitable as a standard form of equipment for use in any tests involving railway hunting.)

After consultation with the factory manager of the Apex Works of Sandvik (Pty) Ltd, it was decided that narrow blank spring set band saw steel strip should be used for the rail simulating surfaces. Butt-welded loops of strips of the correct length supplied by Sandvik performed admirably under the required test conditions with none of the fatigue failures which had hampered test runs with the steel strip used previously (and which had taken up so much time on each occasion it was replaced).

Since the initial test rig was now being used again the strip coming off the driving and idler pulleys was inclined at 30° to the horizontal, and as the cone taper angle in the wheelpair being used was 5° the strip had to be twisted so as to lie at an angle of 5° to the horizontal; it also had to be cambered in order to achieve (as far as this was possible) point contact with the running surfaces of the wheelpair. Furthermore, the strip had to be supported in the contact region between the strip and the wheelpair,

FIG 6- 14 (a)
CAMBERING ROLLERS IN ELEVATION

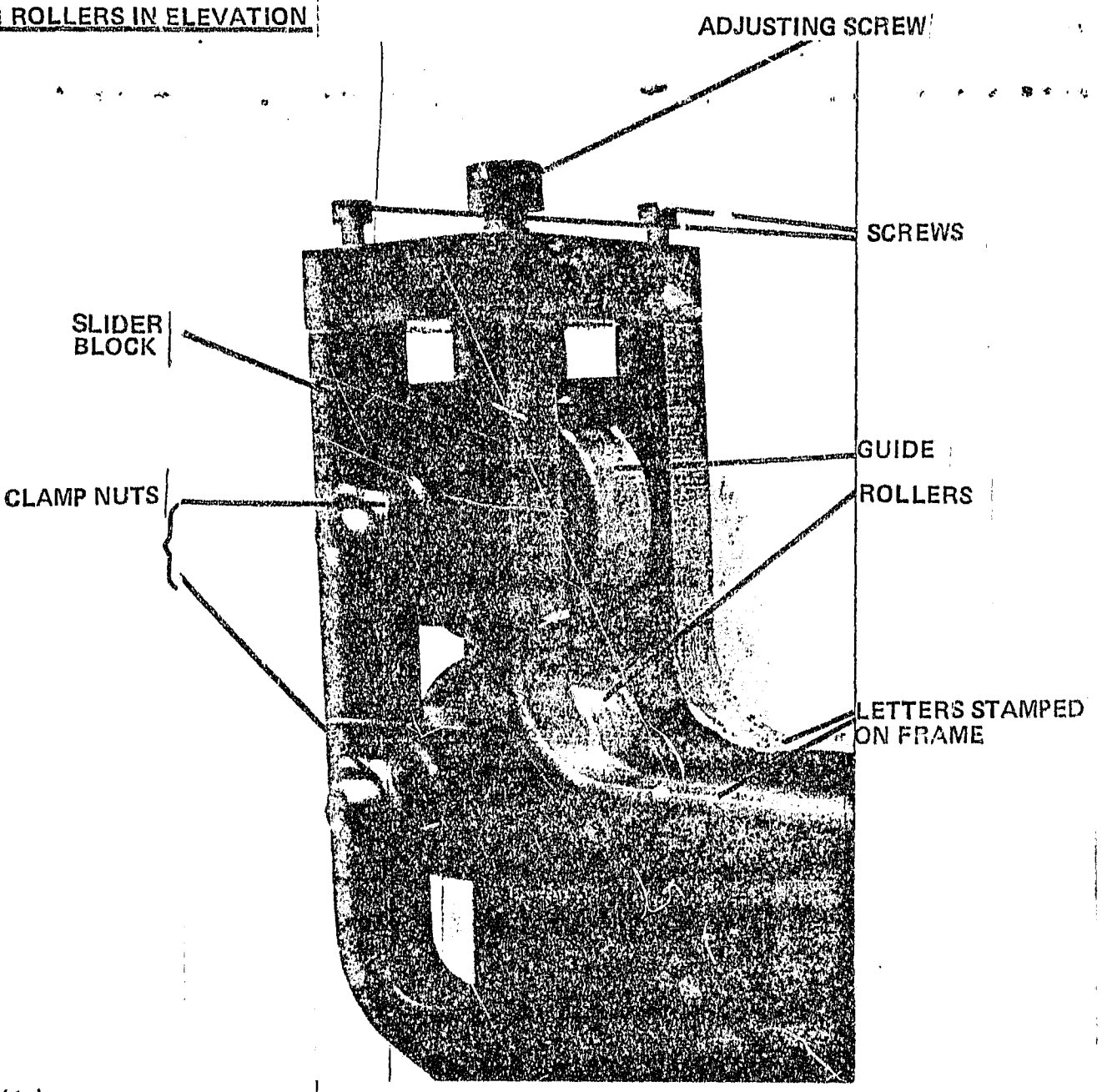

FIG 6 - 14 (b)
CAMBERING ROLLERS IN PLAN

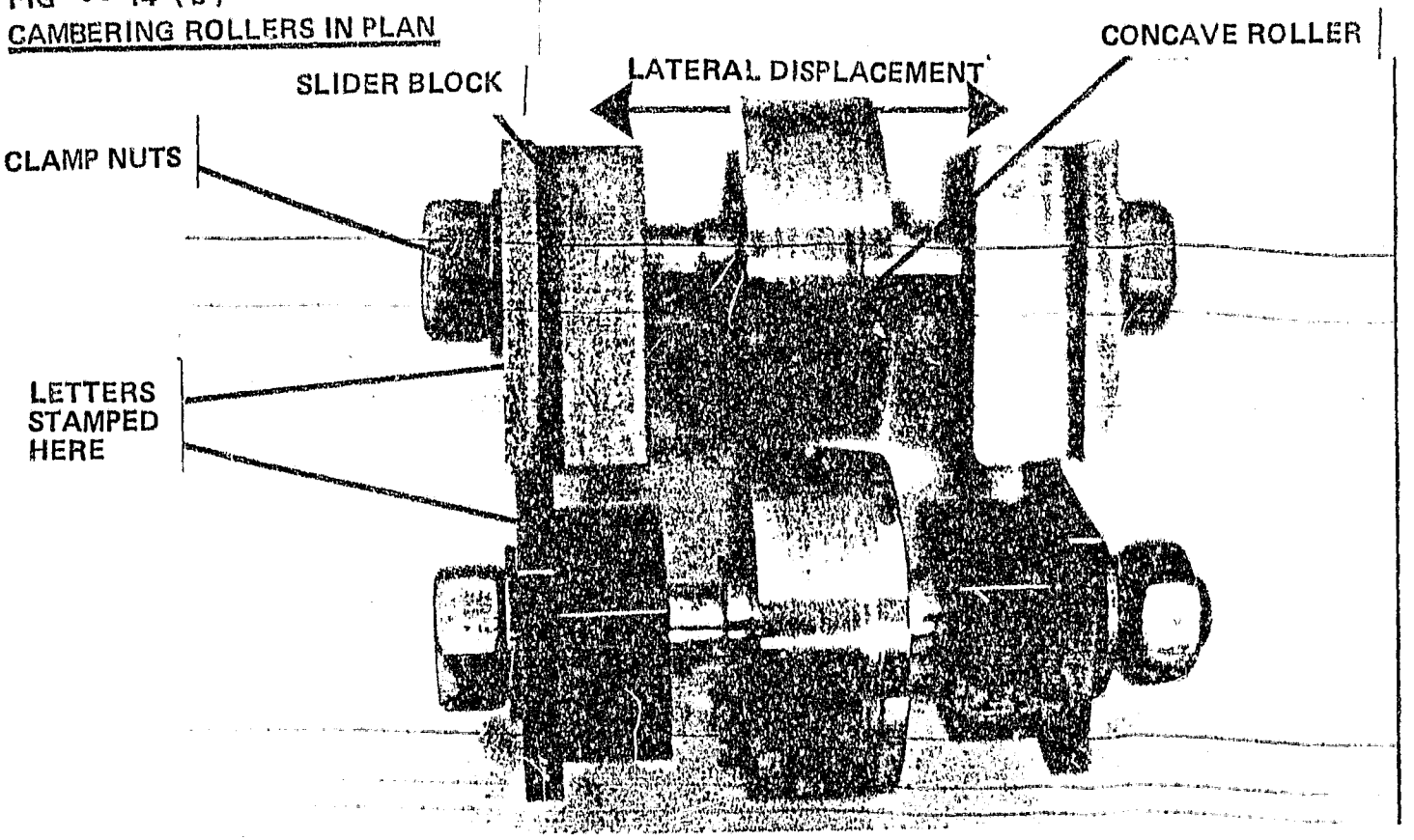

as stated previously, in such a way that its direction of travel was along a straight line with the minimum of frictional resistance on the under side of the strip. This seemed to be an ideal application for air slides and as the subsequent experience showed, this was indeed the case. The roller guides used to twist and camber the strip then had the important additional function of accurately positioning the strip as it entered and left the air slides. These roller guides, with adequate provision for the lateral and vertical adjustment of the position of the strip, are shown in Figures 6.14(a) and 6.14(b). In addition to providing the support for the steel strip in the vital contact region, the air slides had to prevent any tendency, which it might have, for sideways drift to take place. As these air bearings are an important element in the rig as it now stands, certain construction details of the bearings will now be given.

6.3.6 Design of air bearings

Grassam [40] suggests that the design of pneumatic bearings, where the applied loads are as complex as they were in the case of the test rig, tends to be an art rather than a science. Not only must aerodynamic bearings have sufficient load bearing capacity but - because of their sensitivity to out-of-balance loads and to bearing misalignment - adequate allowance has to be made for all possible transient conditions before work is started on the actual bearing design. In the present case, while the normal load would be the weight on the bearing, there would in addition be the dynamic loads brought about as the wheelpair yawed and/or tilted, and lastly, impulse disturbances would occur as the butt-welded joints in the steel bands passed over the bearings. The minimum clearances in the bearings would

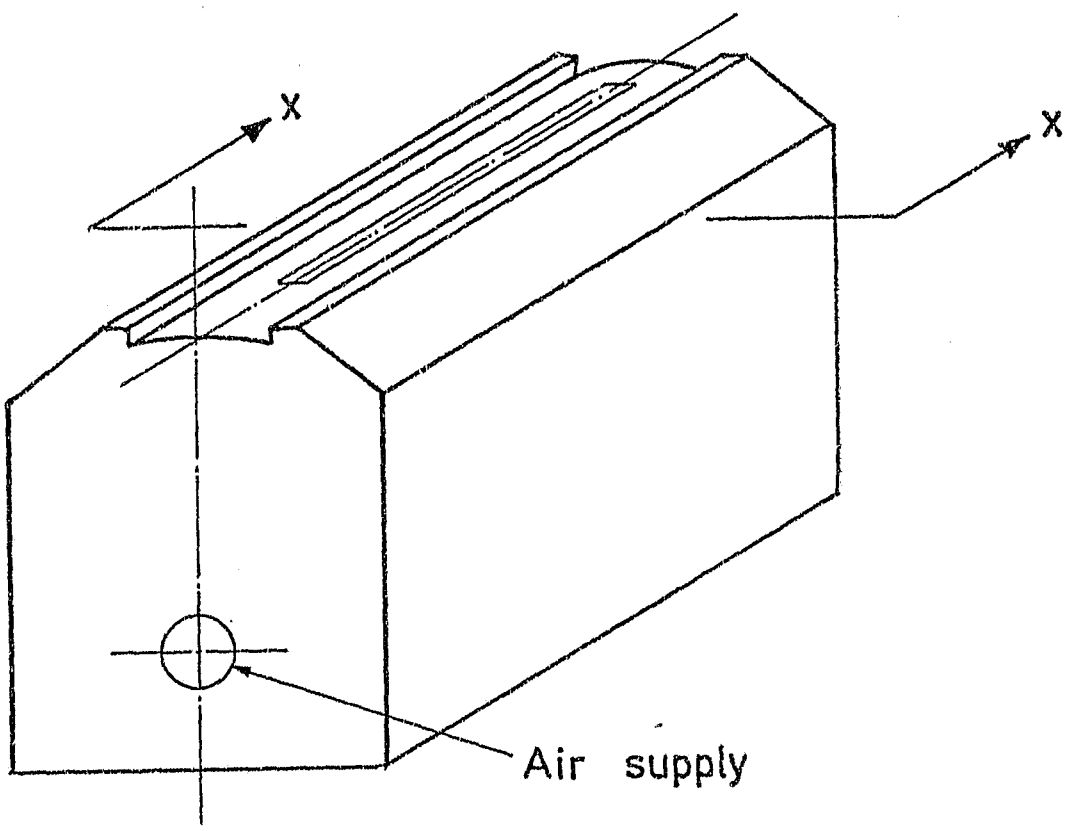

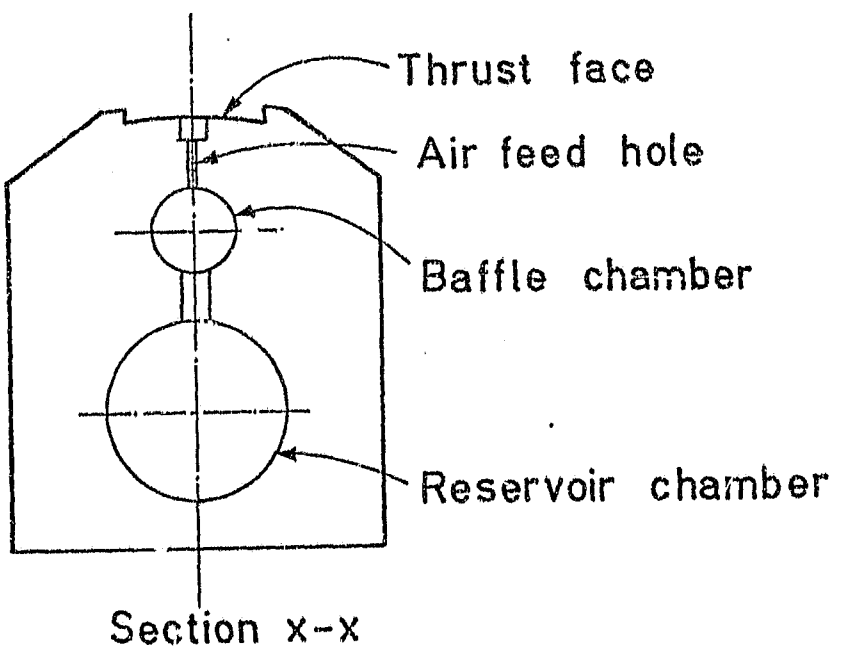

Figure 6.15: ISOMETRIC VIEW AND CROSS-SECTION OF AIR SLIDE

be determined by these forces; furthermore, the bearings had to be stiff and damped so as to restrict their response to impulse forces. As the University of the Witwatersrand is situated at an altitude of approximately 1 800 m, normal changes in the ambient air pressure would be more marked and since changes in pressure and ambient temperatures would cause the air viscosity to vary, the load bearing capacity would be affected ty these changes.

An isometric view of the resulting air slide, as well as of its cross-section, is shown in Figure 6.15. Because no design data was available for determining various dimensions, the calculations proceeded on an *a priori* basis. As the mass of the dicone was 10,45 kg, and based on the arbitrary assumption that the maximum lateral displacement of the wheelpair would be 2,64 cm (this value being related to the track width), it was estimated that the maximum static load on the bearing would be 61,8 N; furthermore, using the same oscillatory frequencies experienced in the earlier test runs, it was calculated that the maximum transverse force would be 6,94 N. Since the steel strip was under tension and cambered, it was further assumed that, as a first approximation, the load on the bearing would be distributed uniformly over its entire length. With a factor of safety of 5, the design load to be supported on the bearings in the normal direction would therefore be 309 N.

Because of the very small clearance between the strip and the air slide bed, the assumption was made that the air flow in this space was laminar. Using a reasonable approximation for the air pressure distribution under the strip, it was concluded that the velocity profile under the strip would be parabolic so that the mass air flow rate could then be found in terms of the pressure gradient. Because little heat would be generated within the bearing and since the

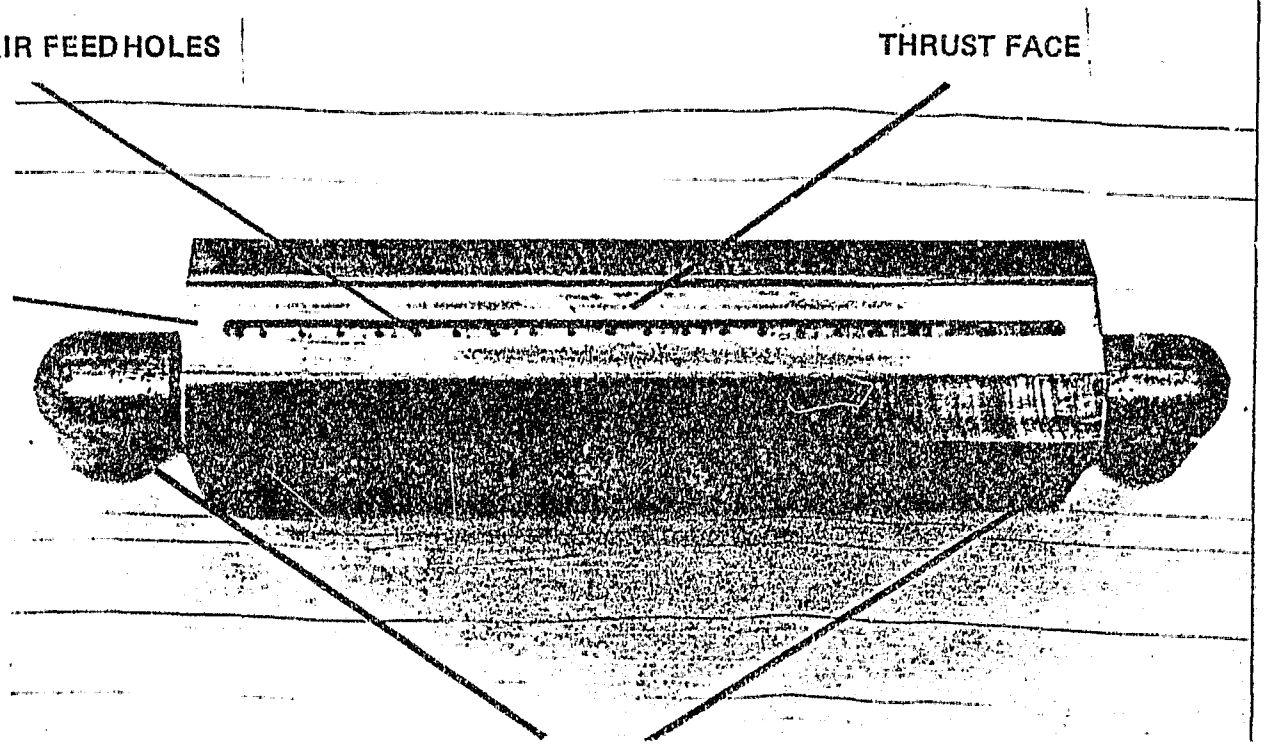

6-16 (a)
AIR BEARING

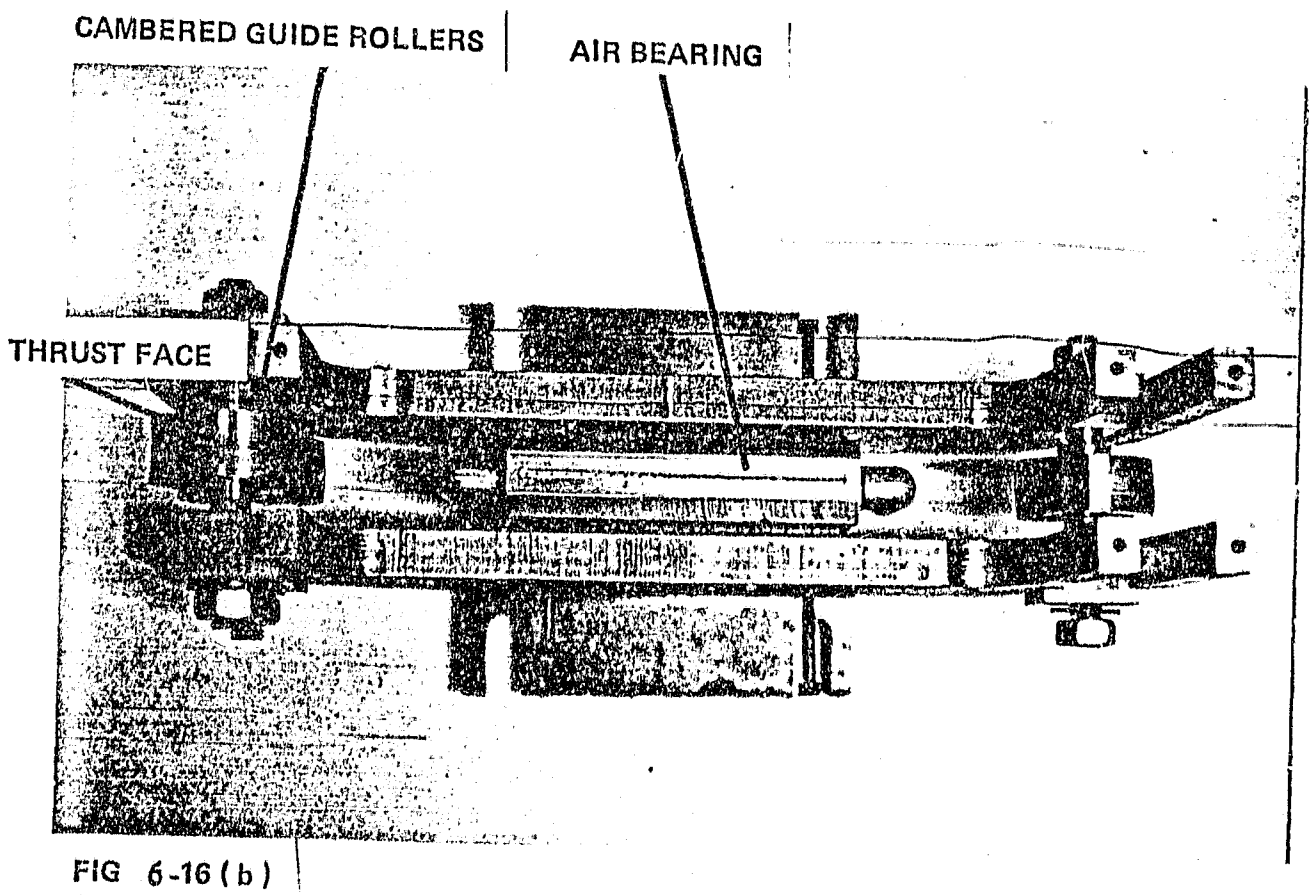

FIG 6-16 (b)
AIR SLIDE & CAMBERING ROLLERS

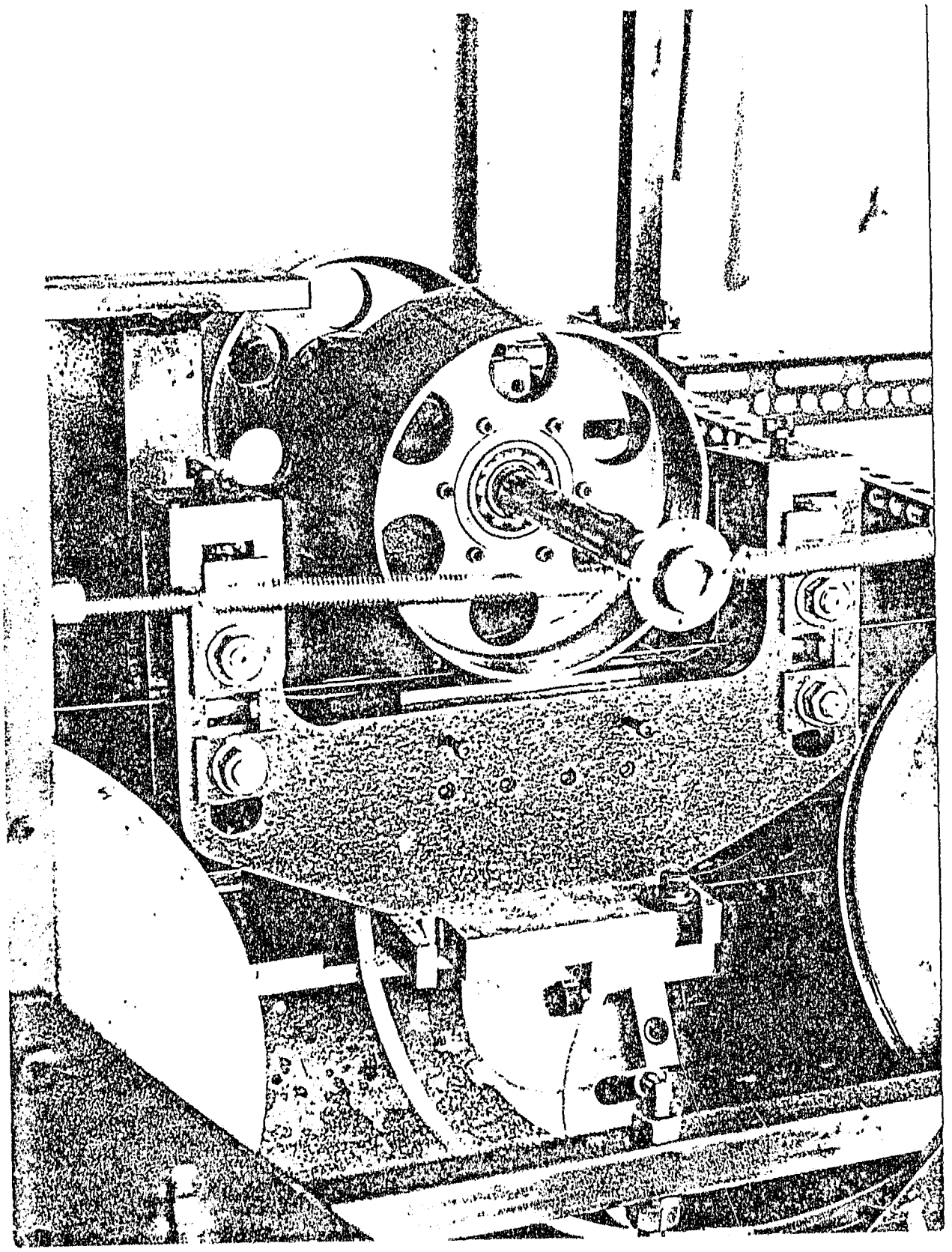

Figure 6.17: AIR SLIDE AND CAMBERING ROLLERS SEEN IN ELEVATION

metallic bearing walls had a high thermal conductivity, isothermal conditions could be assumed. The bearing thrust force had to be 12.7 mm wide so as to accommodate the width of the steel strip used. On the basis that the air supply pressure was 517 Pascals, the estimated bearing length for a maximum external load of 309 N was 93 mm; however, it was thought prudent to extend its length to 120 mm.

An arbitrary volumetric flow rate of feed air, kept at as low a figure as was thought possible, was decided upon, and on the basis of this assumption it was calculated that 21 feed holes, each with a diameter of 0.3 mm, and spaced at intervals of 5 mm were needed. The completed air bearing, as well as a photograph of the assembly of the air bearing and the cambering rollers, is shown in Figures 6.16(a) and 6.16(b). So as to provide enough space between the pulleys for the assembly shown in Figure 6.16(b), the belt idler pulley slides on the rig had to be lengthened. The wheelpair is shown in elevation in Figure 6.17 which illustrates its position relative to the air slide and the cambering rollers.

6.3.7 Optical measuring system

So as to observe the yawing and tilting movement of the wheelpair more closely, the device (based on mirrors) shown in Figure 6.18 was then designed. An extension bar, fixed at one end to the side of the dicone yoke, had a pin fitted into it at the other end. This pin in turn fitted into the fork of a pivotted bar, at the other end of which a mirror was fixed. This mirror reflected the light from a slit source onto a screen to provide a magnification of 15 in the yawing movement of the wheelpair. Similarly, a pin secured to the upper surface of a brass block riding on the wheelpair axle housing between the yoke inner surfaces

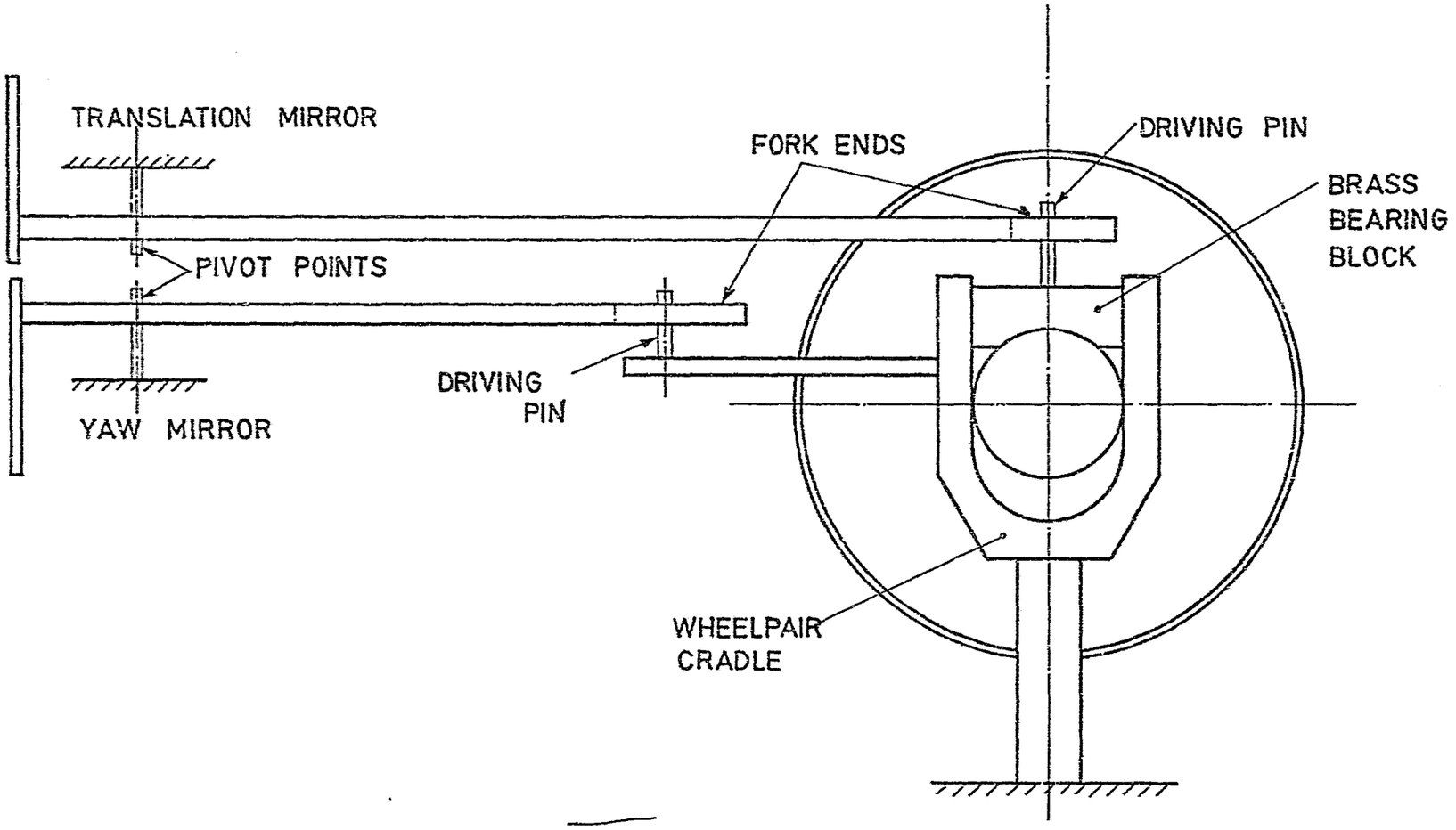

Figure 6.18 MIRROR DRIVING SYSTEM

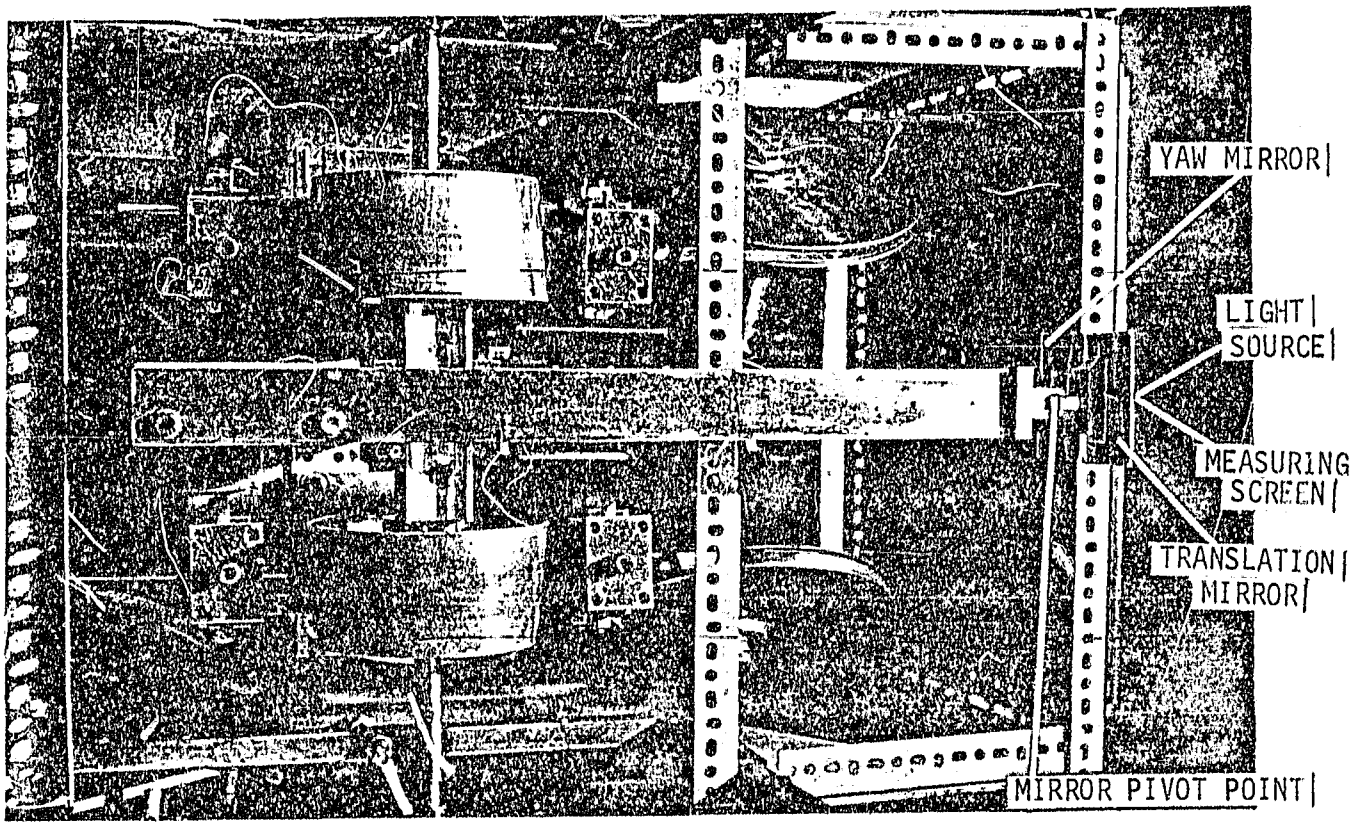

Figure 6.19(a): PLAN VIEW OF MIRROR DRIVING SYSTEM

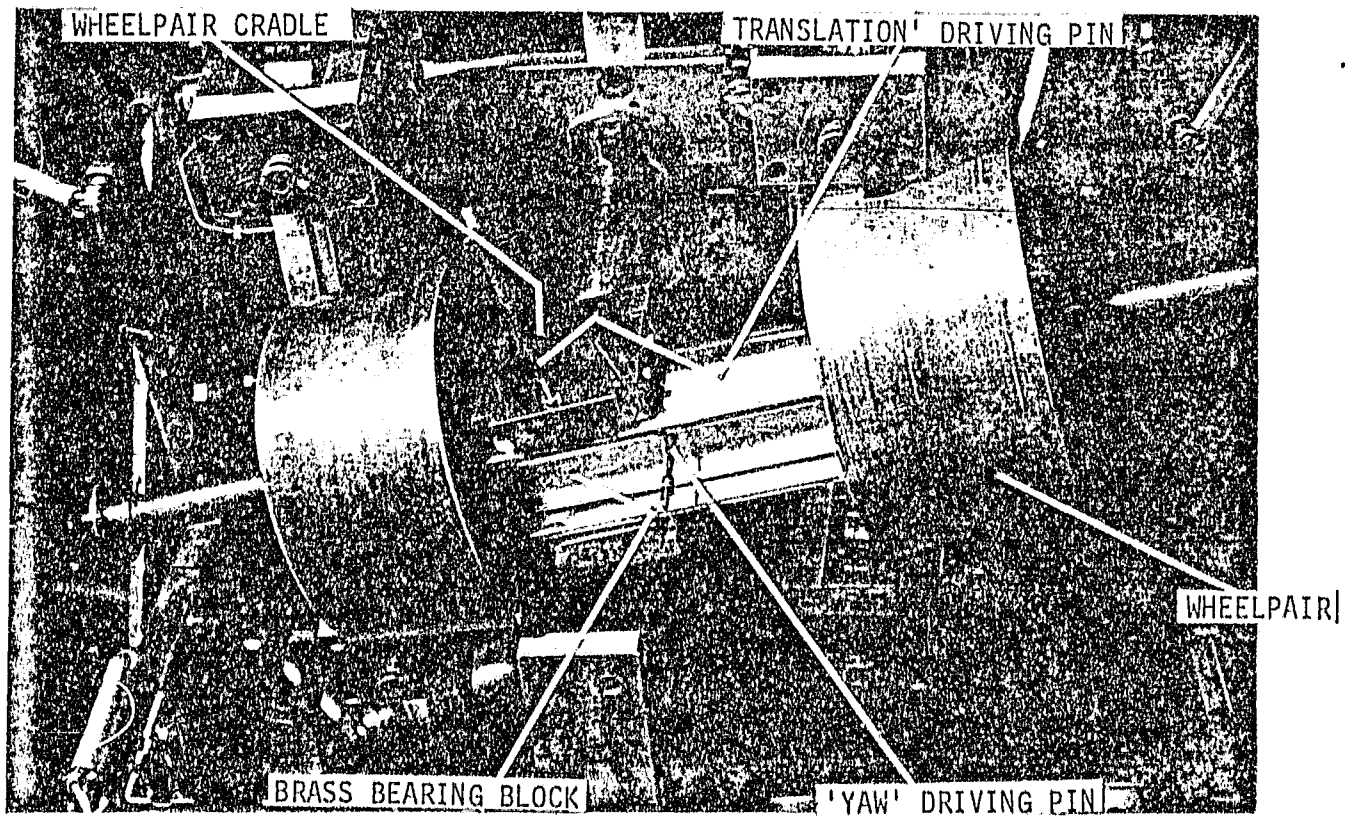

Figure 6.19(b): ELEVATION OF MIRROR DRIVING SYSTEM

followed the tilting movement. A forked lever, the pivot of which was placed sufficiently far from the pin so as to minimise possible interference with the yawing movement, was arranged so that its fork fitted into the pin while a mirror was fixed at the other end. Using the same light source as that employed to follow the yawing movement, the amount of the tilt experienced by the wheelpair could be observed at the same time as the yawing movement. The driving pins are clearly visible in Figure 6.19(a), where the wheelpair is shown in the fully yawed and tilted position. The optical measuring system is shown in plan in Figure 6.19(b).

CHAPTER 7

EXPERIMENTAL WORK PERFORMED ON TEST RIG

7.1 INTRODUCTORY SURVEY

The earlier sets of tests performed on the test rig had as one of their principal objectives the need to investigate possible modifications to the test rig so as to improve its performance, but while this aspect was being given consideration, it was nevertheless possible to gain much useful information as to how the wheelpair behaved in a variety of conditions. (In order that it may be more readily appreciated why certain changes to the test rig were brought about, this account is almost inevitably to some extent historical and it is hoped that this method of presenting the experimental work will be helpful in eliminating some aspects of the wheelpair behaviour.)

In general, the procedure followed in carrying out the tests was to gradually increase the belt speeds (and in this way, cause the wheelpair spin speed to increase) until at some critical speed, the wheelpair would start to oscillate without outside prompting, that is, 'hunting' commenced. Below the critical rail speed, the wheelpair ran stably in the neutral position. The pattern of the hunting movement once it started was recorded in a variety of ways; additionally, attempts were made to investigate

in what manner the oscillatory movements were initiated. New belt materials were being tested as the methods of observing the wheelpair movements were changed, but as the discussion in Section 6.3.3 showed, the type of belt material was not found to alter the hunting pattern.

7.2 FIRST TEST SERIES

In the first series of tests (where the driving belts used consisted of coiled wire springs), photographs of the successive stages of the oscillatory motion were taken with a ciné camera placed sufficiently far away from the test rig for the movement of both ends of the dicone shaft to be included in each frame. Because the ceiling clearance was insufficient, the necessary distance from the wheelpair was achieved by placing a mirror between the test rig and the camera, as shown in Figure 7.1(a).

Figure 7.1(b) shows how squared grids were placed on each side of the rig below the level of the wheelpair shaft. So as to make it easier to identify the ends of the shaft, caps with pointed ends were placed on them. The recording film made it possible to establish the exact positions of the ends of the shaft as the oscillatory motion proceeded. Because of the distance between the camera lens and the grid, there was some lack in the definition of the positions of the ends of the shaft, but despite this, it was possible to establish a sufficiently accurate record of the movements of the ends of the shaft from an arbitrarily selected base line on the grids. These positions were measured on enlarged prints of every second frame of a portion of a ciné film showing complete cycles of the linear and rotary oscillatory movements. A sequence of such frames is shown in Figure 7.2

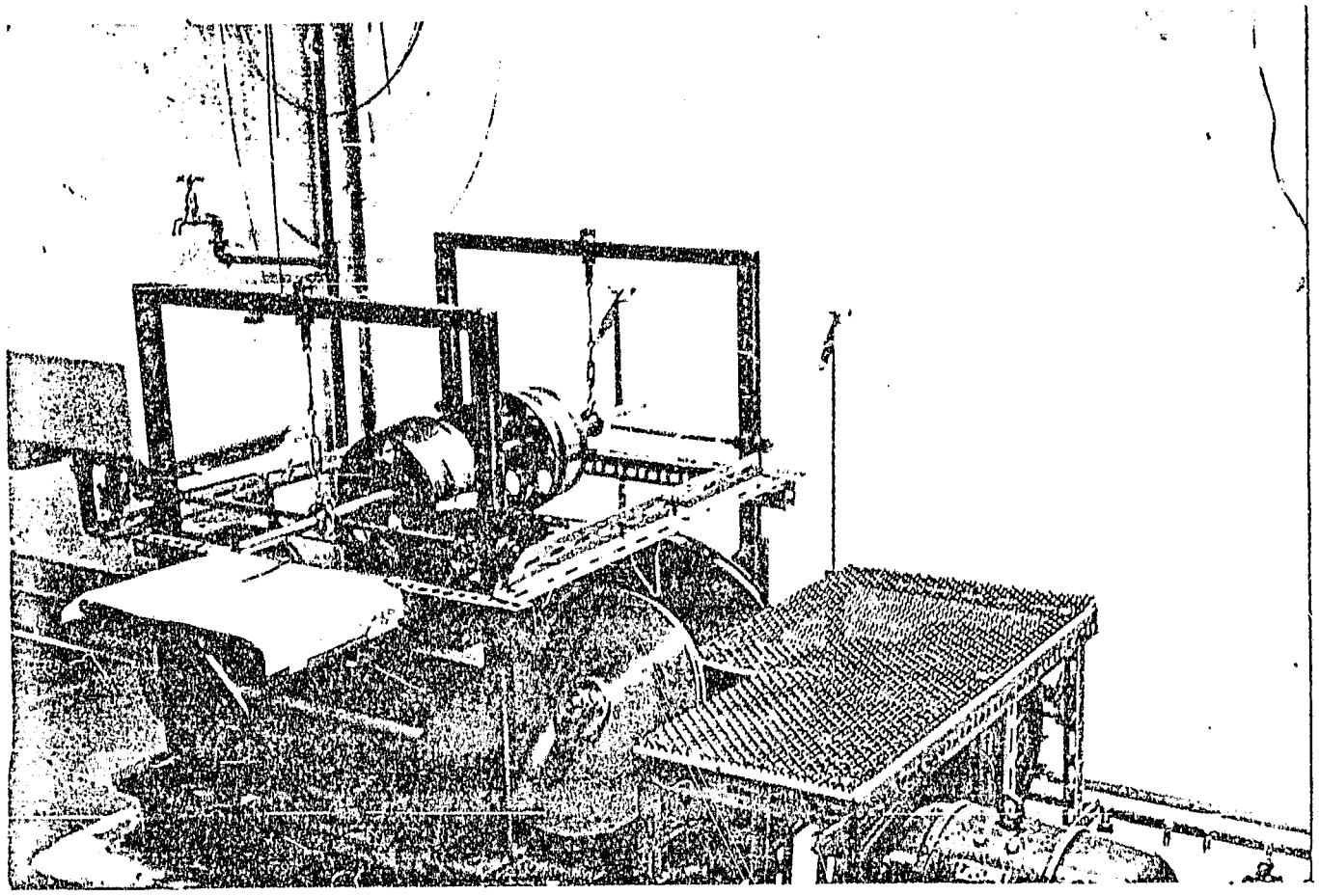

Figure 7.1(a): PHOTOGRAPH SHOWING SQUARED GRIDS PLACED UNDER ENDS OF WHEEL PAIR SHAFT

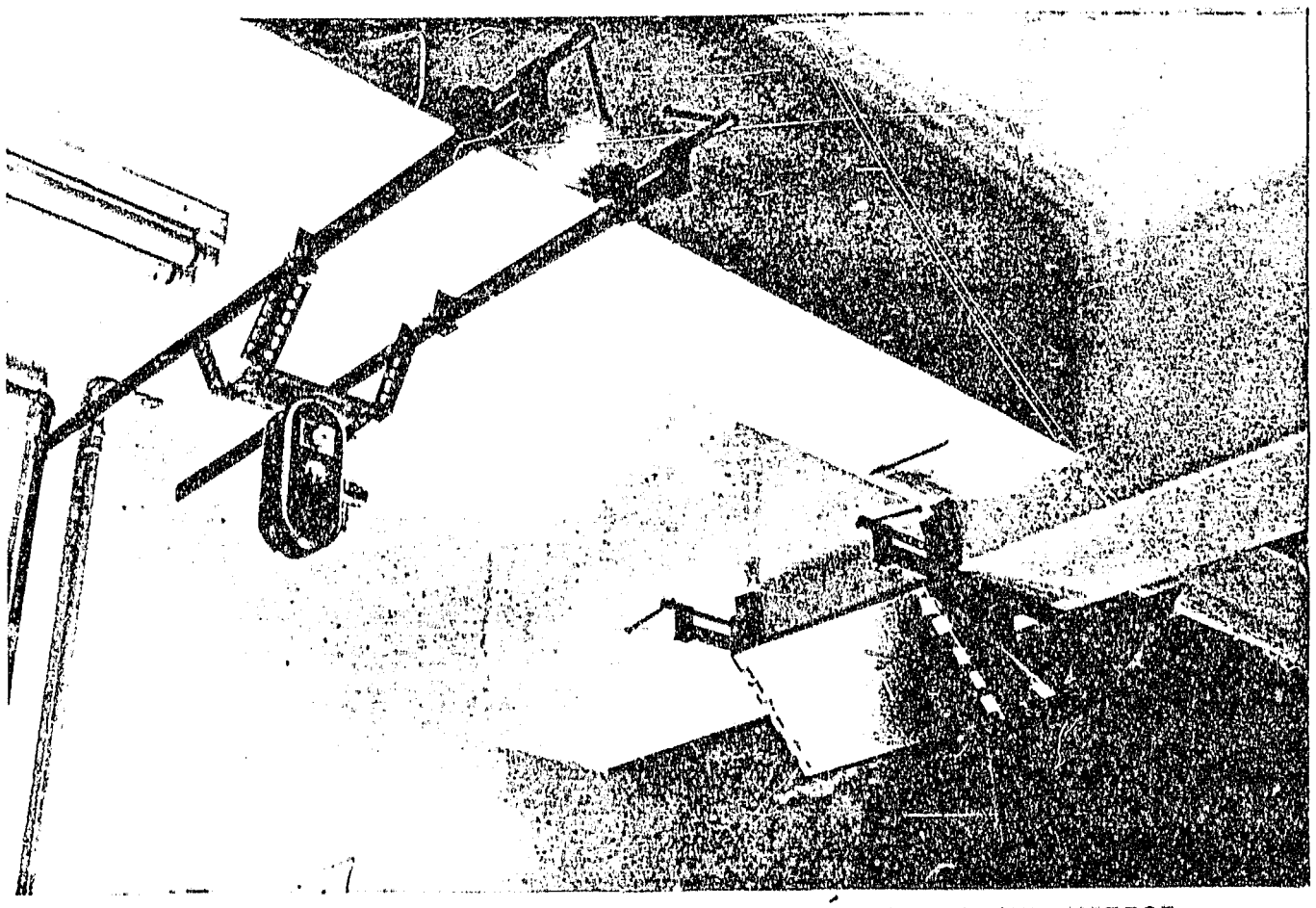

Figure 7.1(b): MOUNTING OF RECORDING CINÉ CAMERA AND MIRROR

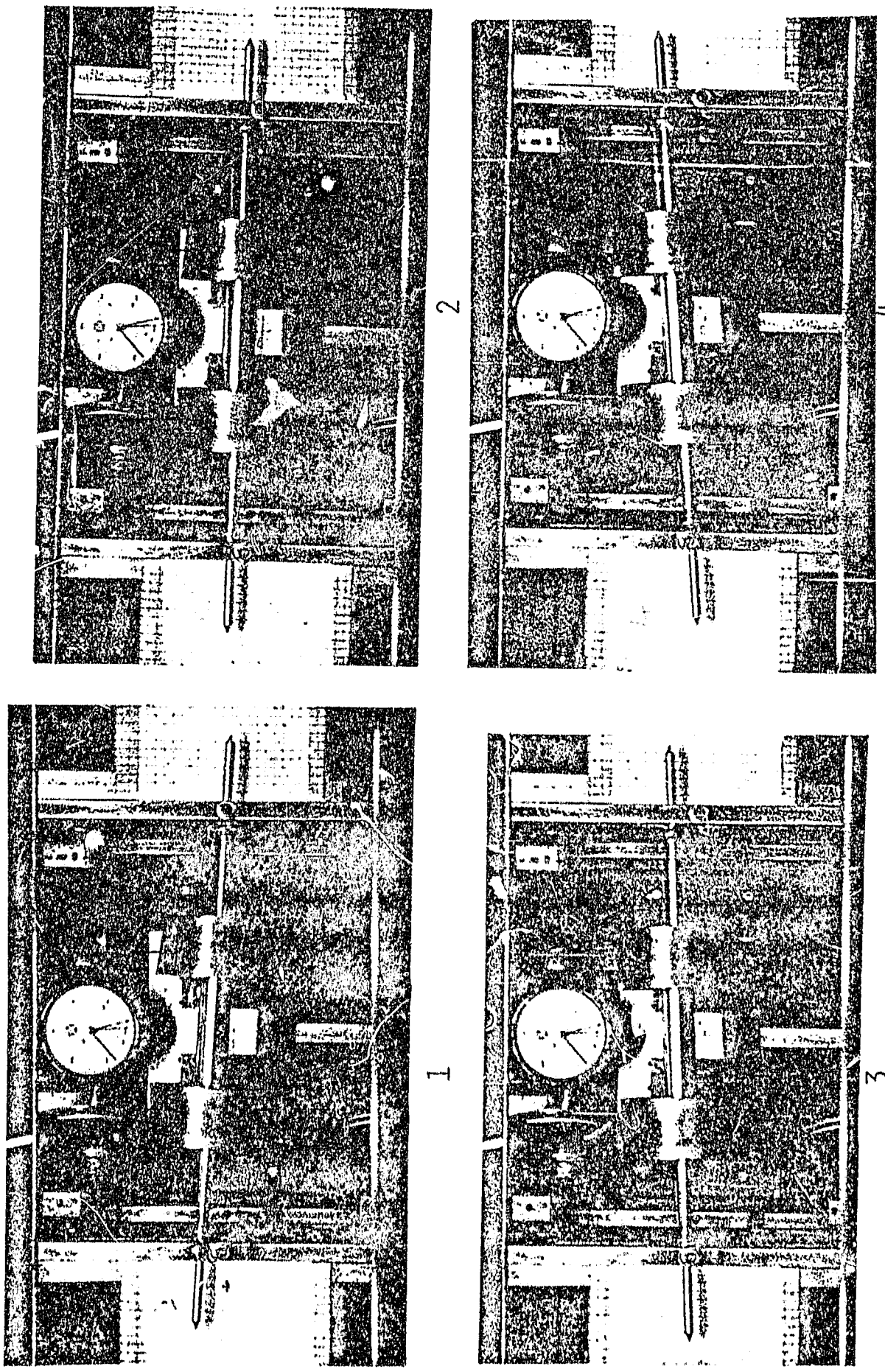

Figure 7.2: SEQUENCE OF WHEELPAIR POSITION IN VARIOUS OSCILLATORY POSITIONS

Author Boyd Charles Olivier
Name of thesis A Three-dimensional Analysis Of The "hunting" Of An Unflanged Railway Wheelpair In Its Motion Along A Straight Track. 1979

PUBLISHER:
University of the Witwatersrand, Johannesburg
©2013

LEGAL NOTICES:

Copyright Notice: All materials on the University of the Witwatersrand, Johannesburg Library website are protected by South African copyright law and may not be distributed, transmitted, displayed, or otherwise published in any format, without the prior written permission of the copyright owner.

Disclaimer and Terms of Use: Provided that you maintain all copyright and other notices contained therein, you may download material (one machine readable copy and one print copy per page) for your personal and/or educational non-commercial use only.

The University of the Witwatersrand, Johannesburg, is not responsible for any errors or omissions and excludes any and all liability for any errors in or omissions from the information on the Library website.